Technical Report Documentation Page

1. Report No.	2. Government Accession No.	3. Recipient's Catalog No.
FHWA/TX-89/473-1		

4. Title and Subtitle	5. Report Date
A Simplified Mechanistic Rut Depth Prediction Procedure for Low-Volume Roads	December 1988
	6. Performing Organization Code
7. Author(s)	8. Performing Organization Report No.
Kashyapa A. S. Yapa and Robert L. Lytton	Research Report 473-1
9. Performing Organization Name and Address	10. Work Unit No. (TRAIS)
Texas Transportation Institute The Texas A&M University System College Station, Texas 77843-3135	11. Contract or Grant No. Study No. 2-18-87-473
	13. Type of Report and Period Covered
12. Sponsoring Agency Name and Address	Interim - September 1986 December 1988
Texas State Department of Highways and Public Transportation; Transportation Planning Division P.O. Box 5051 Austin, Texas 78763	14. Sponsoring Agency Code

15. Supplementary Notes

Research performed in cooperation with DOT, FHWA.
Research Study Title: Investigation of the Effects of Raising Legal Load Limits to 80,000 lbs. on Farm-to-Market Roads

16. Abstract

In this study, a procedure for predicting the number of passes of a wheel load that will cause a specified rut depth is developed, using information which includes the base layer thickness, the resilient moduli and general classification of the granular base course and the subgrade soils. The procedure is mechanistic but simple, and is based on the permanent deformation characteristics of various types of soils determined in the laboratory and also from test results published by other researchers. Resilient moduli of pavement material layers are obtained from the results of non-destructive testing techniques. The validity of predictions of a number of these techniques is verified by comparing them with laboratory test results. Parametric runs were made using the Mechano-lattice program to form a database of rut depths. The procedure uses a multi-parametric interpolation scheme on the database in order to make predictions. Pavement materials were retrieved from six farm-to-market road sections and permanent deformation tests and resilient modulus tests were carried out. The permanent deformation behavior was modeled as a straight line in a logarithmic plot of the residual strain and the number of load repetitions. Typical slopes and intercepts of this line were determined for various soil materials. If the volumetric aggregate and moisture contents are known, an expression is also proposed to calculate the value of the slope. Expressions are giving for the intercept as a function of the resilient modulus and the soil classification. The Mechano-lattice approach, which takes into account the realistic interaction effects of the permanent deformation behavior of the individual layers, is shown to produce results which differ from the more commonly used approximately method of superposition.

17. Key Words	18. Distribution Statement
Residual deformation, rutting, Mechano-lattice analysis, non-destructive testing, resilient modulus	No restrictions. This document is available to the public through the National Technical Information Service 5285 Port Royal Road Springfield, Virginia 22161

19. Security Classif. (of this report)	20. Security Classif. (of this page)	21. No. of Pages	22. Price
Unclassified	Unclassified	145	

Form DOT F 1700.7 (8-72) Reproduction of completed page authorized

A SIMPLIFIED MECHANISTIC RUT DEPTH PREDICTION PROCEDURE FOR LOW-VOLUME ROADS

by

KASHYAPA A.S. YAPA and ROBERT L. LYTTON

Research Report 473-1

Research Study 2-18-87-473

Investigation of the Effects of Raising Legal Load Limits to 80,000 lbs. on Farm-to-Market Roads

Conducted for

Texas State Department of Highways and Public Transportation

in cooperation with the
U.S. Department of Transportation
Federal Highway Administration

by the

Texas Transportation Institute
The Texas A&M University System
College Station, Texas

December 1988

METRIC (SI*) CONVERSION FACTORS

APPROXIMATE CONVERSIONS TO SI UNITS

Symbol	When You Know	Multiply By	To Find	Symbol
LENGTH				
in	inches	2.54	millimetres	mm
ft	feet	0.3048	metres	m
yd	yards	0.914	metres	m
mi	miles	1.61	kilometres	km
AREA				
in^2	square inches	645.2	millimetres squared	mm^2
ft^2	square feet	0.0929	metres squared	m^2
yd^2	square yards	0.836	metres squared	m^2
mi^2	square miles	2.59	kilometres squared	km^2
ac	acres	0.395	hectares	ha
MASS (weight)				
oz	ounces	28.35	grams	g
lb	pounds	0.454	kilograms	kg
T	short tons (2000 lb)	0.907	megagrams	Mg
VOLUME				
fl oz	fluid ounces	29.57	millilitres	mL
gal	gallons	3.785	litres	L
ft^3	cubic feet	0.0328	metres cubed	m^3
yd^3	cubic yards	0.0765	metres cubed	m^3

NOTE: Volumes greater than 1000 L shall be shown in m^3.

TEMPERATURE (exact)

°F	Fahrenheit temperature	5/9 (after subtracting 32)	Celsius temperature	°C

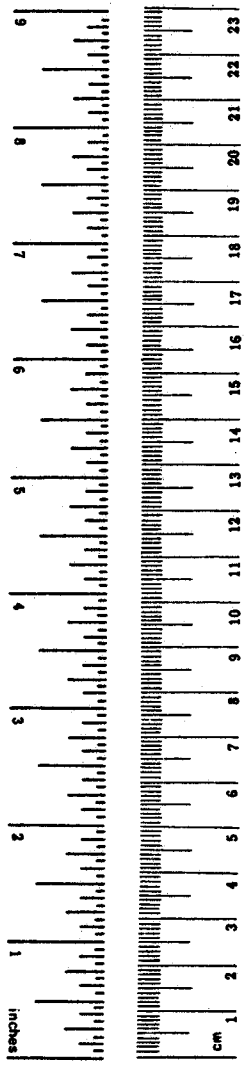

APPROXIMATE CONVERSIONS TO SI UNITS

Symbol	When You Know	Multiply By	To Find	Symbol
LENGTH				
mm	millimetres	0.039	inches	in
m	metres	3.28	feet	ft
m	metres	1.09	yards	yd
km	kilometres	0.621	miles	mi
AREA				
mm^2	millimetres squared	0.0016	square inches	in^2
m^2	metres squared	10.764	square feet	ft^2
km^2	kilometres squared	0.39	square miles	mi^2
ha	hectores (10 000 m^2)	2.53	acres	ac
MASS (weight)				
g	grams	0.0353	ounces	oz
kg	kilograms	2.205	pounds	lb
Mg	megagrams (1 000 kg)	1.103	short tons	T
VOLUME				
mL	millilitres	0.034	fluid ounces	fl oz
L	litres	0.264	gallons	gal
m^3	metres cubed	35.315	cubic feet	ft^3
m^3	metres cubed	1.308	cubic yards	yd^3

TEMPERATURE (exact)

°C	Celsius temperature	9/5 (then add 32)	Fahrenheit temperature	°F

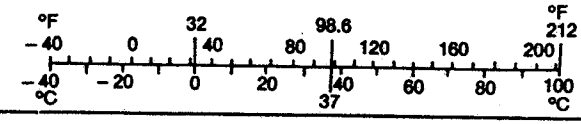

These factors conform to the requirement of FHWA Order 5190.1A.

* SI is the symbol for the International System of Measurements

ABSTRACT

Rutting has always been recognized as a major problem in low-volume roads. Thin pavements can easily face rapid deterioration because of rutting caused by increased overweight vehicle traffic. The present trend in pavement design and analysis is towards describing material properties in terms of resilient moduli.

In this study, a procedure for predicting the number of passes of a wheel load that will cause a specified rut depth is developed, using information which includes the base layer thickness, the resilient moduli and general classification of the granular base course and the subgrade soils. The procedure is mechanistic but simple, and is based on the permanent deformation characteristics of various types of soils determined in the laboratory and also from test results published by other researchers. Resilient moduli of pavement materials are obtained from the results of non-destructive testing techniques. The validity of a number of these techniques is verified by comparing them with laboratory test results. Parametric runs were made using the Mechano-lattice program to form a database of rut depths. The procedure uses a multi-parametric interpolation scheme on the database in order to make predictions.

Pavement materials were retrieved from six farm-to-market road sections, and permanent deformation tests and resilient modulus tests were carried out. The permanent deformation behavior was modeled as a straight line in a logarithmic plot of the residual strain and the number of load repetitions. Typical slopes and intercepts of this line were determined for various soil materials. Typical values for the slope are given for different soil types. If the volumetric aggregate and moisture contents are known, an expression is also proposed to calculate the value of the slope. Expressions are given for the intercept as a function of the resilient modulus and the soil classification. The Mechano-lattice approach, which takes into account the realistic interaction effects of the permanent deformation behavior of the individual layers, is shown to produce results which differ from the more commonly used approximate method of superposition.

SUMMARY

Rutting has always been recognized as a major problem in low-volume roads. Thin pavements can easily face rapid deterioration because of rutting caused by increased overweight vehicle traffic. As a part of a previous study by Texas Transportation Institute, "Load Rating of Light Pavement Structures" (Study No. 2-8-80-284, sponsored by Texas State Department of Highways and Public Transportation), a computer program, "LOADRATE", was developed. It predicts the rut depth of a low-volume pavement using an empirically developed database. This study refines that process by using a mechanistic approach for predicting rut depth.

This procedure predicts the number of passes of a wheel load that will cause a specified rut depth, using information which includes the base layer thickness, the resilient moduli and general classification of the granular base course and the subgrade soils. The procedure is mechanistic but simple, and is based on the permanent deformation characteristics of various types of soils determined in the laboratory and also from test results published by other researchers. Resilient moduli of pavement material layers are obtained from the predictions of nondestructive testing techniques. The validity of predictions of a number of these techniques is verified by comparing these predictions with laboratory test results. Parametric runs were made using the Mechano-lattice program to form a database of rut depths. The procedure uses a multi-parametric interpolation scheme on the database in order to make predictions.

Pavement materials were retrieved from six farm-to-market road sections, and permanent deformation tests and resilient modulus tests were carried out. The permanent deformation behavior was modeled as a straight line in a logarithmic plot of the residual strain and the number of load repetitions. Typical slopes and intercepts of this line were determined for various soil materials. Typical values for the slope are given for different soil types. If the volumetric aggregate and moisture contents are known, an expression is also proposed to calculate the value of the slope. Expressions are given for the intercept as a function of the resilient modulus and the soil classification. The Mechano-lattice approach, which takes into account the realistic interaction effects of the permanent deformation behavior of the individual layers, is shown to produce results which differ from the more commonly used approximate method of superposition.

A computer program is written incorporating the rut depth database and the

interpolation scheme. It can be used alone if the resilient moduli of the pavement layers are known beforehand. Otherwise, it can be incorporated with another program like LOADRATE, which can estimate the resilient modulus using deflection data in the field. Rut depth is predicted for a given traffic volume.

This simple but mechanistic means of estimating the service life of a pavement will help the Texas SDHPT in precisely planning future rehabilitation works of its extensive farm-to-market road system.

IMPLEMENTATION STATEMENT

This report describes the development of a new rut depth prediction scheme for low-volume roads. The prediction procedure uses the resilient moduli and the material type of the pavement layers and the thickness of the base layer. It predicts the rut depth for a volume of traffic given in terms of Equivalent Single Axle Loads. The program developed here will be available for implementation as a part of a software package which will be produced towards the final stage of the Study 2-18-87-473.

DISCLAIMER

The contents of this report reflect the views of the authors who are responsible for the facts and the accuracy of the data presented within. The contents do not necessarily reflect the official views or the policies of the Federal Highway Administration. This report is not a standard, a specification nor a regulation.

TABLE OF CONTENTS

TABLE OF CONTENTS (Continued)

LIST OF TABLES

LIST OF FIGURES

LIST OF FIGURES (Continued)

CHAPTER I

INTRODUCTION

In recent years, low-volume roads (e.g., farm-to-market roads in Texas) have received much attention from various highway agencies because of the rapid deterioration due to the increased heavy vehicle traffic. Rutting, or excessive permanent deformation in the wheel path, has been identified as a major failure criterion in flexible pavements. A low-volume road is essentially a two-layer pavement. It consists of a granular base layer laid over in situ or imported subgrade. The pavement is protected from rainfall infiltration by a thin asphalt surface treatment, which also serves as a wearing course. Because the properties of the base and the subgrade are not perfectly elastic, a load/unload cycle of a traveling wheel will cause a small permanent deformation in each layer. In time, due to repeated loading and unloading sequences, each layer will accumulate a significant amount of permanent deformation. The deformations in individual layers are reflected in the surface as rutting. A long rut in the wheel path is not only uncomfortable to the motorists, but also a severe safety hazard. It can cause hydroplaning of the vehicle during wet conditions. This has been recognized by the highway agencies and as such, is given due consideration in various design guides (1) and maintenance manuals (2). It is generally considered that one to two inches of rut depth in a pavement is a serious problem (3). Hence it is important to be able to estimate the time before rutting exceeds a certain terminal level, in order to plan pavement rehabilitation works.

Scope of the Study

This study undertakes to develop a simple and mechanistic method of predicting the rutting behavior of a low-volume road. There are numerous nondestructive testing [NDT] devices available for structural evaluation of pavements. Because these devices are readily available to most of the highway agencies and are easy to use, the prediction procedure will be based on the measured response from an NDT device. There exist a number of computer codes to interpret an NDT response and estimate the stiffness (resilient modulus) of each pavement layer. But only a few instances of laboratory verification of these predictions have been reported in the literature. This study will investigate the validity of the field estimated resilient moduli by comparing them with laboratory measurements. The behavior of pavement materials under

repeated loading is a dominant factor in the growth of surface rutting. Therefore, the laboratory investigation will also include repeated load tests for a number of base and subgrade materials. (In low-volume roads, the effect of the thin asphaltic surface treatment layer on the structural performance of the pavement is negligible. Therefore, the permanent deformation behavior of asphalt concrete will not be investigated in this study.) Formulation of a simple method of estimating the permanent deformation behavior of a pavement material will also be investigated. One method of predicting the rut depth of a pavement is by using superposition, or adding the permanent deformation in each different material layer, calculated separately. Another method claims to be more accurate in that it takes into consideration the interaction effects of permanent deformation between layers. While using the latter method, this study will also examine these interaction effects.

Chapter II provides the necessary background for further investigations. It describes the various NDT devices and computer codes available for structural evaluation of pavements and discusses their relative merits. The factors influencing permanent deformation behavior in different materials will be discussed using the observations made by other investigators. The two main methods of calculating rut depth will also be evaluated. Chapter III describes the laboratory and field test procedures adopted in this study. Chapter IV presents the test results and compares the field and laboratory results. It also includes the formulation of a method to estimate the permanent deformation behavior of a material based on data from past research work. The proposed rut depth prediction procedure is described in Chapter V. The importance of the interaction effects of the residual deformation behavior in predicting pavement rut depth and the effect of the moisture content on the rate of residual deformation are discussed in Chapter VI. The complete set of laboratory test results, the database of rut depths created using the Mechano-lattice program and the computer program developed in this study are given in the Appendices.

CHAPTER II

RELATED TECHNICAL BACKGROUND

This chapter describes the nondestructive evaluation techniques that were considered in this study. Laboratory testing procedures are briefly explained but will be covered in more detail in a later chapter. Factors affecting the permanent deformation behavior of different pavement materials, as reported in the literature, are also discussed. This will form the basis for identifying the critical parameters that describe the rutting behavior of pavement soil materials. The different approaches used by other investigators in predicting the rut depth of a pavement are also described.

A. Methods for Nondestructive Evaluation of Pavements

There exist a number of techniques to evaluate strength characteristics of pavement structures. Measurement of the pavement surface deflection basin under an applied load is the most popular and widely used of these techniques. But the deflections depend heavily on the way the load is applied and its magnitude (4).

The Benkelman Beam, which is one of the earliest items of equipment used to generate a deflection basin, employs a dual wheel load of 9 kips moving at creep speed and measures the rebound deflection. The Road Rater and the Dynaflect both apply steady-state harmonic loads. The Road Rater can develop a load of about 8 kips between the peaks, and the load can be applied at a frequency range between 6 and 60 Hz. The Dynaflect applies a load of an amplitude of about 500 lb. at a steady frequency of 8 Hz. The Falling Weight Deflectometer [FWD] uses an impulse load which can be varied from 1.5 to 24 kips and is transmitted to the pavement within 30 milliseconds. Velocity transducers, or geophones, are used in all of the devices (with the exception of the Benkelman Beam) to detect the response. All of these items of equipment attempt to reproduce a response which in the ideal situation should reflect the deflection under a single wheel load of 9 kips. Hoffman and Thompson (4) compared the deflection basins measured by the Benkelman Beam, the Road Rater and the FWD, against the deflections under moving trucks of different weights, measured by an accelerometer. After testing a large number of in-service pavements and test sections of different configurations, it was concluded that the FWD performs best in simulating the moving load. It was found that the Road

Rater induces comparatively low deflections because of its harmonic type loading of low magnitude.

The Pavement Dynamic Cone Penetrometer [PDCP] (5) correlates the effort required to penetrate a pavement layer to its stiffness. Blows from a free-falling hammer drive a steel rod with a tempered steel cone at the tip into the pavement layers. The PDCP can easily penetrate the thin asphalt surface treatment of a low volume road, and hence offers a very simple and quick method of estimating layer stiffnesses. Usually the depth penetrated in every 5 blows is recorded, and readings up to a total depth of about 30 inches can be obtained.

B. Backcalculation of Moduli from Nondestructive Tests

The purpose of all of the NDT devices mentioned earlier is to estimate the stiffness of the pavement. Measurement of the deflection basin under a given load provides a means of backcalculating the stiffness, or the resilient modulus, of each of the pavement layers. Boussinesq's formula gives the stresses at any point under a given load of a single layered pavement if the modulus is known (6). Burmister and later Acum and Fox, provided solutions giving stresses, strains and deflections in a multi-layered pavement with known moduli (6). There are currently two major approaches that reverse the process, that is, backcalculate the modulus of each layer using measured deflection readings (7). The first approach uses an iterative technique to match the measured deflections and the calculated deflections of a pavement with assumed moduli under a similar load. CHEVDEF, BISDEF, ELSDEF and MODCOMP2 use this approach and, assume a linear variation of moduli with the applied stress (7). ISSEM4 backcalculates nonlinear parameters of elastic moduli (7). The other approach is to use a data base of calculated deflection values to draw upon, to match the deflection basin. ILLI-CALC (8) uses ILLI-PAVE, a finite element program which allows the use of nonlinear parameters, to generate the database, and MODULUS (9) uses BISAR, a linear elastic computer code. LOADRATE (10), which was developed especially for evaluation of low-volume roads, uses regression models based on a set of ILLI-PAVE runs on thin pavements to match the deflection basin. Chua (7) compared a number of computer codes, namely, BISDEF, CHEVDEF, ELSDEF, MODCOMP2, ISSEM4, LOADRATE and MODULUS, to ascertain the consistency and efficiency of predicting the moduli of low-volume pavements. It was suggested that the programs using the database approach, namely, MODULUS and LOADRATE, have an advantage in

that they are faster and can be used simultaneously with an NDT response.

With the exception of the Benkelman Beam, all of the other NDT devices for deflection basin measurement impose dynamic loads on the pavement. Both the Dynaflect and the Road Rater use harmonic (steady-state) loading to generate the deflections while the FWD imposes an impact load. Mamlouk (11) suggested that the static analysis, as used in the elastic multi-layered theory, may result in significant errors in stiffness calculations as compared to the dynamic analysis, which considers the inertial effects of the pavement structure. But much more work is still needed to be done to successfully employ this approach.

The rate at which the PDCP penetrates a pavement will give an indication of the pavement stiffness. Chua (12) related the penetration index, or the depth penetrated per blow, to the elastic modulus of the medium using an analytical procedure. Penetration is assumed to occur due to plastic deformation caused by a plastic shock wave imposed on an axisymmetric soil disc at the cone tip. The elastic modulus, which matches the measured penetration rate at a point in the medium, is backcalculated by using the Mohr-Coulomb yield criterion to obtain the stress at which plastic strain begins.

C. Laboratory Verification of NDT Predictions of Resilient Moduli

Even though various NDT techniques have been widely used in many parts of the world to assess pavement strength, there have been only a few studies done to verify the NDT predictions of resilient moduli of in-service pavements with laboratory tests. Monismith and others (13) measured the deflections of a four-inch thick asphalt pavement by using the California Traveling Deflectometer (Benkelman Beam) and then sampled the section. The laboratory measured resilient moduli were used to calculate possible deflections under the same load using Burmister's solution. The predictions were found to be in the same order as the measured deflections.

Hoffman and Thompson (8) used the Road Rater to measure deflections and then converted them to comparable FWD readings. Samples from test sections were tested for moduli and ILLI-CALC was used to predict deflections under a similar load. This extensive test program involved a thin and a thick pavement, and the field testing and the sampling were done under several different environmental conditions. Satisfactory agreement was achieved between the measured and the predicted modulus values and deflection basins.

In an attempt to select the "best" NDT device for the evaluation of aggregate-surfaced roads of the U.S. Forest Service, Rwebangira and others (14) performed a testing program using the FWD, the Road Rater and the Dynaflect. Comparisons were made between moduli backcalculated using computer codes BISDEF and MODCOMP2 and those determined in the laboratory. It was found that the FWD and MODCOMP2 combination gave predictions much closer to the measured modulus values. It must be noted that in this case, FWD readings were normalized to a standard load level which essentially neglects the nonlinear behavior of pavement materials.

D. Repeated Load Triaxial Tests

Relations between the applied stress and both the resilient and the permanent (residual) strain of a pavement material are required for most design or evaluation procedures. Laboratory testing is the primary means of establishing these relations. The overall objective of laboratory material testing is to reproduce the in situ pavement conditions including stress and moisture levels, under circumstances which permit accurate measurement of the deformation. In the context of estimating resilient strength and rutting, the repeated load triaxial test is considered to be the best practical method for the testing of pavement materials (15). In addition to the various factors that heavily influence the resilient and plastic behavior of the materials, there are a number of critical problems associated with the testing and the measuring apparatus and also with the method of preparing the sample. In the past, researchers had adopted widely varied techniques in conducting repeated load triaxial tests. However, standard procedures have now been made available (16, 17) in an attempt to standardize the testing procedures. Still there is some controversy as to whether these methods accurately reflect the in situ conditions.

E. Factors Affecting the Permanent Deformation Characteristics of Pavement Materials

There are no specific standard procedures developed for the determination of the behavior of residual deformation (rutting) of pavement materials under repeated loading. But the procedures established for the purpose of measuring resilient modulus, AASHTO (16) and ASTM (preliminary) (17), can be extended to satisfy the research needs because of the similarity in the behavior of the materials under each of the processes. In fact, many researchers have investigated the factors affecting the

residual deformation of both coarse and fine grained materials using the methods for testing resilient behavior (18, 19, 20, 21, 22).

Number of Load Repetitions

In laboratory repeated load tests, the resulting permanent strain levels are often reported with the corresponding number of repeated loads applied. This is because it is recognized that the accumulation of residual deformation varies directly with the number of load repetitions. For the first few cycles of loading, the rate of accumulation also varies significantly. However, after some number of load cycles, the rate of accumulation of residual deformation levels off.

Lentz (23, pp. 92–93) describes vividly what happens in a granular test specimen during a loading and unloading sequence. Three mechanisms may occur simultaneously in soil deformation under load: elastic compression of soil grains, crushing of grains at interparticle contact points, and interparticle sliding. Elastic compression of soil grains causes some energy to be stored in the soil skeleton during the application of the load. When shearing resistance between grains (friction) is exceeded, sliding may occur. Also, if stresses at intergranular contact points exceed the yield strength, some crushing of grains will occur. All of these movements will cause stress redistribution among particle contact points. Elastic compression and sliding will continue until the rearrangement of particles results in a structural equilibrium. When the load is released, the elastic energy stored during compression will cause the soil skeleton to expand. Further rearrangement of particles will occur due to this expansion. Part of the energy input is lost as heat generated by particle movements during loading and unloading. Hence all of the strain will not be recovered, resulting in a net permanent strain. The next application of the load will again activate the previous mechanisms, but this time the particle movements will occur from a slightly more stable condition than before. Thus one can expect a comparatively lower net permanent strain during the second loading cycle. This process continues making net permanent strains at subsequent cycles gradually smaller.

Khosla and Singh (24) describe the residual deformation behavior as commonly occurring in three stages of strain development and they are, the transient, the steady and the tertiary stages (Figure 1). The transient stage is where the rate of accumulation of plastic strain varies with the number of load repetitions and is usually observed at the beginning of the test. In the steady stage, the rate of accumula-

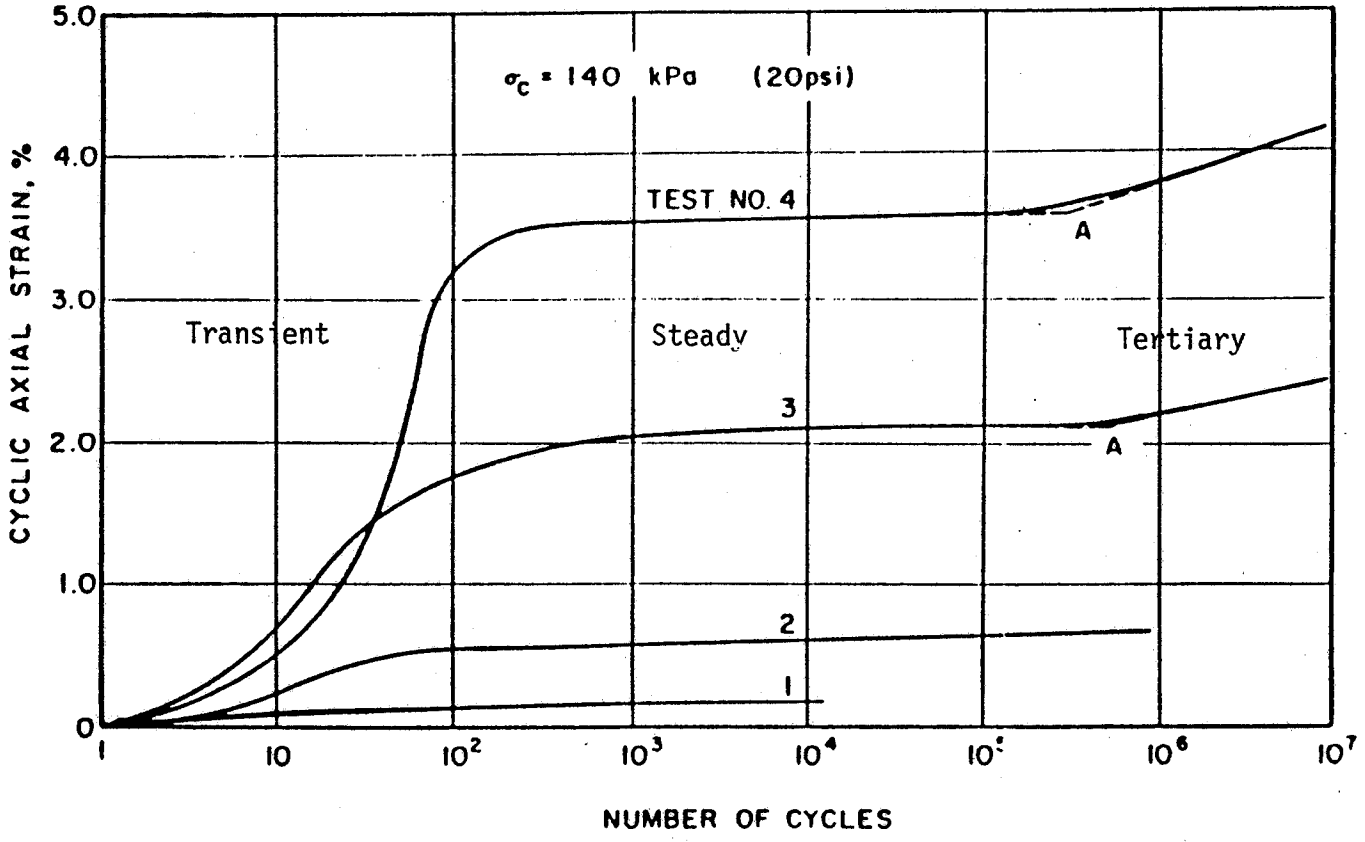

FIGURE 1 Different stages of permanent strain development (24)

tion reaches a constant level. Permanent deformation tests on uniform Ottawa sand were performed for up to 10,000,000 load repetitions. At lower deviator stress levels (Tests 1 and 2 in Figure 1), only the transient and the steady stages were observed. But at higher deviator stress levels (Tests 3 and 4), axial strains increased again after about 100,000 cycles. It was described as the tertiary stage. Similar observations were made by Gaskin et al. (25) in uniform fine sand specimens (Figure 2) under higher deviator stress levels. The same phenomena is seen in the data presented by Lentz (23) in a study involving silty sand subgrade material (Figure 3). It can also be seen in the tests by Chisolm and Townsend (26) on gravelly sand base course material (Figure 4). Barksdale (18), tested Granite Gneiss base course materials and observed that as the deviator stress increases, a critical level will be reached beyond which the rate of strain accumulation tends to increase with increasing load repetitions. There is no indication that this tertiary stage in plastic strain development has been observed in any of the cohesive material types.

There are two popular models used to relate plastic strain accumulation with the number of load repetitions. The first identifies a linear relationship between the accumulated residual strain and the logarithm of the number of load repetitions (22, 23, 24, 25, 26, 27) and is given by,

$$\epsilon_p = a_1 + b_1 \log N \tag{1}$$

where,

ϵ_p = total residual strain at the end of N cycles and,

a_1, b_1 = material constants.

Lentz (23) claims to have obtained a better correlation with this model than any other for his experimental data on silty sand. It must be noted here that this model does not consider the transient and the steady stages of residual strain accumulation separately (Figure 3).

The other model uses a linear relation in a log-log plot between the accumulated permanent strain and the number of load repetitions (20, 28) and is given by,

$$\log \epsilon_p = \log a + b \log N \tag{2}$$

where,

a, b = material constants.

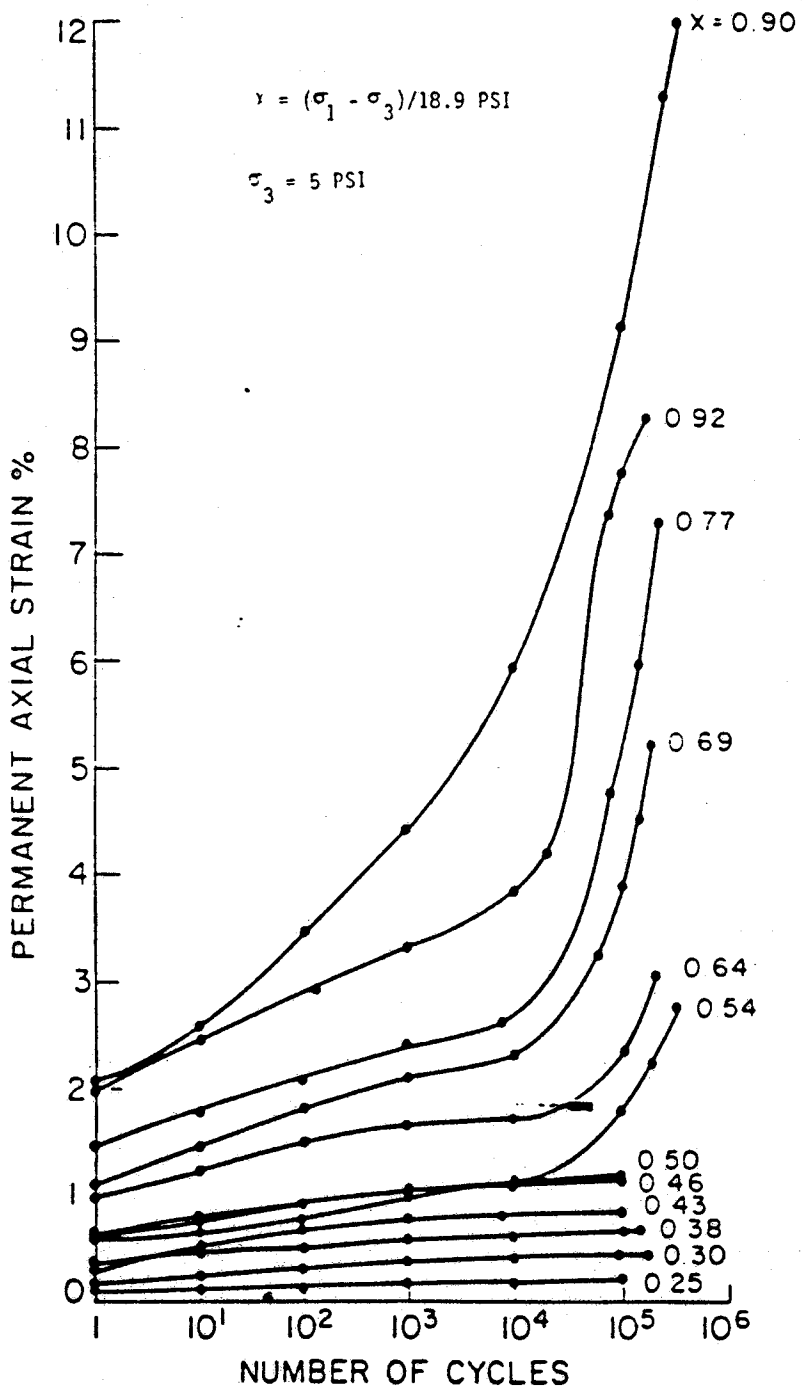

FIGURE 2 Change of permanent strain behavior with applied stress (25)

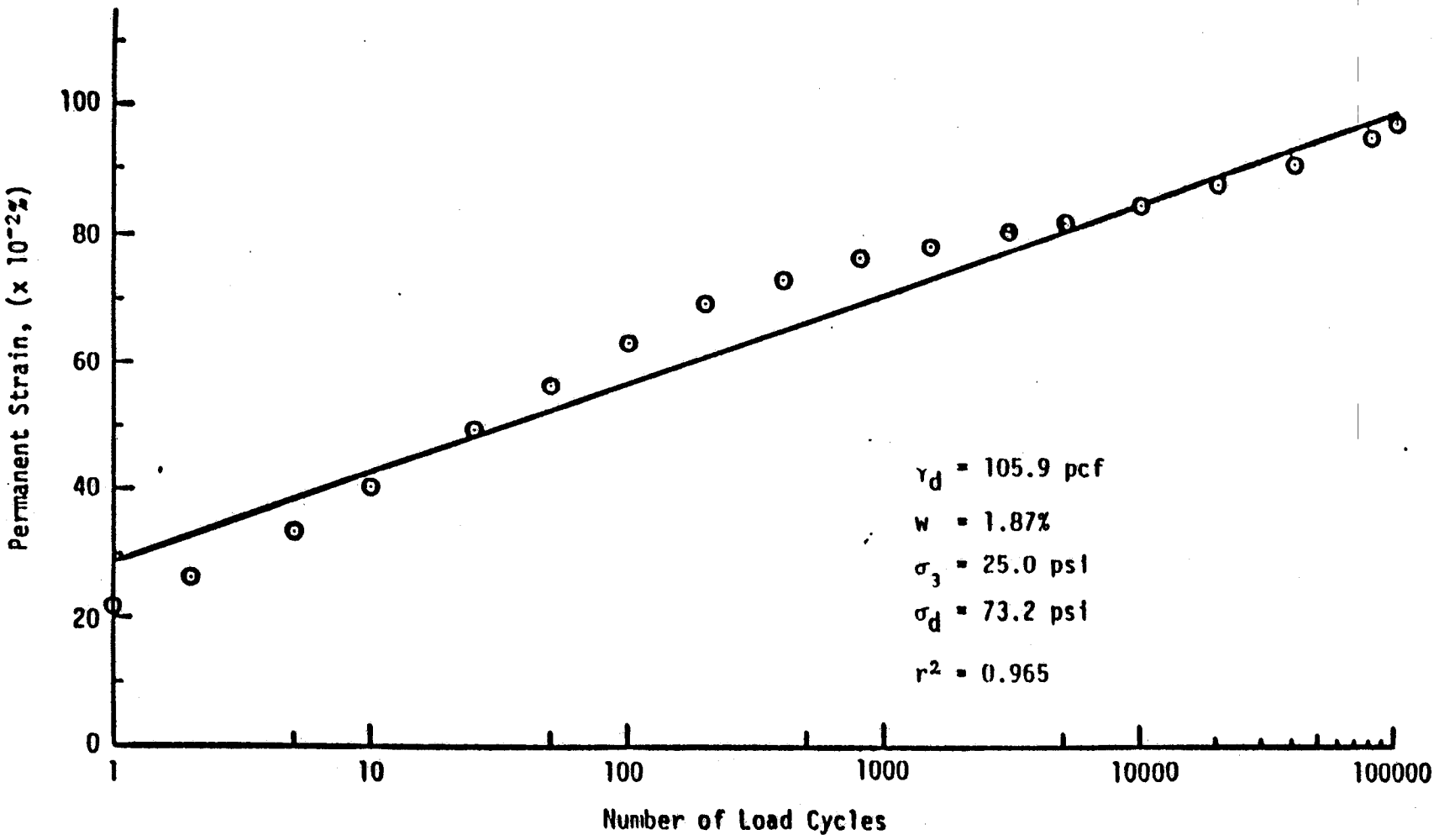

FIGURE 3 Permanent strain behavior of silty sand subgrade (23)

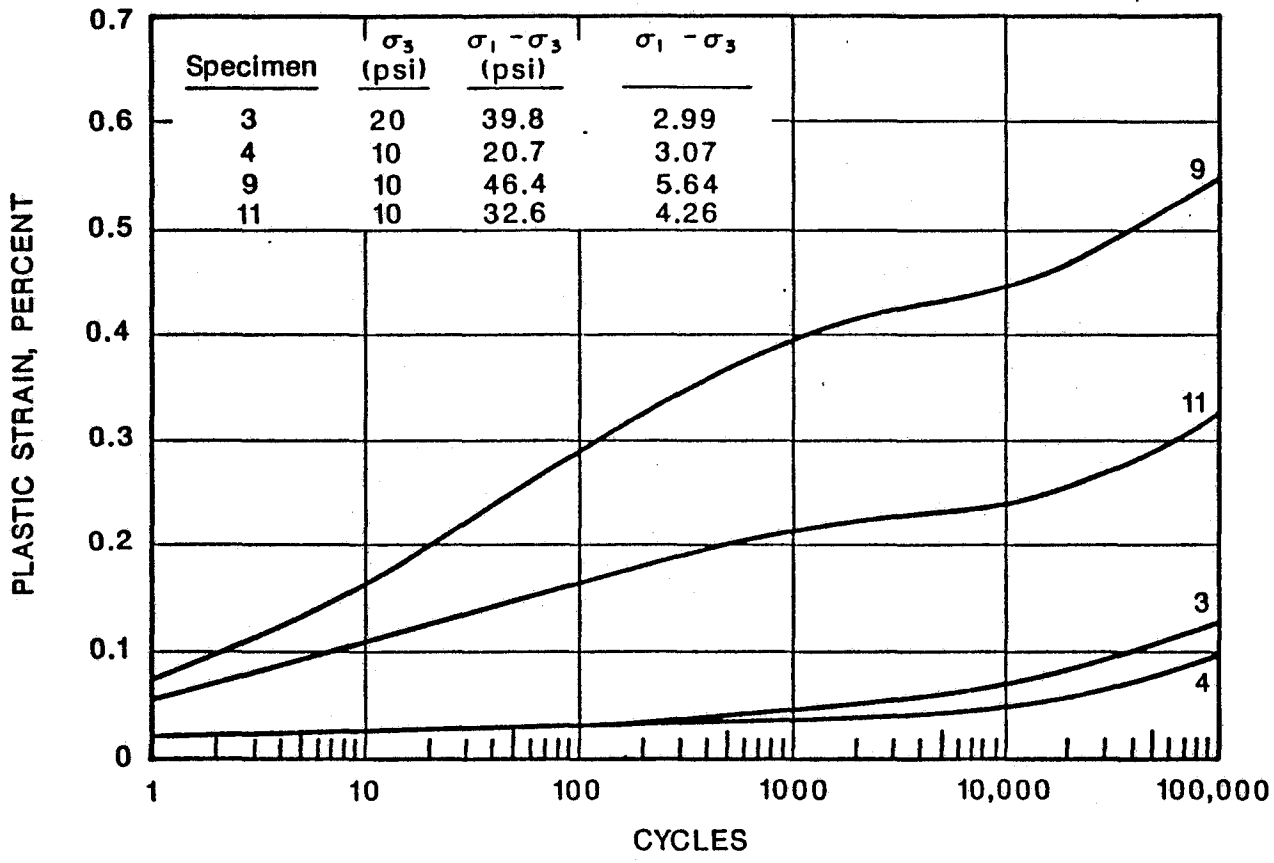

FIGURE 4 Permanent strain behavior of gravelly sand base course (26)

Monismith et al. (20), in representing their experimental data on silty clay by this model, had neglected the transient stage of plastic strain accumulation (Figure 5). Furthermore, they remarked that it is possible for the constant 'b' to be dependent only on the soil type, and that the coefficient 'a' may be a function of the stress level, the stress history, and the placement conditions. In the VESYS pavement evaluation program (29, 30) a similar model is used and it is,

$$\epsilon_p = \frac{R_\delta \, \mu}{1-\alpha} \, N^{1-\alpha} \tag{3}$$

where,

R_δ = total deflection amplitude and,

α, μ = material constants.

Equation (3) can be reduced to Equation (2) if,

$$\mu = a\,(1-\alpha)/\,R_\delta \qquad \text{and} \qquad \alpha = 1 - \mathrm{b}\,.$$

Rauhut and Jordhal (30) observed that for subgrade materials, the α value varies with the deviator stress and the moisture content within a narrow range, and is also affected greatly by the clay content of the material. They observed that for granular base course materials, α is essentially independent of the stress state.

Majidzadeh et al. (31, 32), Bayomy (33) and Khedr (34), used the Rate Process Theory to arrive at the following relationship,

$$\frac{\epsilon_p}{N} = A \, N^{-m} \tag{4}$$

where,

A, m = material parameters.

This is equivalent to Equation (2) for,

$$A = a \qquad \text{and} \qquad \mathrm{m} = 1 - \mathrm{b}\,.$$

Majidzadeh et al. (31) showed that for silty clays, 'm' is probably a constant (Figure 6), while 'A' varies inversely with the dynamic modulus and is not significantly dependent on the applied stress (Figure 7). Khedr (34) showed that 'm' is probably

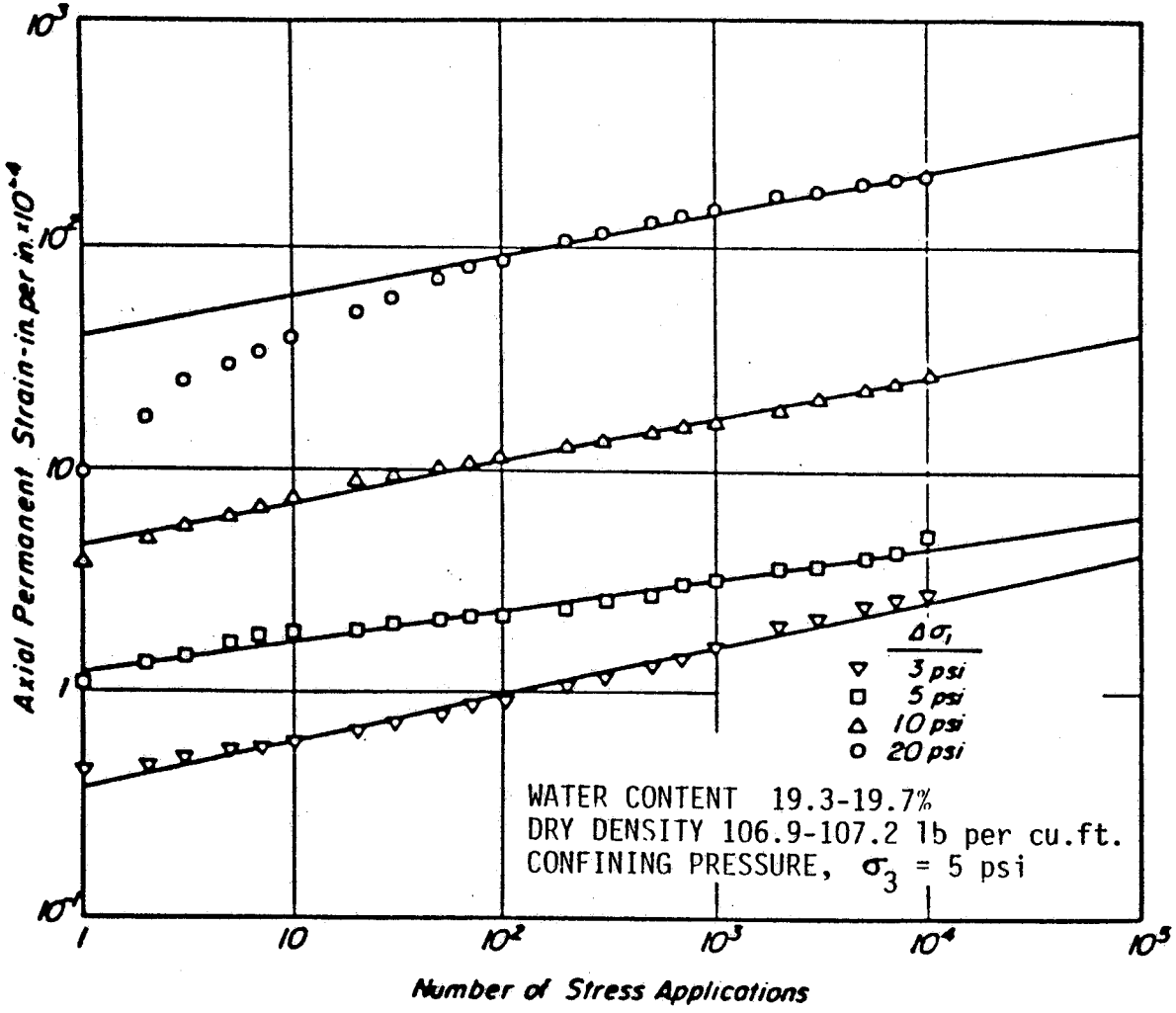

FIGURE 5 Log-log representation of permanent strain behavior (20)

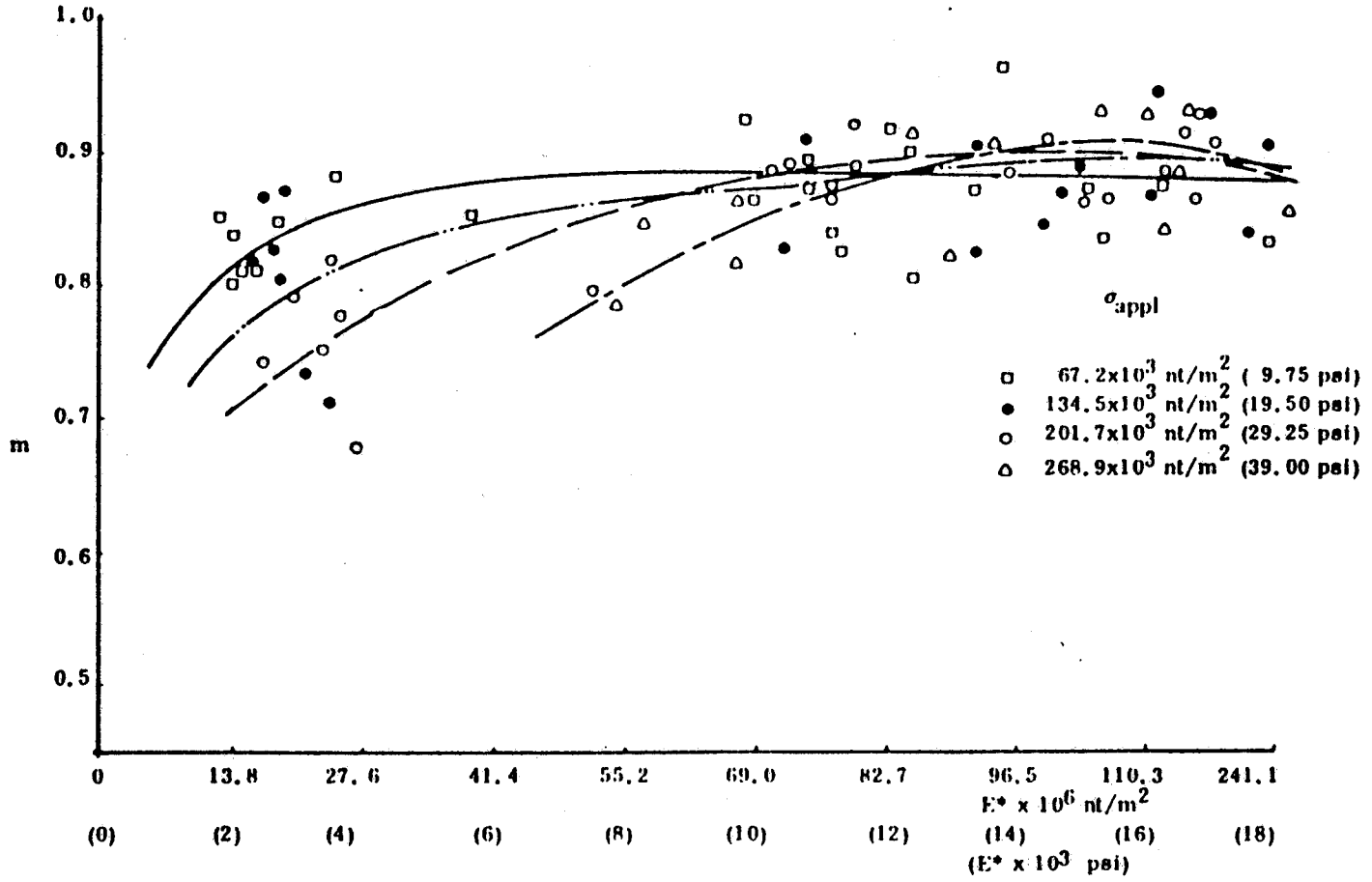

FIGURE 6 Variation of 'm' with dynamic modulus E^*—silty clay (31)

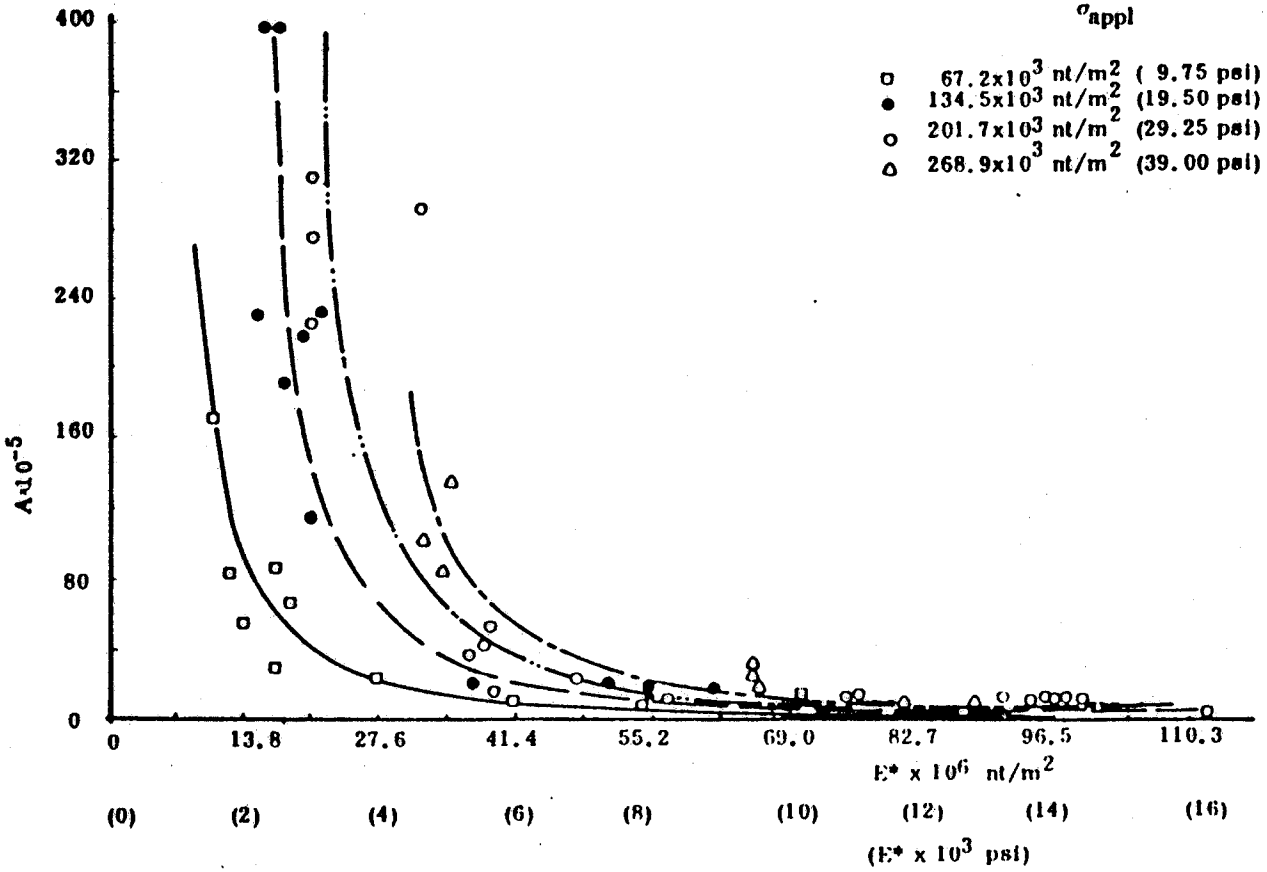

FIGURE 7 Variation of 'A' with dynamic modulus E^*—silty clay (31)

a constant for crushed limestone base material (Figure 8). The 'A' value was given as a function of resilient modulus (M_R) and the octahedral stress ratio (R_0):

$$A = 0.0358\ R_0^{2.135}\ M_R^{-0.304}\ .$$

where,

$R_0 = \tau_0/\sigma_0$

τ_0 = octahedral shear stress ($\sqrt{2}(\sigma_1 - \sigma_3)/3$), and

σ_0 = octahedral normal stress ($(\sigma_1 + 2\sigma_3)/3$).

In 1986, Tseng and Lytton (35) proposed a three parameter model using incremental plasticity theory to predict residual strains:

$$\epsilon_p = \epsilon_0\ e^{-(\rho/N)^\beta} \tag{5}$$

where,

$\epsilon_0,\ \rho, \beta$ = material parameters.

Using data compiled from several sources, it was shown that for base course materials, ϵ_0, ρ and β are dependent on the water content, the bulk stress and the resilient modulus. For subgrade materials, ϵ_0, ρ and β were shown to be dependent on the deviator stress level and less so on the water content. The parameter ϵ_0 was shown to be related also to the resilient modulus.

Applied Stress

Barksdale (18) conducted a thorough investigation on the effects of deviator and confining stresses on the residual deformation of granular base course material. Figure 9 illustrates a typical plot between the deviator stress and the residual strain at 100,000 cycles. Increasing deviator stress caused greater residual deformation while increasing confining pressure reduced it. It was found that a hyperbolic stress-strain law can be used to explain plastic strain behavior in base course material. Monismith et al. (20) investigated the effect of deviator stress on residual deformation of silty clay and the results are similar to those of Barksdale (18), as shown in Figure 10. They suggested a relationship between the applied stress and the plastic strain in the form:

$$\epsilon_p/\Delta\sigma = l + m\ \epsilon_p \tag{6}$$

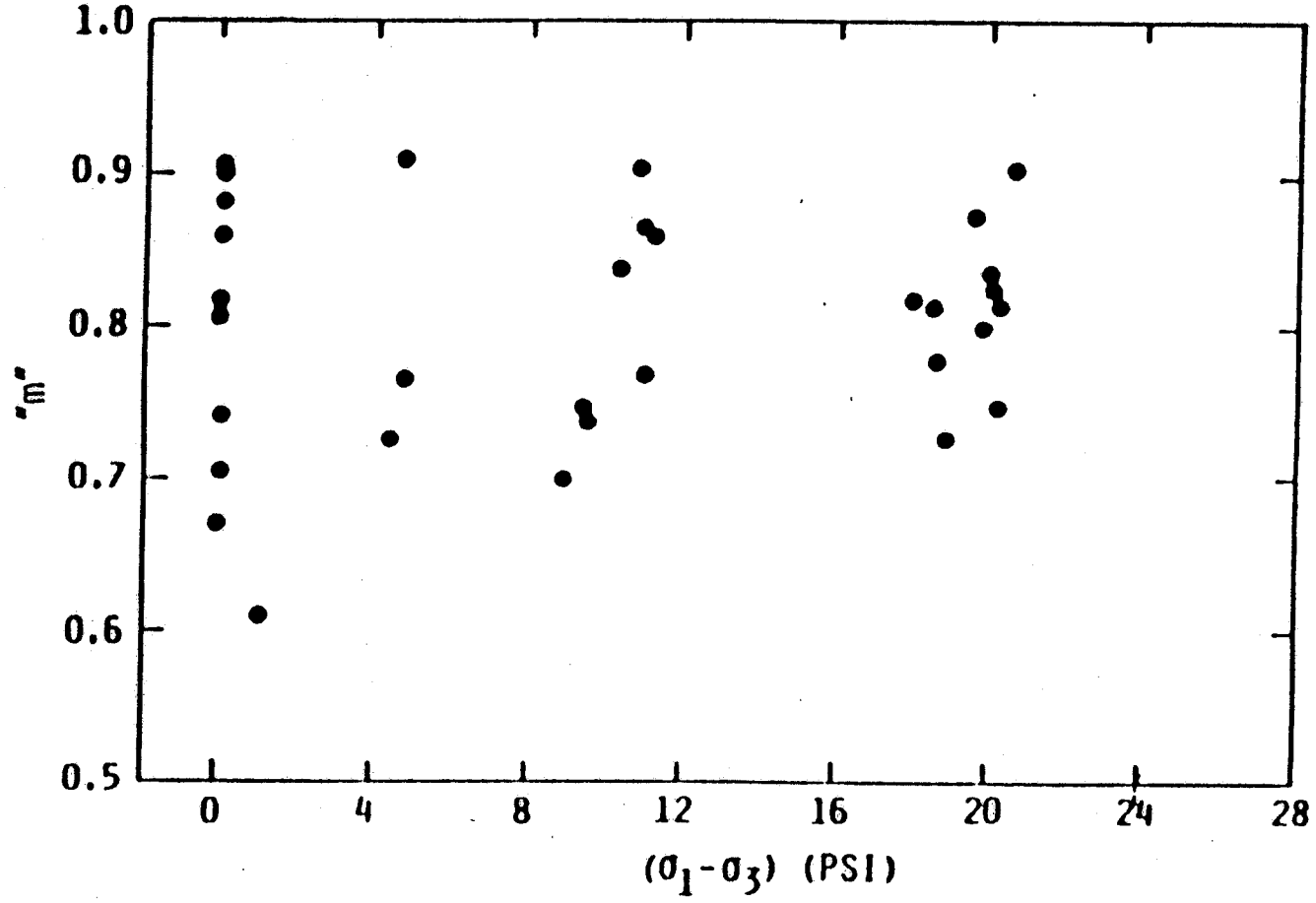

FIGURE 8 Variation of 'm' with applied stress--crushed limestone (34)

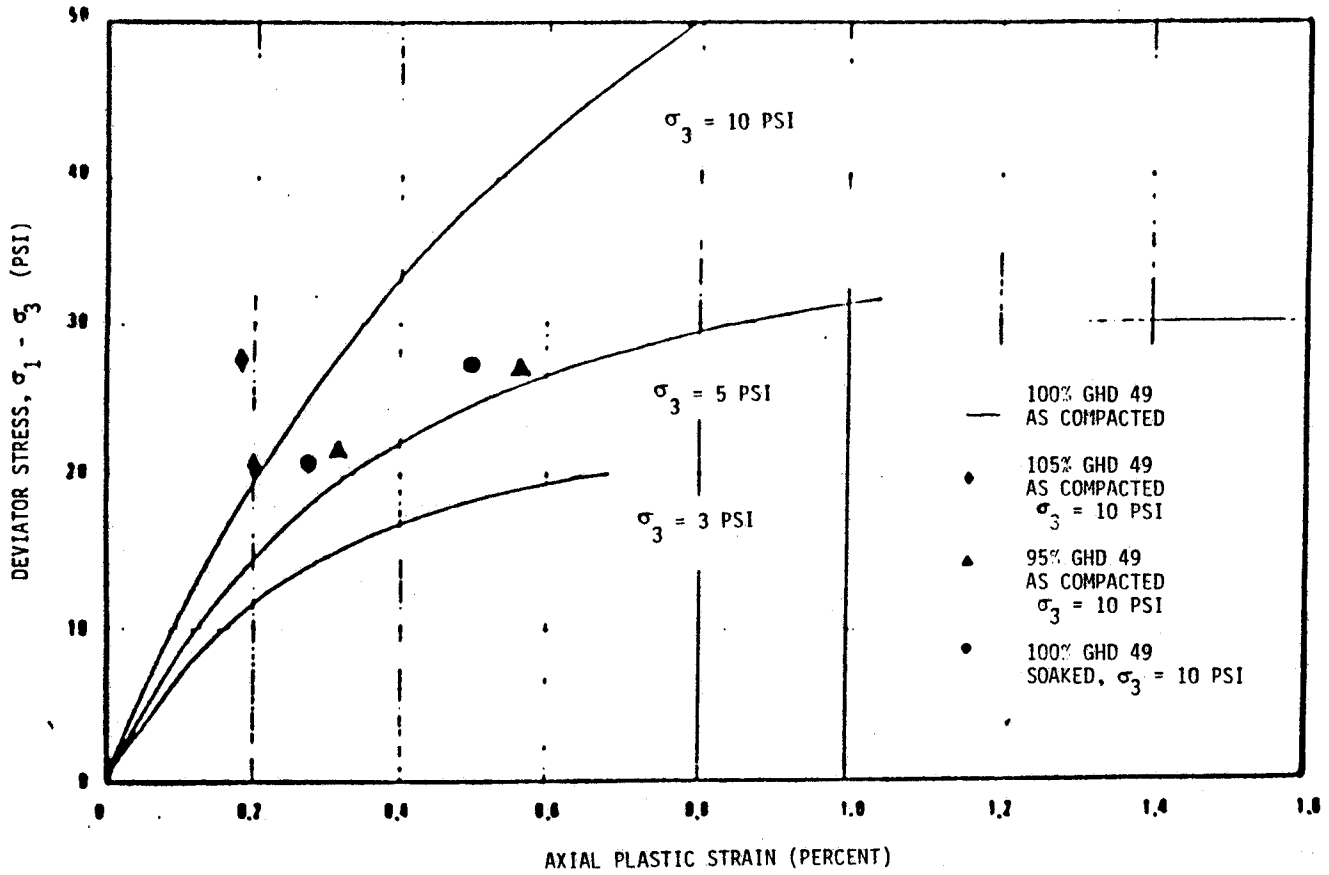

FIGURE 9 Variation of residual strain with applied stress—granular materials (18)

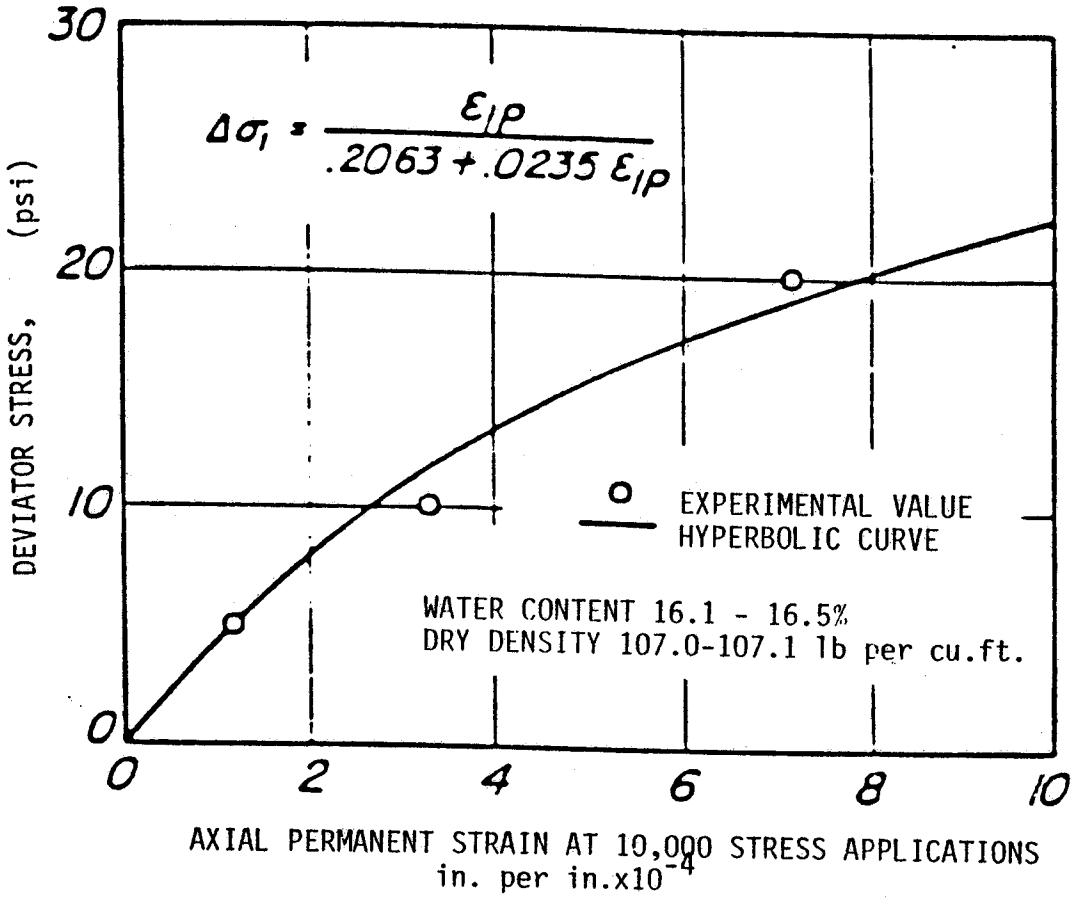

FIGURE 10 Variation of residual strain with deviator stress—silty clay (20)

where,

$\Delta\sigma$ = applied axial stress and

l, m = material constants.

Stress History

Kalcheff and Hicks (19) investigated the effects of stress history on several different base materials (Table 1). It was observed that when a sample is subjected to stages of gradually increasing stress conditions, the resulting residual deformation is lower than when compared to the same with the loading sequence reversed. Monismith et al. (20) studied this effect on silty clay and found a similar behavior (Figure 11).

Specimen Density

Barksdale (18) prepared three specimens at 95%, 100% and 105% of the maximum density and under repeated loading, the specimen at 95% density showed about 185% increase in residual deformation as compared to the 100% dense sample. The difference in deformation between the specimens at 100% and 105% density was only about 10%. He remarked that an extensive study would show the differences better.

Moisture Content

Barksdale (18) conducted some repeated load tests under a "soaked" condition which showed an average of 68% increase in the plastic strain. But it was cautioned that this would be an underprediction in an actually saturated situation, because the tested specimens had been allowed a free flow of water in and out. Edris and Lytton (22) performed a number of tests on silt to heavy clay specimens. It was observed that there is a marked increase in residual strain when moving from specimens compacted dry of optimum moisture content to very wet specimens (Figure 12). Similar increases in residual strain were noted by Morgan (21) when the sand samples were saturated. However, Lentz (23) reported that a variation of the degree of saturation from 0 to 47% during compaction (the maximum possible in the silty sand material) did not result in any significant variation in permanent strain. Majidzadeh and others (32) brought a few clay samples to saturation after 2000 cycles of loading and retested them for another 8000 cycles. They noted that the slope (m) of the

TABLE 1 EFFECT OF STRESS SEQUENCE ON PERMANENT STRAIN—GRANULAR MATERIALS (19)

Material		Source A, Pa. 2A Subbase, (144 lb/ft³)			
Loading Condition		Partially Saturated Load Duration: 0.10 s Rate of Application: 30 cpm			
Confining Stress/ Deviator Stress	Number of Load Repetitions	Permanent Strain, 10^{-6} in./in.			
		No. 1	No. 2	No. 3	No. 4
2/6		c[1]	a	a	c
	10	0	0	0	0
	100	6	220	70	25
	1 000	14	430	150	50
	10 000		650	220	
	50 000				
5/15		a	b	b	b
	10	0	0	0	0
	100	320	60	160	95
	1 000	640	110	320	185
	10 000	950	170	480	
	50 000	1180	210	600	
20/60		b	c	c	a
	10	0	0	0	0
	100	990	640	590	1050
	1 000	1980	1280	1180	2720
	10 000	2980	1930	1760	4260
	50 000	3670	2380		4780

[1] The order of test sequence was a, b, c, d.

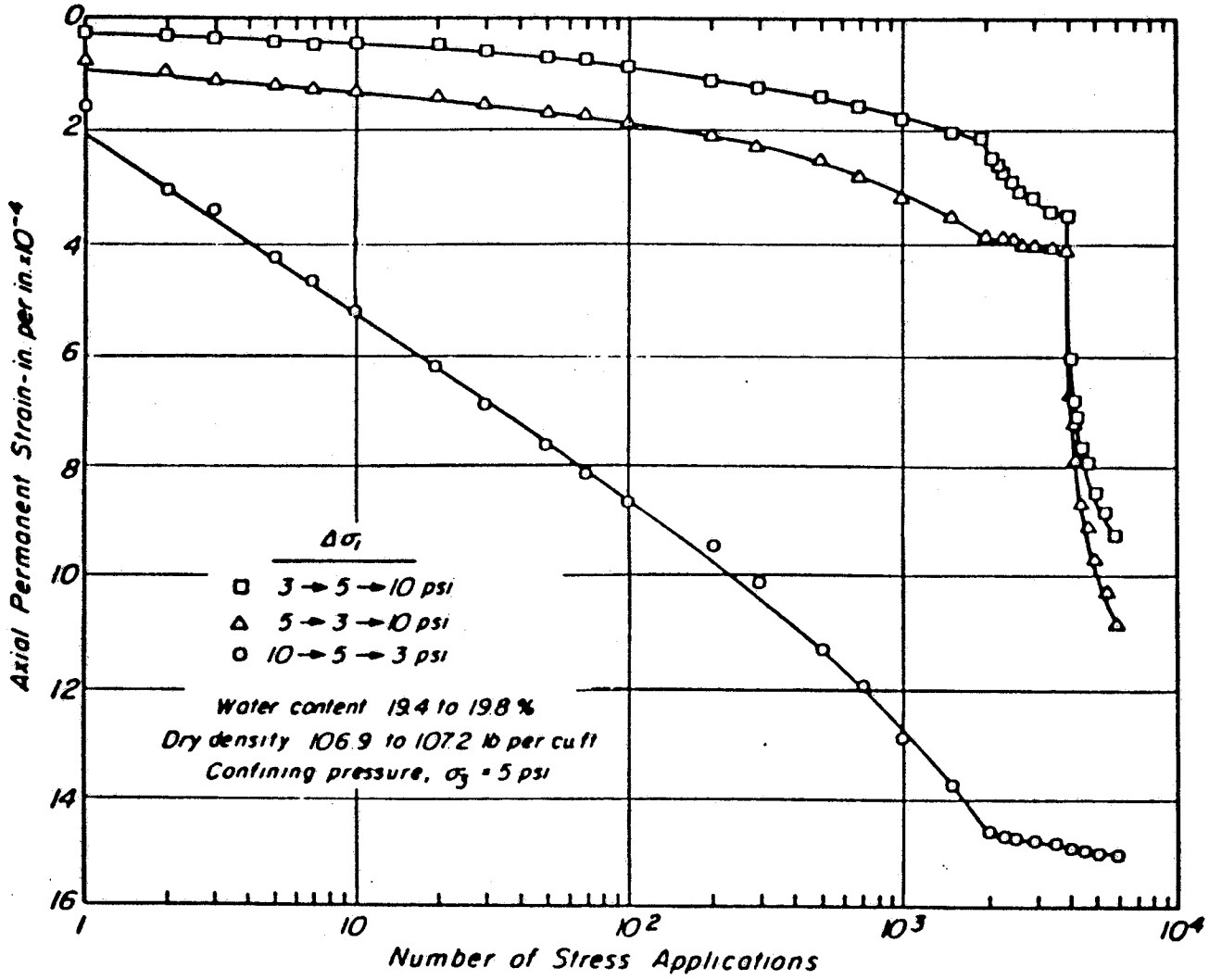

FIGURE 11 Effect of stress sequence on permanent strain—silty clay (20)

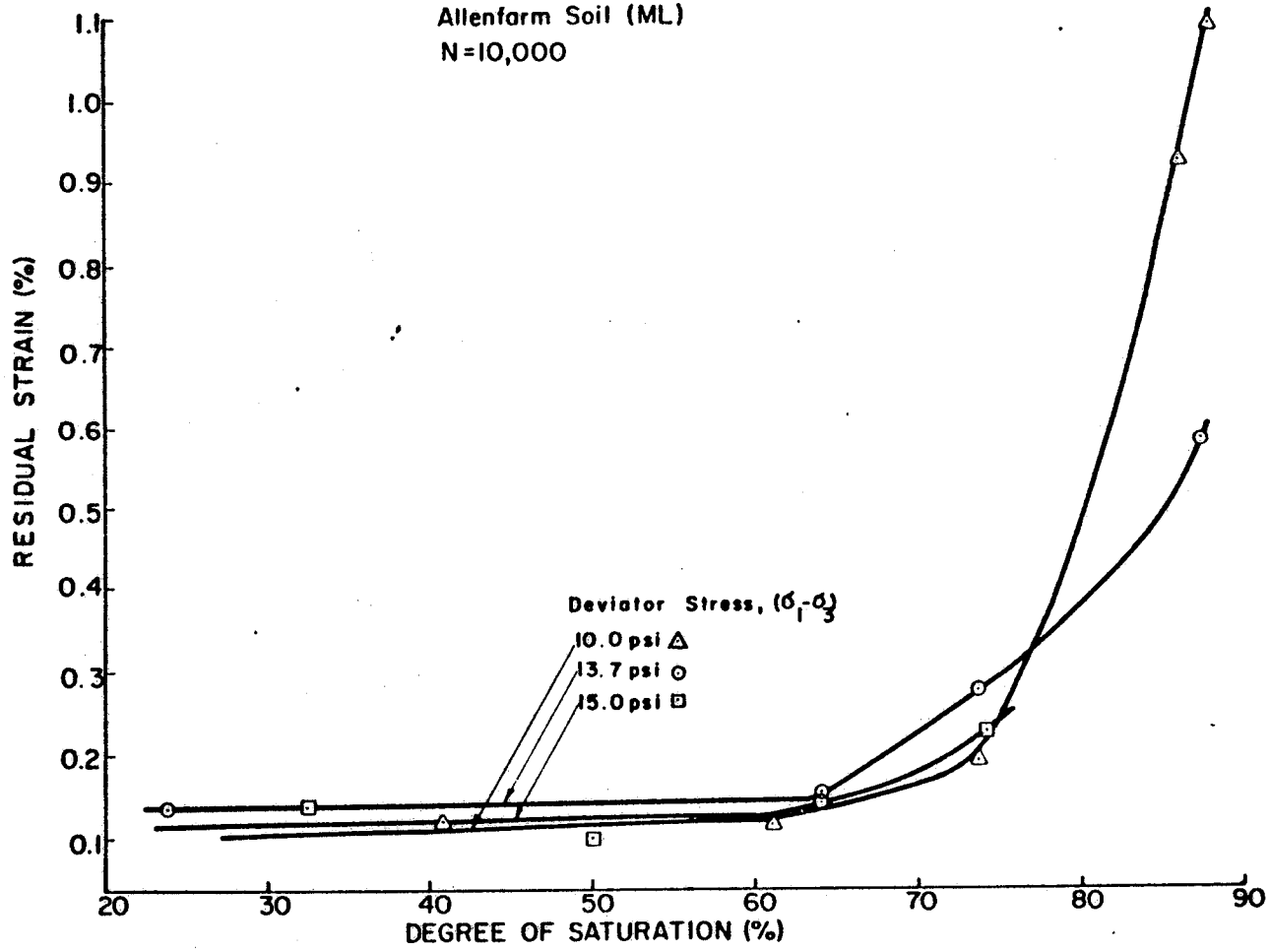

FIGURE 12 Variation of residual strain with moisture content—silt (22)

log-log plot between the permanent strain per cycle and the number of cycles stayed the same, while there was a large increase in the intercept (A) (Figure 13).

Fines Content

Barksdale (18) found that the amount of fines have a significant influence on residual strain in granular materials. It was observed that the residual strain increased greatly with the increase in fines at high deviator stress levels (Figure 14). Edris and Lytton (22) used three different subgrades with the percent passing #200 sieve at 72, 71 and 91, and with the clay contents (minus 2 micron size) at 20%, 39% and 70% respectively. Even though the effect of the clay content was not shown separately, it was noted that a soil of high clay content would have higher residual strains.

F. Prediction of Rutting in a Pavement

Rutting in a pavement is regarded as a major safety hazard and is also a cause for further deterioration of the pavement. Hence, it will be advantageous to limit the amount of rutting that can occur during the service life of a pavement. Two different approaches are identified in this regard (36). The first assumes most of the rutting is caused by permanent deformation in the subgrade layer and limits the vertical compressive strain at the surface of the subgrade with the aim of controlling residual strain (37, 38). This can be considered primarily a design oriented technique, where the magnitude of the compressive strain at the surface of the subgrade can be controlled by an appropriate selection of materials and layer thicknesses and also by appropriate construction techniques. It has a disadvantage because one cannot predict the amount of rutting using this method. The other approach aims to estimate or predict the amount of rutting that will occur as a function of time or traffic loadings. First, permanent deformation behavior of each material layer is estimated or measured with regard to its dependency on the compressive stress. The layered elastic or viscoelastic theory is used to estimate the stress distribution. The total amount of rutting is then calculated by considering the contributions from each layer in the system. Since the aim of this study is mainly to predict rut depth, the latter approach will be discussed in detail as to identify an appropriate methodology in combining permanent deformations in individual layers into rutting in the whole system.

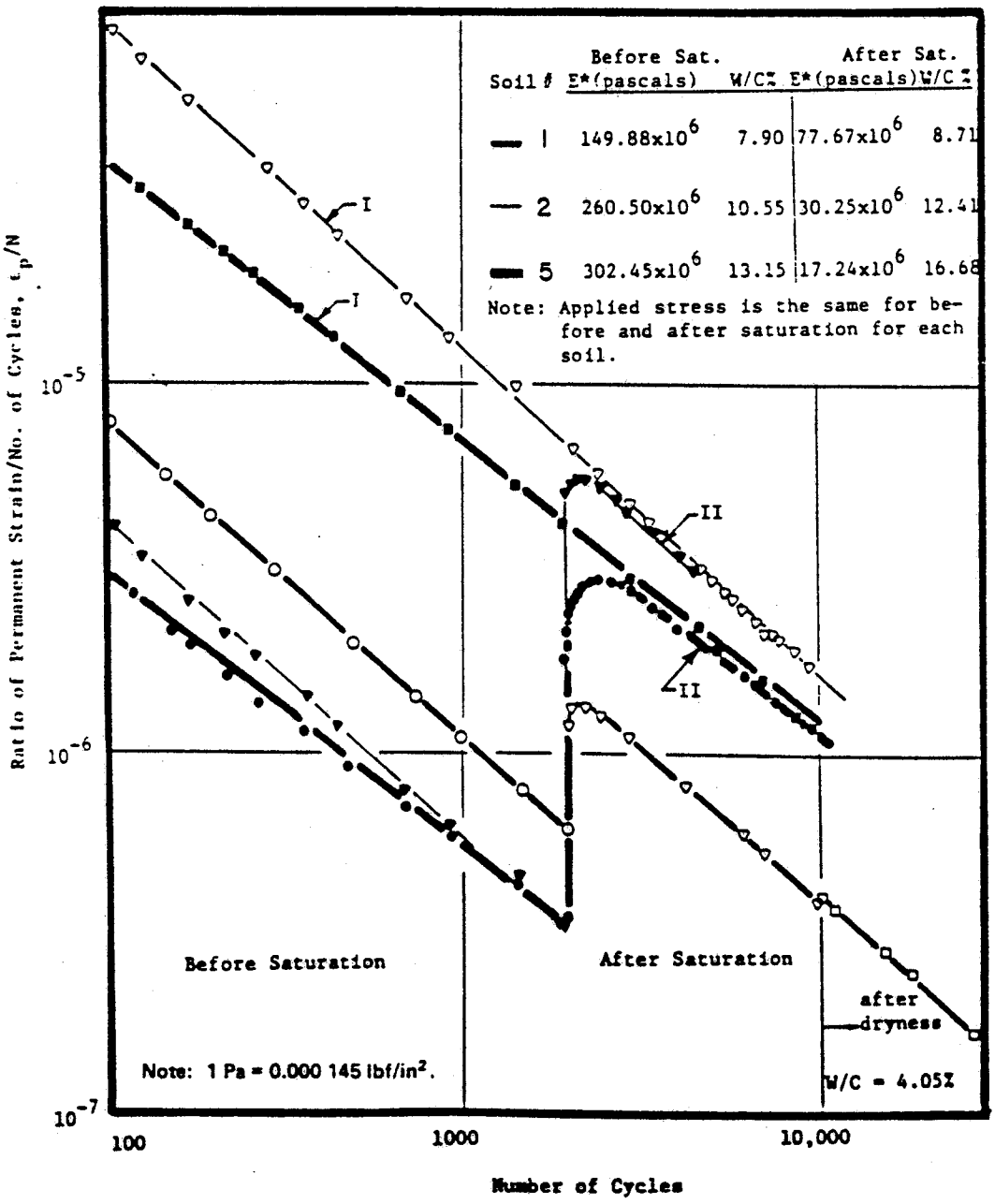

FIGURE 13 Effect of saturation on residual strain—clay (32)

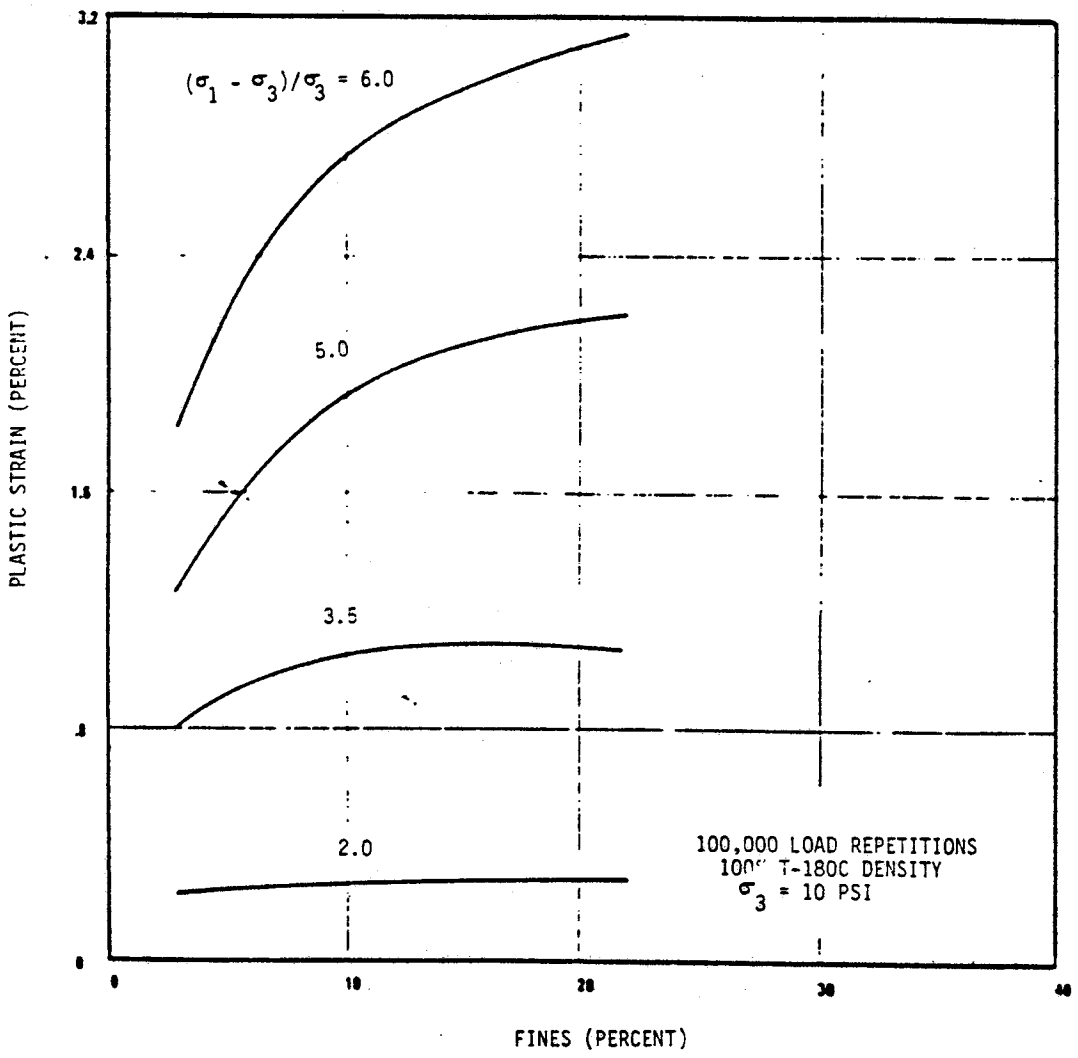

FIGURE 14 Influence of fines on residual strain—granular materials (18)

Method of Superposition

In the more widely used method employing the latter approach, each material layer is divided into a number of sublayers and, the stress states (σ_{ij}) in each of these layers are estimated using the layered theory. The permanent strain and hence the permanent deformation at each sublayer can then be estimated using the relationship $\epsilon_p = f(\sigma_{ij})$. As mentioned before, for different materials, different relationships between the permanent strain and the applied stress have been proposed (18, 20). Total rutting at the surface is calculated as the summation of permanent deformation in all of the sub-layers. This method, which will be identified hereafter as the method of superposition, had been used to predict rutting in either a portion of, or the total pavement structure by Barksdale (18), Kenis (29), Majidzadeh and others (32), Khedr (34) and Tseng and Lytton (35).

Mechano-lattice Program

Yandell (39, 40) used a different approach to the problem of combining different subsystems in the pavement. His MECHANO-LATTICE program (40) considers a layered pavement as a three-dimensional assembly of numerous cube-shaped units (Figure 15). Semi-infinite subgrade is represented by one layer of cubic units by the use of influence factors developed from Boussinessq theory. Each cubic unit has 28 spring-like elements (Figure 16) which allow simulation of not only axial strains, but also shear as well as volumetric strains. Each element in a unit is assumed to behave like an energy-absorbing material under loading and unloading by an elasto-plastic mechanism (Figure 17). The slope of the unloading path of the stress-strain curve, which is referred to as the unloading modulus, is calculated based on the permanent deformation behavior and the state of stress in the modeled pavement layer. This three-dimensional assembly of units, connected by frictionless joints at the ends, is loaded by a traveling wheel load (Figure 18). When the wheel approaches a unit in the assembly—or to be exact, when the assembly of units is moved towards the wheel, as done in the calculations—the elements of each unit will experience loading or unloading, depending on whether the strain is tensile or compressive, and whether it is increasing or decreasing. The stresses in elements are continually changing as the unit moves under and away from the wheel. Beyond the influence of the wheel, the elements recover most of the energy by rebounding, but the residual strains in

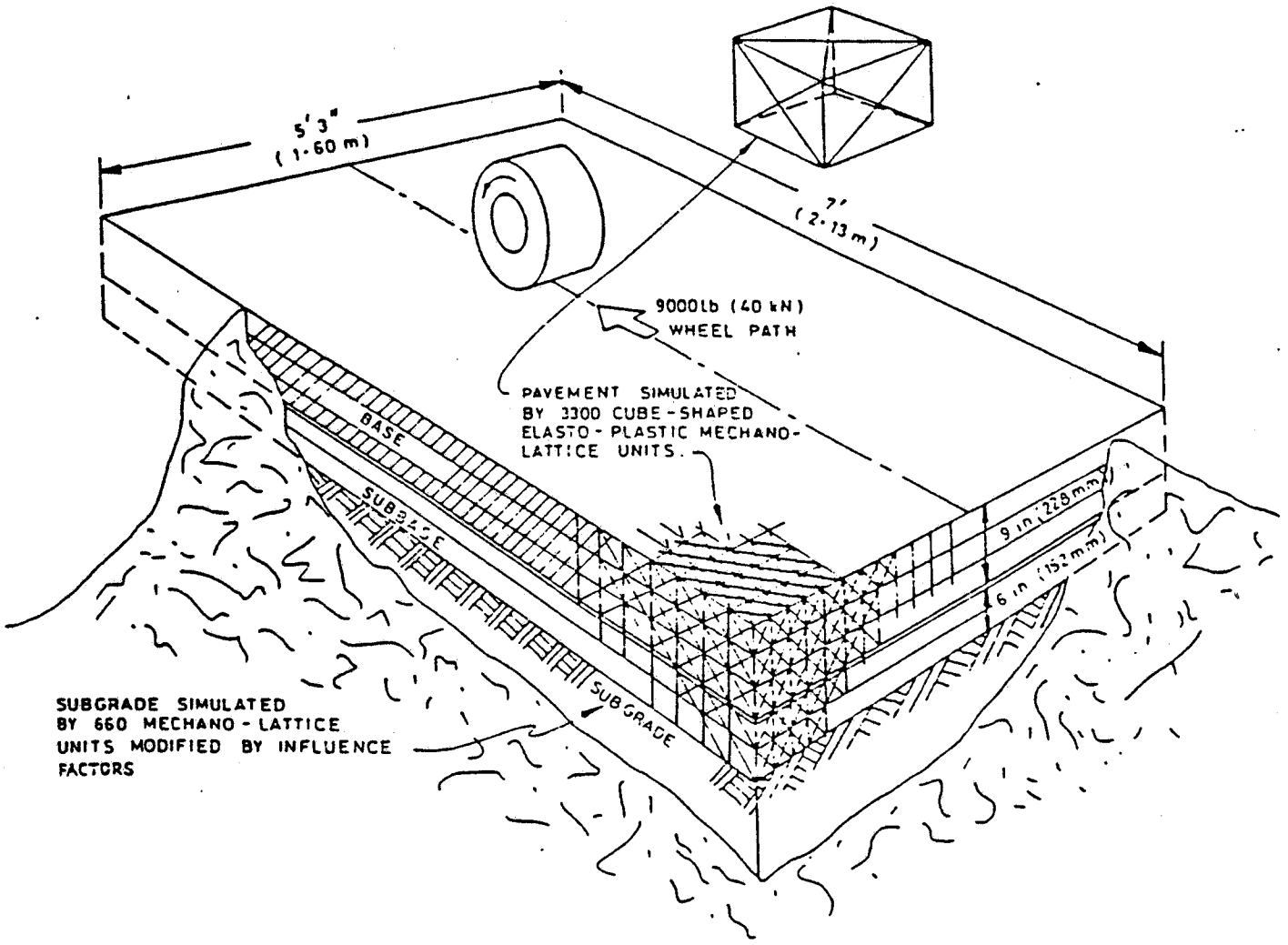

FIGURE 15 Assembly of Mechano-lattice units to simulate a pavement (40)

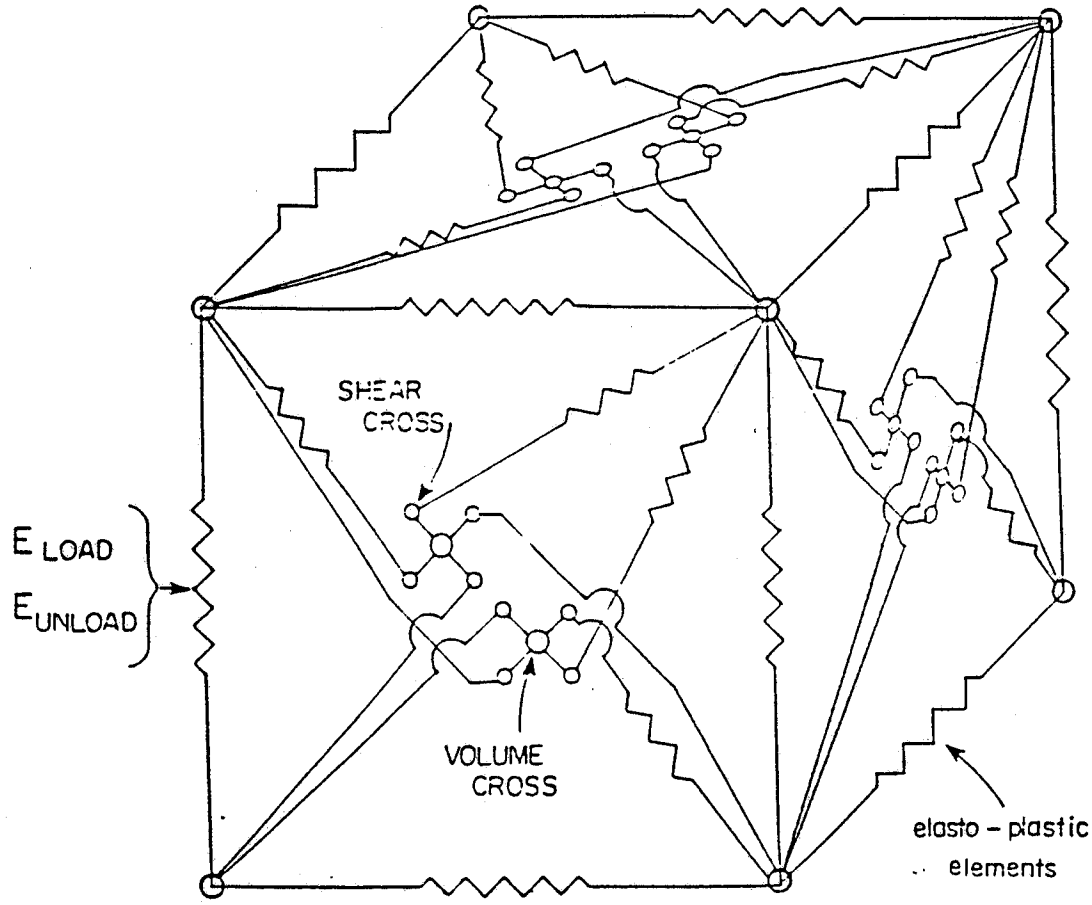

FIGURE 16 Approximate analogue of a Mechano-lattice unit (40)

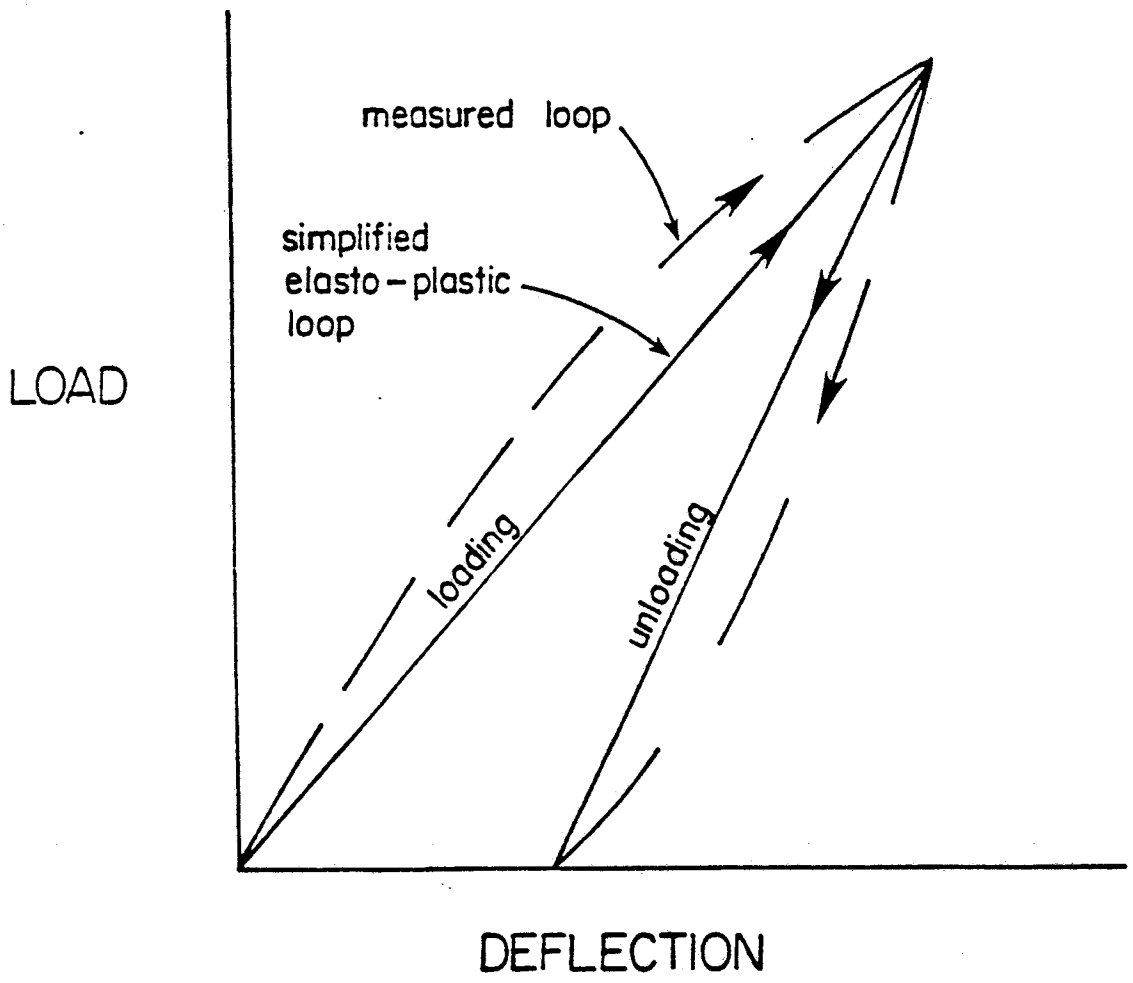

FIGURE 17 Simplified elasto-plastic behavior of a Mechano-lattice element (40)

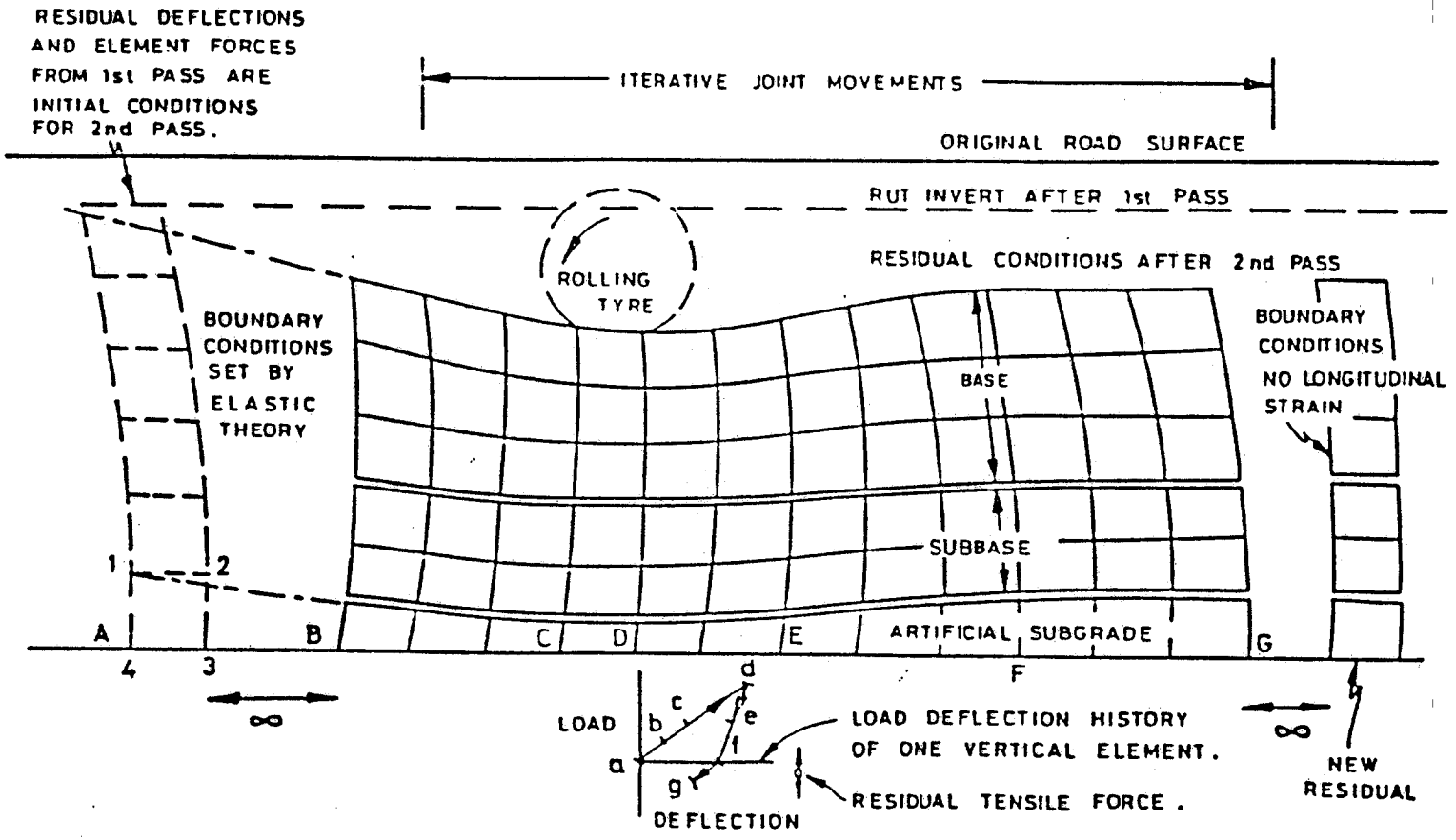

FIGURE 18 Simulation of a wheel load on a pavement (40)

each element will accumulate as residual deformation in the pavement. For the next pass of the wheel, the initial conditions in the assembly will be re-initialized to these stored residual stresses and strains.

Yandell claims (40) that the method of superposition ignores the interaction effects between elastic and plastic behavior in different material layers, and also the effects of a traveling wheel. The Mechano-lattice program has been used with the results from several test track experiments and has been shown to give acceptable predictions (39, 41). Figure 19 shows the Mechano-lattice-predicted and the measured rutting profiles at the Sydney test track. Figure 20 compares the predicted and the measured absolute rut depths at the same test site. Figure 21 shows comparisons of the rut depths predicted by the VESYS and the Mechano-lattice program against the measured values at the Pennsylvania State University test track.

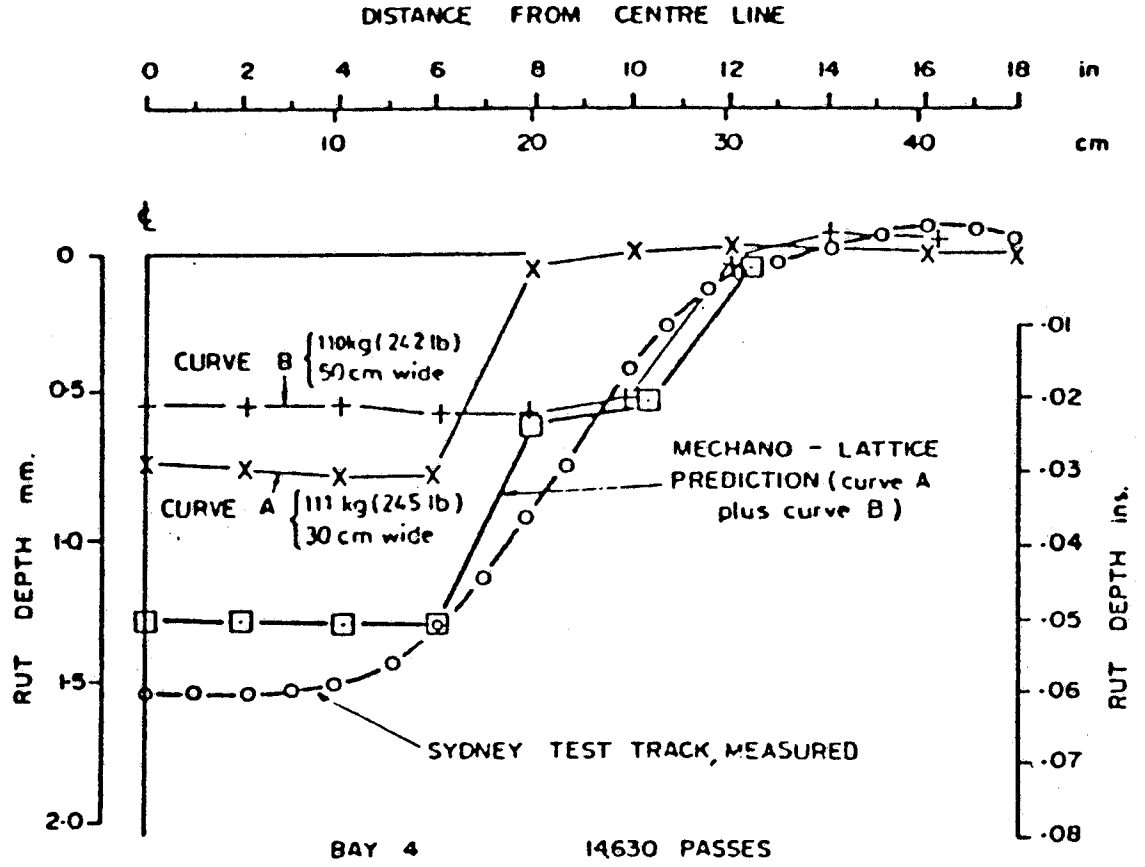

FIGURE 19 Comparison of rutting profiles after 14,630 wheel passes (41)

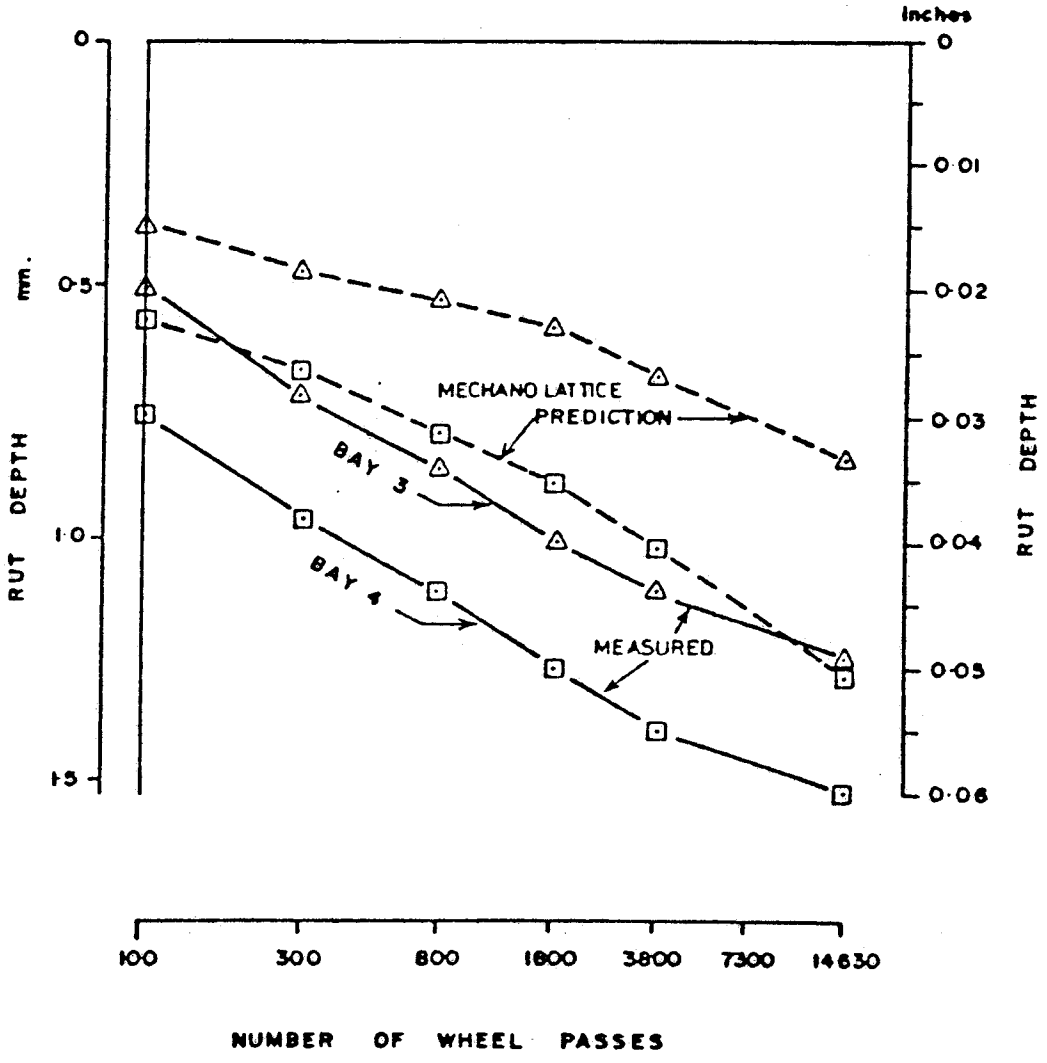

FIGURE 20 Comparison of absolute rut depths after 14,630 wheel passes (41)

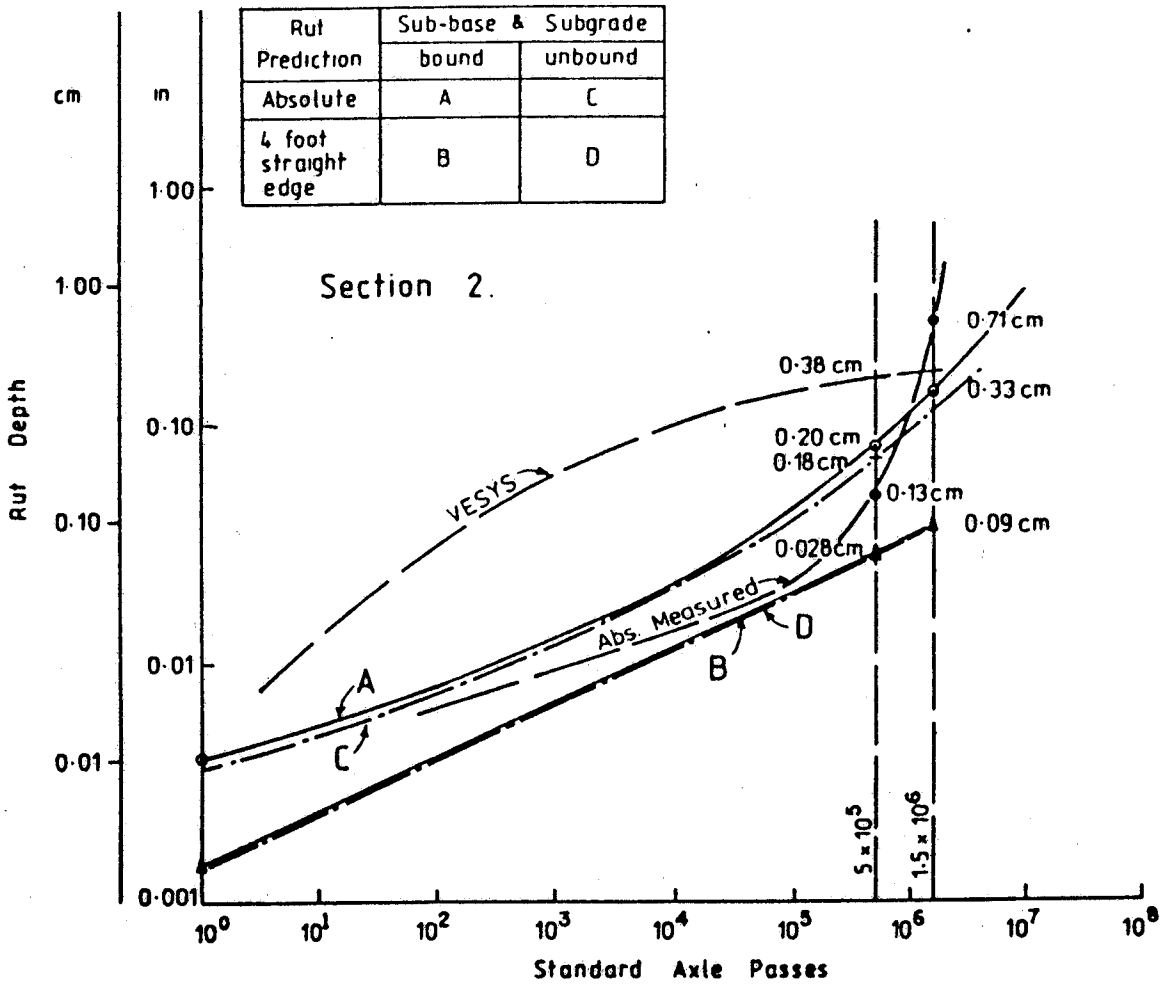

FIGURE 21 Comparison of VESYS and Mechano-lattice rut depth predictions (39)

CHAPTER III

FIELD AND LABORATORY TESTING

This chapter describes the selection process of the test sites, sampling techniques and the laboratory test procedures used in the study. Laboratory test procedures are discussed in detail, with the intention of properly simulating the field conditions in the laboratory. Investigations and suggestions by other researchers are used to formulate a more suitable test procedure. The process of preparation of samples for testing is also described in the sections to follow.

A. Selection of Test Sites

Since this study is mainly concerned with the low-volume roads in the state of Texas, the test sites were chosen so that they include the different types of materials used as well as the different climatic conditions throughout the state. Districts 21, 11 and 8 were chosen and test sections were to be located in these districts. District 21 represents the southern dry land area, while District 11 is representative of the eastern wet lands in the state. District 8 was picked as it is representative of both the northern high lands with long winters and the western region with very dry climatic conditions. In the preliminary investigation, most of the low-volume roads in each of the three districts were tested using the FWD to select roads which are in satisfactory condition, in the sense that no major rehabilitation work should be needed in the next 5 to 10 years. FWD tests were made at half-mile intervals along the roads and the results were analyzed using the LOADRATE program, which, as mentioned before, was developed for evaluating low-volume roads. Two farm-to-market roads meeting the following criteria were selected from each of the districts.

1. The roads should not include either stabilized base or subbase because the use of either is not common in low-volume roads.

2. Subgrades are to include a sandy soil and a clayey soil.

3. Modulus values of the pavement layers should be consistent throughout for at least a two-mile long stretch.

4. The base course thickness should remain the same throughout the section.

After selecting the test roads (Table 2), each was tested at a closer interval with the FWD to find a suitable location with consistent responses.

B. Field NDT Testing and Sampling

At each test site, a 100-ft. long section was marked and the FWD test was performed at 10-ft. intervals along the outer wheel path. At the midpoint of the 100-ft. section, a 2-ft. long and 2-ft. wide pit was dug and base course materials were retrieved. At the level of the subgrade layer, core samples were retrieved using 2.81-in. diameter Shelby tubes. Sampling was made to a depth of 8 to 10 feet or until the water table was reached. The moisture contents and the density measurements were obtained using a nuclear density gage. Later, in the laboratory, the soil samples were extruded "undisturbed" from the Shelby tubes, sealed with wax and stored in a 95% constant humidity room until the time of testing.

C. Laboratory Test Procedure

Selecting Appropriate Loading Conditions

A major limitation of the triaxial test is that the stresses can be applied only along the principal directions of a test specimen. Furthermore, two of the three principal stresses are necessarily equal because of the axial symmetry of the arrangement. However, the stress distribution at a point in a pavement is much more complex. The triaxial test can reproduce the stresses only at a point directly under a uniform axisymmetric load (15). Even at such a point, tensile stresses as well as rotation of the principal axes may occur under a moving wheel load (42). After successfully introducing tensile loads together with a 90^0 rotation of principal axes on a triaxial specimen, McVay and Taesiri (42) found that the stress path has a pronounced effect on the resilient modulus at low confining pressures. Sousa and Monismith (43) developed an innovative way of applying a predetermined stress path, axial as well as torsional loads with rotation of principal axes, on a hollow cylindrical sample. These techniques are still at the preliminary stages of development and are very expensive to apply. Allen and Thompson (44) used cyclic confining pressure, instead of keeping it constant as practiced conventionally. It was found that the change in the response was not significant enough to warrant the use of the complicated procedure of varying the confining pressure.

TABLE 2 SELECTED LOW-VOLUME ROADS AND TEST SITES

District	Road	Location
8	FM 1235	MP 21.0
	FM 1983	MP 1.0
11	SH 7	MP 7.8
	FM 2864	MP 6.5
21	FM 186	MP 33.2
	FM 491	MP 6.1

Since the applied state of stress is very influential in both the resilient and the residual strain of a specimen, the correct choice of the deviator and the confining stress is very important. The stress states suggested in the standard procedures (16, 17) are typical for a thick pavement. However, these stress values appear to be too low for use on materials from a low-volume road, because of the lack of a thick and strong asphalt concrete layer which distributes the load and reduces the stress. As such, it was decided to employ loading conditions that are representative of the actual situation in a surface-treated pavement. The CHEVDEF elastic layered program was used to calculate the stress distribution in such a pavement under a standard 9,000 lb. wheel load. A wide range of possible resilient modulus values were assumed for the base and the subgrade, and several different base thicknesses were also used in these calculations. A one-inch thick asphalt layer with a low resilient modulus of 30,000 psi was used to represent the surface treatment in every case. This produced a range of vertical and horizontal stresses, to which the base course and the subgrade would be subjected, under a standard single wheel load (Table 3). After comparing these values with the stress states suggested in the standard procedures as well as those that were used by other researchers, a suitable set of deviator and confining stress levels were chosen for the laboratory tests (Table 3).

In performing the resilient modulus test, the lowest deviator stress and the highest confining pressure were applied first, and the responses were recorded at the end of 200 cycles. The confining pressure was then reduced to the next level and the process was repeated. For subgrade samples all the stress combinations were used. However, for the base course samples, all the confining stress levels were used only with the lowest deviator stress level. With the increase of the deviator stress to the next higher level, the current lowest confining stress was left out to avoid subjecting the sample to unusually high stress ratios. This resulted in only 15 stress combinations.

It was decided to conduct only one permanent deformation test per test site per material layer (base course or subgrade). Deviator and confining stress combinations of 20 and 10 psi respectively were chosen for the base course samples, and 8 and 4 psi respectively for the subgrade samples. These stress combinations were within the probable range of the stresses in the field.

The actual shape of the loading pulse under a moving vehicle, measured by an accelerometer (4), strongly suggests that a sinusoidal input is more appropriate for loading the specimen. Some researchers had used continuous cycling of the deviator

TABLE 3 LOADING CONDITIONS FOR RESILIENT TESTING

Reference	Base course Materials		Subgrade Materials	
	Confining pr. (psi)	Deviator st. (psi)	Confining pr. (psi)	Deviator st. (psi)
AASHTO (16)	1,5,10,15,20	1,2,5,10,15,20	0,3,6	1,2,4,8,10
ASTM (17)	1,3,6	0.5,1,2,5,10	1,3,6	0.5,1,2,5,10
SR 162 (45)	1,3,5,..,15,20	1-75	1-5	0.5,1,2,..,10
HICKS (46)	1,2,3,..,30,50	3,5,10,..,30,35		
KALCHEFF..(19)	2,5,20	4,6,10,..,60,80		
EDRIS..(22)			3.5,15,20	10,13.7,15
TOWNSEND..(27)			2,4,6	2-21
CHEVDEF runs	1-11	42-50	0.5-2	6-12
Selected for This Study	1,5,10,20,30	10,20,35,45,60	1,4,8	2,5,8,12

load, but Brown (15) suggests that a short rest period between pulses would be required in order to accommodate any delayed elastic recovery in the specimen. The frequency of the load pulse being applied has been found to be not influential within the range of 10 to 80 rpm for granular materials (19). Similar results have been reported for cohesive materials (47). The deviator load pulse adopted for this test program was that of a sinusoidal shape with a loading and unloading period of 0.1 second and a rest period of 0.9 second. A servo-controlled Material Testing Systems (MTS) machine was used in the tests.

Preconditioning of the Specimens

The AASHTO (16) and the ASTM (17) standard procedures differ on the recommendations for preconditioning of the sample. AASHTO suggests applying each of the different deviator stresses 200 times while maintaining the maximum confining pressure in the chamber. ASTM, on the other hand, recommends applying only the smallest deviator stress 1200 times with the maximum confining pressure. Although no studies had specifically evaluated the effects of preconditioning, the investigations on the effect of stress history on resilient and plastic behavior of materials could serve as a guide. Kalcheff and Hicks (19) did not find any significant dependence of the sequence of loading on the resilient modulus values of granular materials. But as mentioned in Chapter II, the stress history has a significant effect on the residual deformation of both granular (19) and cohesive (20) materials. According to the AASHTO standard procedure (16), the purposes of sample-conditioning are to eliminate the effects of the interval between compaction and loading, to minimize the effects of imperfect contact between end platens and the specimen, and also, to eliminate the differences between initial loading versus reloading.

From a number of trials with undisturbed samples it was found that, if a higher deviator stress is applied during preconditioning, it may result in very high deformations. Thus it was decided to follow the ASTM procedure (17) in pre-conditioning all of the subgrade samples, most of which were undisturbed, in order to make comparisons on an equitable basis. For remolded base course samples, 200 cycles each of the combinations of the minimum deviator stress and the confining pressures were applied, starting with the highest confining pressure. In the permanent deformation tests sample conditioning was not done. To eliminate errors due to any imperfect contact between the end platens and the sample in that case, the initial reading was

recorded at the end of the first load cycle.

Measurement of Deformations

Both the AASHTO (16) and the ASTM (17) standard procedures suggest measuring axial deformations using two Linear Variable Displacement Transformers (LVDTs) mounted on the test specimen with clamps. AASHTO allows an exception in the case of softer specimens (resilient modulus less than 15,000 psi), in which case it suggests mounting the LVDTs externally, thus measuring between the platens. Brown (15) cautions against mounting the LVDTs on weak samples:

> it may introduce larger errors than those associated with external or overall measurement, unless very light equipment can be developed.

In such situations, he suggests using lubricated contacts (e.g., Silicon grease and a rubber membrane) between the platens and the sample in order to reduce errors in the measurement of overall deformation.

Before the actual test, several trials were conducted with LVDTs mounted on the undisturbed samples. It was found that the clamps used to mount LVDTs either restrict the lateral expansion of the sample if it is too soft or start to slip if the sample is too rigid. Thus, to maintain uniformity in measurements, it was decided to mount LVDTs from platen to platen (Figure 22) for tests on the subgrade samples. To reduce the end effects, two Teflon sheets with Graphite powder in between were placed at the top of the sample, which provided free lateral movement during loading. For the base course specimens, clamps could be fixed tightly around the specimen because of its rigidity, and they were placed at the middle half of the sample. The LVDTs were connected to a signal conditioner to process the output signal. In both test setups, an additional set of displacement measurements was made using another LVDT mounted at the top of the loading ram of the MTS machine. This reading may actually include errors due to any end effects and also, the probable elastic deformations of the loading ram itself. Even though this served as an extra measurement, calibration runs were made using an aluminum block in place of the soil sample.

Measurement of the Load

The positioning of the load cell to record the deviator load is also important (15). If the load cell is mounted outside the the triaxial chamber, friction between the load-

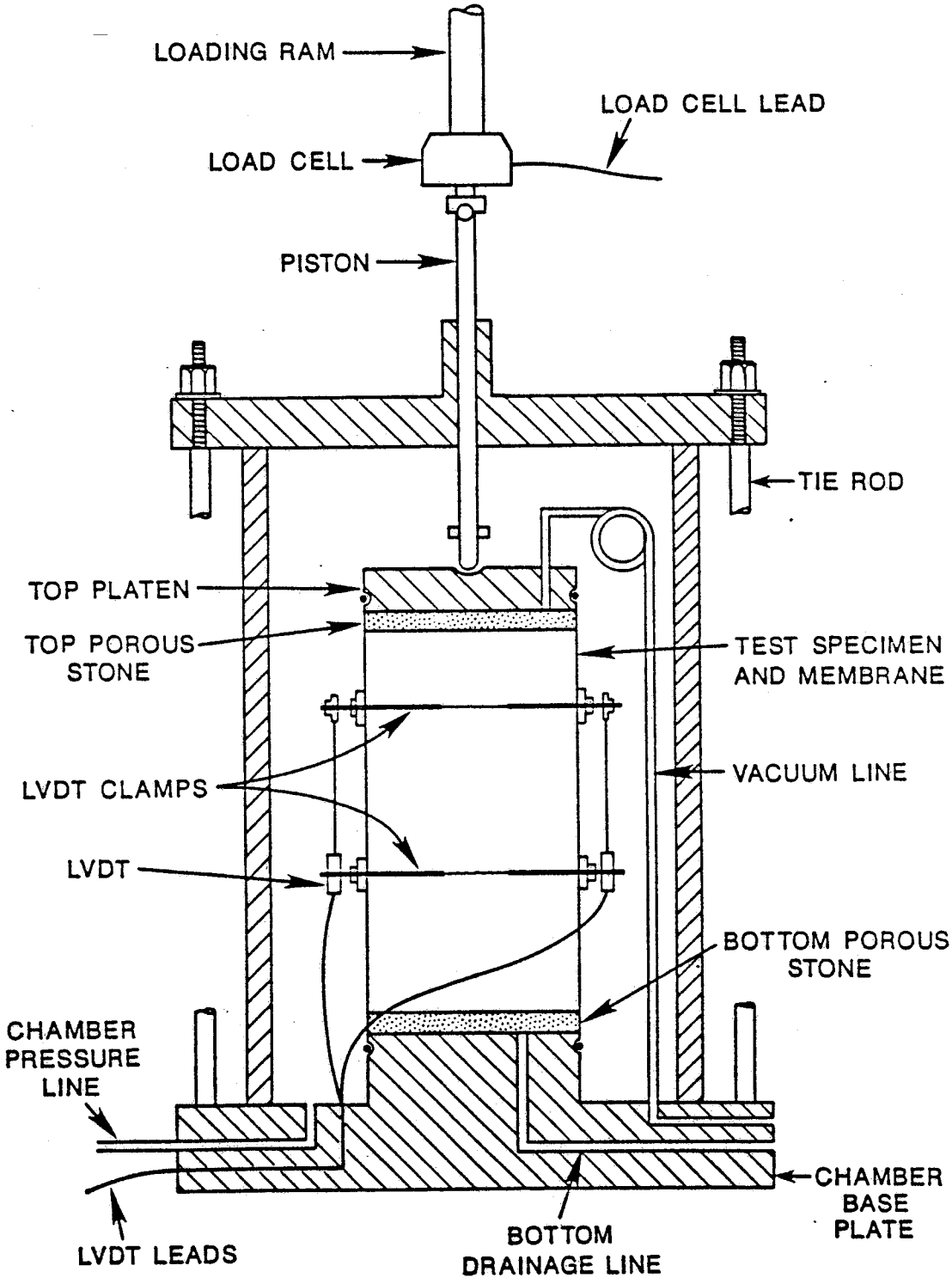

FIGURE 22 Schematic triaxial test setup for base course specimens

ing piston and the top of the chamber may cause inaccuracies in the load measurement. In the MTS machine available for the tests, the load cell had to be mounted externally. Therefore extra measures were taken to reduce friction at the loading piston.

Recording of the Output

Most of the published reports of the repeated load tests indicated that either the pen recorders or the Brush chart recorders were used for recording the output. During the trial runs, the pen recorder showed smaller peak input loads than the actual peak input which could be directly read off the machine. It was found that, the pen recorder was unable to respond as quickly as the input load pulse. The Brush chart recorder performed better, but it had a disadvantage in that the scales of recording did not allow a large enough output to avoid inaccuracies when values are read off the charts. The final choice was a computerized data acquisition system (Digital Minc-23) which allowed simultaneous recording from three channels. In the resilient modulus tests, 400 data points per cycle were recorded in order to obtain an almost continuous and smooth response curve (Figures 23 and 24). In the permanent deformation tests, data points describing one cycle were captured for every 500 cycles (Figure 25). The ability of the device to automatically set the gain allowed very accurate recording of data even when the signals were very small.

D. Preparation of Samples

Subgrade Materials

Before testing, undisturbed samples were trimmed to a diameter of 2.81 in. and to a height of about 6 in. A membrane was placed around the sample to prevent pressurized confining air from leaking into it. After placing the sample inside the triaxial chamber, the setup was tested for any leakage by applying a vacuum of about 5 psi inside the membrane. This vacuum was released after applying the initial confining pressure but before applying any deviator load. LVDTs were mounted with the help of clamps set up at the top and the bottom platens. Epoxy glue was used to prevent any slip between the clamp and the membrane.

Since sandy subgrades cannot be retrieved undisturbed, those samples were remolded using a 2.81 inch split mold and a vibratory table. While remolding, field

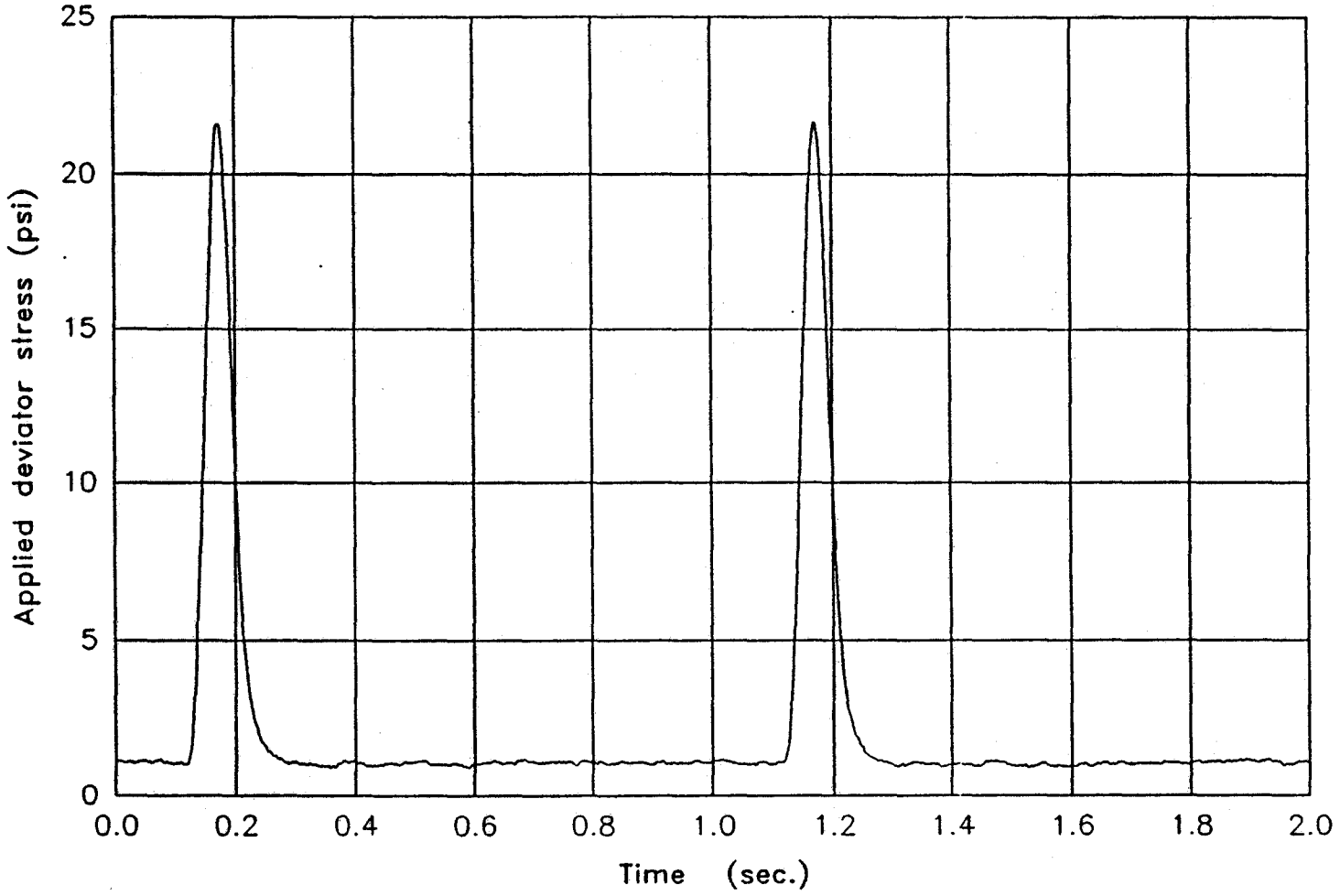

FIGURE 23 Typical plot of applied deviator load

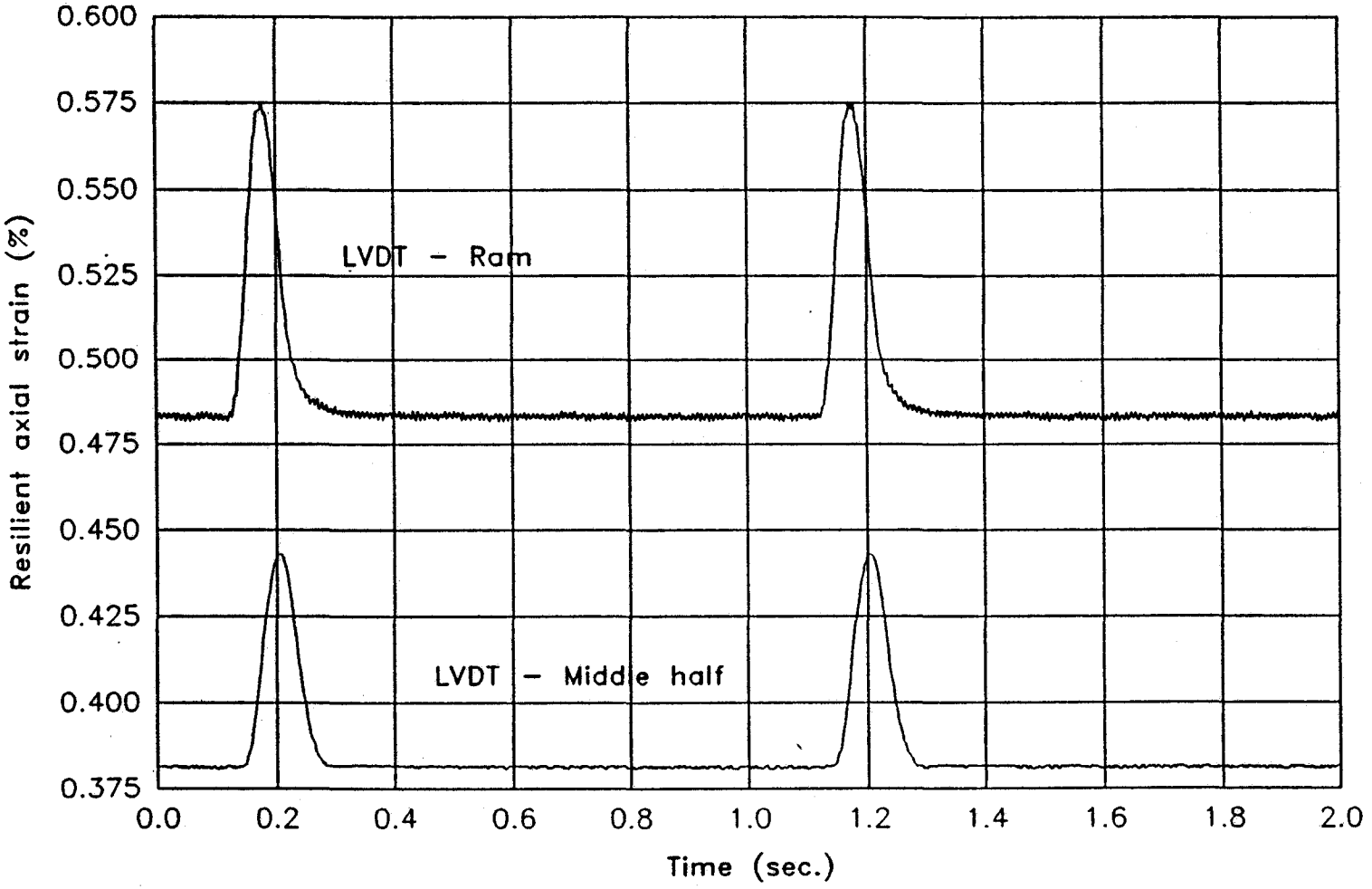

FIGURE 24 Typical axial resilient strain response—base course

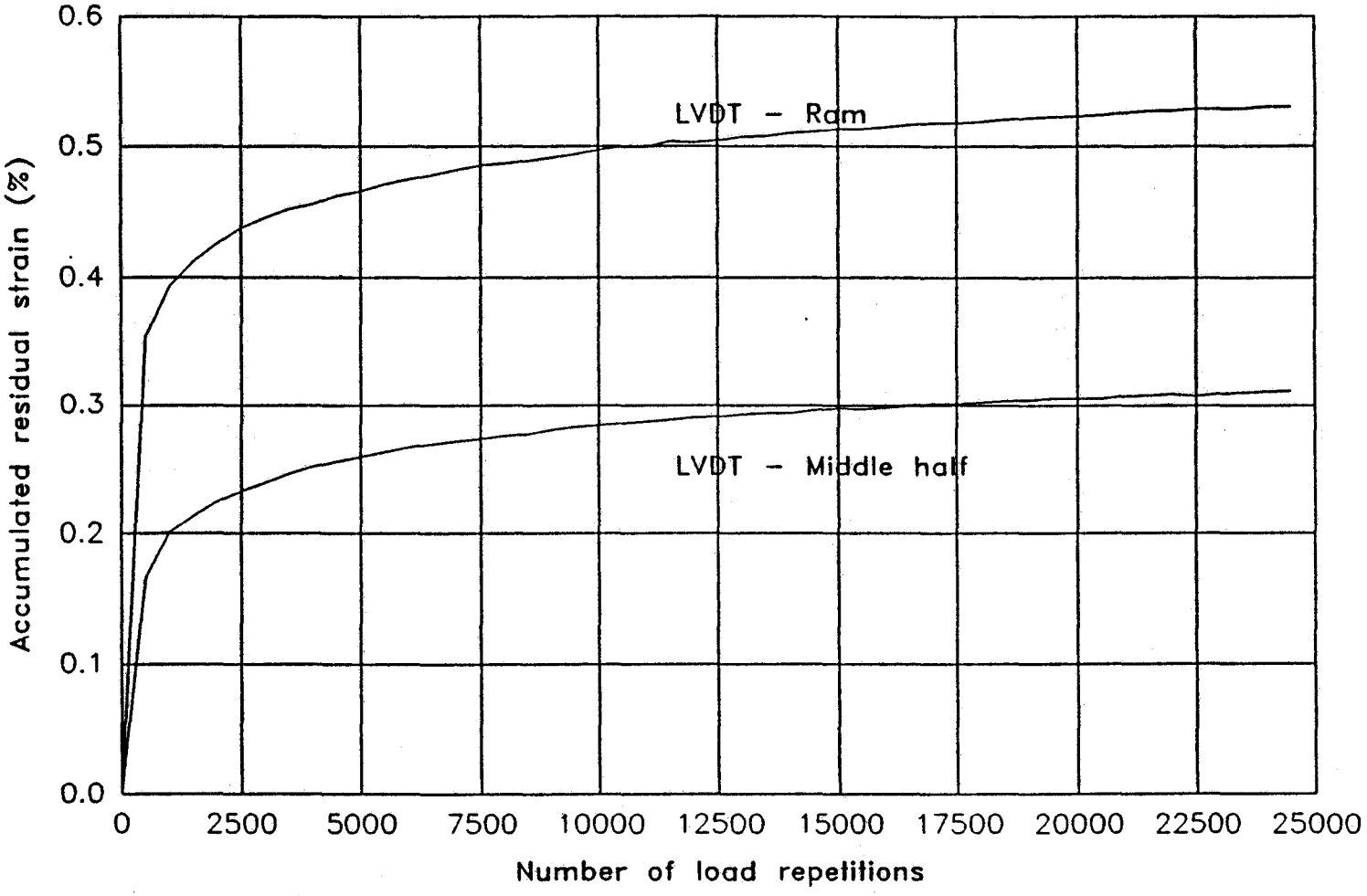

FIGURE 25 Typical plot of residual deformation—base course

measured density and moisture levels were reproduced as closely as possible.

Base Course Materials

All of the base course samples had to be remolded. Because the top size of the materials was about 1.5 in., it was decided to test cylindrical specimens of 6 in. in diameter and 12 in. in height. A special split mold was made for this purpose (Figure 26). A guide sleeve was provided at the top to keep extra loose material in place. A membrane was stretched inside the mold and a vacuum was applied to keep the membrane glued to the inside wall of the mold. Meanwhile, the amount of material sufficient to give the field measured unit weight in the mold was weighed and thoroughly mixed with the appropriate amount of water in order to achieve the field measured water content. After several trial runs, the number of material lifts required to obtain the density was determined. Only the exact amount of material needed for each lift was poured into the mold. The surcharge load, a steel cylinder weighing 126 lbs, was lifted by a small crane and placed on the material. Vibration was kept on until the material was compacted down to the required height for that lift. Once a lift is completed, the surcharge is removed and the top of the material is scarified. Material for the next lift is then placed and the next stage of vibration is begun with the surcharge load in place. When the final lift is completed, the top surface is made smooth and the top porous stone and the top platen is placed. Since the original membrane gets damaged frequently during compaction, a second membrane is stretched over the sample. To prevent high pressure air from leaking inside the specimen, both platens had to be grooved and the grooves are filled with high vacuum silicon grease before placing the membranes and the O-rings. A full vacuum is then applied to check for leaks in the system. LVDTs are then setup in the middle half of the sample using aluminum clamps. Because of the rigidity of the base course samples, stronger springs can be used on the clamps to secure them onto the sample wall.

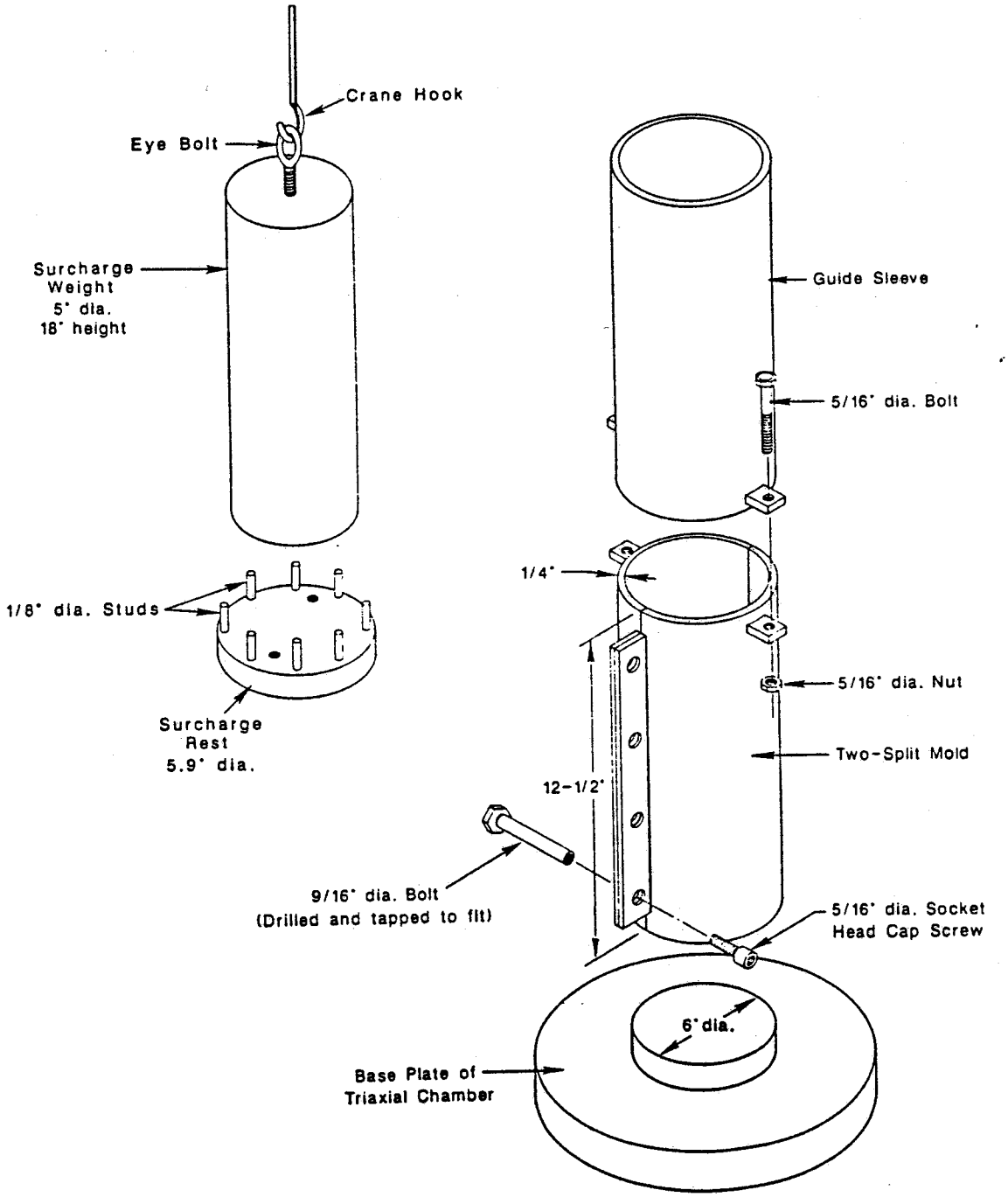

FIGURE 26 Assembly of apparatus for remolding base course samples

CHAPTER IV

TEST RESULTS AND ANALYSIS

Resilient modulus values of the pavement layers at test locations, estimated by field NDT techniques, are compared in this chapter with the modulus values measured in the laboratory. The FWD responses were analyzed with the computer programs LOADRATE (10) and BISDEF (48). The PDCP results were interpreted through another computer program (12). Permanent deformation characteristics of each of the pavement material layers were also examined in the laboratory and are presented in this chapter. A linear relationship on a log-log plot between the accumulated permanent strain and the number of load repetitions is employed to analyze the data. Permanent deformation properties of many different materials, as reported by other researchers, are also presented in order to characterize rutting behavior according to the material classification. It is shown that the subgrade materials can be categorized into three broadly defined groups based on their rutting behavior. A method is proposed which can identify the rutting parameters 'a' and 'b' of a pavement material, when the material classification and the resilient modulus are known.

A. Verification of NDT Predictions of Resilient Moduli

Resilient modulus tests were performed on all of the base course and subgrade samples retrieved from the six test sites. The material classifications and the other characteristics of the samples are given in Tables 4 and 5. As described in Chapter III, the resilient modulus of a specimen was measured under various stress states. The complete set of resilient test data are given in Appendix A. Table 6 presents a summary of the laboratory test data for the purpose of comparison with NDT predictions. It considers only those modulus values that were measured under the stress states representative of those at the middle of the base course layer, or in the top 6 to 12 inches of the subgrade layer at the corresponding test site. The subgrade test data considered for the comparison are from the samples retrieved within the top 1 to 1.5 feet of the subgrade layer. Out of the many remolded base course and subgrade specimens, test results from only those specimens which closely represent the field conditions were selected for comparison.

The FWD responses were analyzed using the LOADRATE (10) and the BISDEF (48) computer programs. The range of the resilient modulus value at a test site,

TABLE 4 CHARACTERISTICS OF BASE COURSE SAMPLES

Sample	Location	Material	Classification AASHTO	Unified	Top Size (in)	% Pass. #200	Density (pcf) In-situ	Lab.	MC %	Type of Test*
D21/FM491										
BE0	#5	Calcite	A-1-a	GW	1.5	4.0	113.0	106.7	11.3	1
BE1	#5	Calcite	A-1-a	GW	1.5	4.0	113.0	106.7	10.2	1
BERT	#5	Calcite	A-1-a	GW	1.5	4.0	113.0	117.2	12.0	3
D21/FM186										
BC0	#6	Calcite	A-1-a	SP-SM	1.5	7.0	101.2	101.5	10.0	1
BC1	#6	Calcite	A-1-a	SP-SM	1.5	7.0	101.2	104.9	12.5	1
BCRT	#6	Calcite	A-1-a	SP-SM	1.5	7.0	101.2	107.0	14.8	2
D8/FM1983										
BA1	#5	Grav. w/Li.	A-1-b	SW	1.5	5.0	127.6	121.6	7.8	1
BART	#5	Grav. w/Li.	A-1-b	SW	1.5	5.0	127.6	122.1	5.6	2
D8/FM1235										
BD0	#5	Cru. Lime.	A-1-a	GP	1.5	3.0	126.5	105.9	4.8	1
BD1	#5	Cru. Lime.	A-1-a	GP	1.5	3.0	126.5	110.8	1.0	1
BDRT	#5	Cru. Lime.	A-1-a	GP	1.5	3.0	126.5	125.8	6.1	3
D11/FM2864										
BB0	#3	Iron Ore Gr.	A-1-b	SW-SM	1.0	11.0	125.3	119.2	7.6	1
BB1	#3	Iron Ore Gr.	A-1-b	SW-SM	1.0	11.0	125.3	122.7	8.9	1
BB2	#3	Iron Ore Gr.	A-1-b	SW-SM	1.0	11.0	125.3	129.9	11.0	1
BBRT	#3	Iron Ore Gr.	A-1-b	SW-SM	1.0	11.0	125.3	130.3	10.5	2
D11/SH7										
BF0	#4	Iron Ore Gr.	A-1-b	SP-SM	1.5	7.0	144.9	123.0	4.6	1
BFRT	#4	Iron Ore Gr.	A-1-b	SP-SM	1.5	7.0	144.9	146.5	7.7	3

* Test Type -
1 - Resilient Test only
2 - Rut Test only
3 - Both Resilient and Rut Tests

TABLE 5 CHARACTERISTICS OF SUBGRADE SAMPLES

Sample	Location	Material	Classification AASHTO	Unified	Depth (ft)	LL/PI	% Pass. #200	Density (pcf) In-situ	Density (pcf) Lab.	MC %	Type of Test*
D21/FM491											
P0	#7(top)	Dark	A-6	SC	1.00	30/18	41.5		93.5	16.5	1
M0	#8(top)	Brown	A-6	SC	1.50	34/17	40.5		102.0	16.9	1
F0	#10(top)	Clayey	A-2-6	SC	3.50	36/23	16.3		102.0	19.8	1
RUT02	#8(bot)	Sand	A-6	SC	2.00	26/17	43.0		119.5	20.7	2
D21/FM186											
H0	#8(bot)	Dark Br.	A-2-6	SC	1.00	29/19	21.0		100.0	16.3	1
K0	#9(bot)	Clayey	A-6	SC	1.50	26/16	40.0		102.0	16.3	1
RUT03	#12(bot)	Sand	A-2-6	SC	5.50	31/20	31.5		125.8	20.2	2
D8/FM1983											
S1	#7,9,10	Red. Br.	A-2-4	SP-SM	1.50	19/-	11.5	91.0	104.7	14.4	1
S3	#7,9,10	Silty Sand	A-2-4	SP-SM	1.50	19/-	11.5	91.0	113.8	13.5	1
RUT05	#11	RB Cl. Sand	A-2-6	SC	4.50	25/16	27.0		124.4	12.7	2
D8/FM1235											
I0	#8(top)	Dark Br.	A-6	CL	1.25	37/17	64.0		126.0	20.6	1
L0	#8(bot)	Loamy	A-7-6	CL	2.00	41/25	67.2		127.0	19.4	1
G0	#9(top)	Clay	A-7-6	CL	2.50	42/24	44.4		127.0	18.3	1
RUT01	#13(top)	Yell. Br. Clay	A-7-6	CH	8.50	43/31	58.0		128.0	18.2	2
D11/FM2864											
O0	#5	Grey. Clay w/ RB Grav.	A-7-6	CH	1.50	86/70	75.0		110.0	34.6	1
U0	#8(top)	Yell. Clay	A-7-6	CL	4.00	42/28	45.8		125.1	13.3	1
E0	#8(bot)	w/ RB Grav.	A-7-6	CL	6.75	44/23	49.9		107.0	22.2	1
N0	#9(top)	Grey. Clay w/ RB Grav.	A-7-6	CH	7.25	78/61	73.0		106.0	30.1	1
RUT04	#10	Yell. Clay	A-7-6	CH	11.50	43/33	58.0		123.7	20.2	2
D11/SH7											
T2	#5	Light Br.	A-2-4	SP-SM	1.25	18/-	4.8	113.0	109.4	7.8	1
T1	#6	Silty	A-2-4	SP-SM	1.75	17/-	11.7	113.0	109.5	5.4	1
RUT06	#5	Sand	A-2-4	SP-SM	1.25	18/-	4.8	113.0	109.7	7.0	2

* Type of Test - 1 - Resilient Test only
2 - Rut Test only

TABLE 6 COMPARISON OF FIELD AND LABORATORY RESILIENT MODULI

Site	Material	Resilient Modulus (ksi)			
		LOADRATE	PDCP	BISDEF	Lab Tests
FM 491	Base	25.8-39.9	43.4-48.3	24.4-33.5	22.6-42.0
	Subgrade	5.3	9.5-13.2	6.9- 7.6	7.4-10.6
FM 186	Base	36.3-55.8	41.8-46.1	29.0-39.6	14.0-28.8
	Subgrade	5.4	16.0-21.3	9.4-10.4	7.6-12.3
FM 1983	Base	58.4-85.4	39.6-42.0	35.0-44.9	27.4-48.7
	Subgrade	7.1-10.1	31.3-32.1	17.4-20.2	21.1-25.0
FM 1235	Base	51.2-83.6	62.3-69.1	34.6-42.8	41.3-61.4
	Subgrade	6.0- 7.2	8.9-12.0	13.7-14.8	9.0-14.2
FM 2864	Base	11.1-17.3	38.0-46.0	15.0	25.1-38.8
	Subgrade	9.6-12.6	20.0-24.0	16.5-20.5	11.2-15.2
SH 7	Base	56.5-71.0	57.0-75.0	44.9-49.4	25.2-43.8
	Subgrade	5.5- 5.9	42.0-55.0	13.0-17.4	44.7-59.5

shown in Table 6 incorporates modulus values backcalculated from FWD readings at five test stations, each 10 ft. apart with the middle one at the location of the test pit. The PDCP test was performed only at the location of the test pit. The computer program used to analyze the PDCP data predicts the modulus values at any point of the depth of penetration (12). Table 6 includes the range of resilient modulus values close to the middle of the base course layer and in the top 6 to 12 inches of the subgrade layer.

The PDCP seems to be the most consistent out of the three NDT techniques in predicting the resilient modulus of the base course layer. Its predictions of moduli were either within the range of the laboratory measurements (FM 1983), or varied within a narrow range near the upper limit of the laboratory-measured values (FM 491, FM 1235 and FM 2864). Exceptions were FM 186 (varied in a narrow range above that of laboratory measurements) and SH 7 (where the variation was unusually high), but still the predictions were on the high side of the measured modulus values. This trend compares well with the comparatively low stress state produced in the pavement by the PDCP. The BISDEF predictions of the modulus of the base course were within the laboratory measured values at three test sites (FM 491, FM 1983 and FM 1235), and for two other sites, predictions were not too far away. However, at FM 2864, it failed to predict a reasonable value of modulus for the base layer within the tolerances given and, the final output of 15.0 ksi was the minimum threshold value. The LOADRATE program was able to predict the modulus value of the base course of FM 491 with satisfactory results. At all of the other sites, its predictions were always on the higher side of the measured values, except at FM 2864 where the prediction was on the lower side.

Both the PDCP and the computer program BISDEF predicted the subgrade modulus values fairly well. The PDCP predictions were within the laboratory measured values except at FM 1983 and FM 2864, in which cases the predictions were slightly on the higher side. The BISDEF prediction of the subgrade modulus at FM 2864 was slightly on the higher side (the output itself was not within acceptable tolerances), and at SH 7, it was predicting modulus values below the measured ones. The LOADRATE program successfully predicted the subgrade modulus at FM 2864. With the exception of SH 7, predictions at all of the other test sites were somewhat below the measured values. At the test site SH 7, the subgrade modulus predicted was far below the measured range.

In general, the PDCP predicted the modulus values of both the base course and the subgrade satisfactorily. Although only one PDCP test was done per test site in this study, the influence of possible localized effects could be reduced by performing more than one test. The BISDEF program also performed fairly well except at FM 2864 and at SH 7. None of the NDT techniques that use FWD responses were able to predict the modulus values of both the base course and the subgrade successfully at either of these sites. It must be noted that both of the sites are located in the wet region of the state and the samples retrieved recorded comparatively high moisture levels. One possibility could be that the high moisture concentration underneath the pavement may affect the FWD responses, which as a result may not reflect the true strength of the pavement. The LOADRATE program fared poorly, mostly where there is sandy subgrade. It always underpredicted the modulus of a sandy subgrade while heavily overpredicting the base course stiffness.

B. Laboratory Repeated Load Tests

One specimen each of the base and the subgrade layers from a test site was subjected to the permanent deformation test in the laboratory. For a base course specimen, a deviator stress of 20 psi and a confining pressure of 10 psi were applied throughout the 25,000 repetitions. For a subgrade specimen, a deviator stress of 8 psi and a confining pressure of 4 psi were used.

Figures 27 and 28 show the log-log plots between the accumulated residual strain and the number of load repetitions. Table 7 gives the intercept (a) and the slope (b) of the straight line fit on the log-log plot for each sample and also the resilient modulus value under the same loading conditions, measured after the completion of 25,000 cycles. It must be noted that the straight line in each case was fitted only to the data points beyond the transient stage of rutting even though all the data points are shown in the figures. It will be of interest to note the increasing trend in residual strain towards the end of the steady stage in samples with high sand content (subgrades of FM 1983 and SH 7). It may indicate the existence of the tertiary stage of residual deformation which was described in Chapter II.

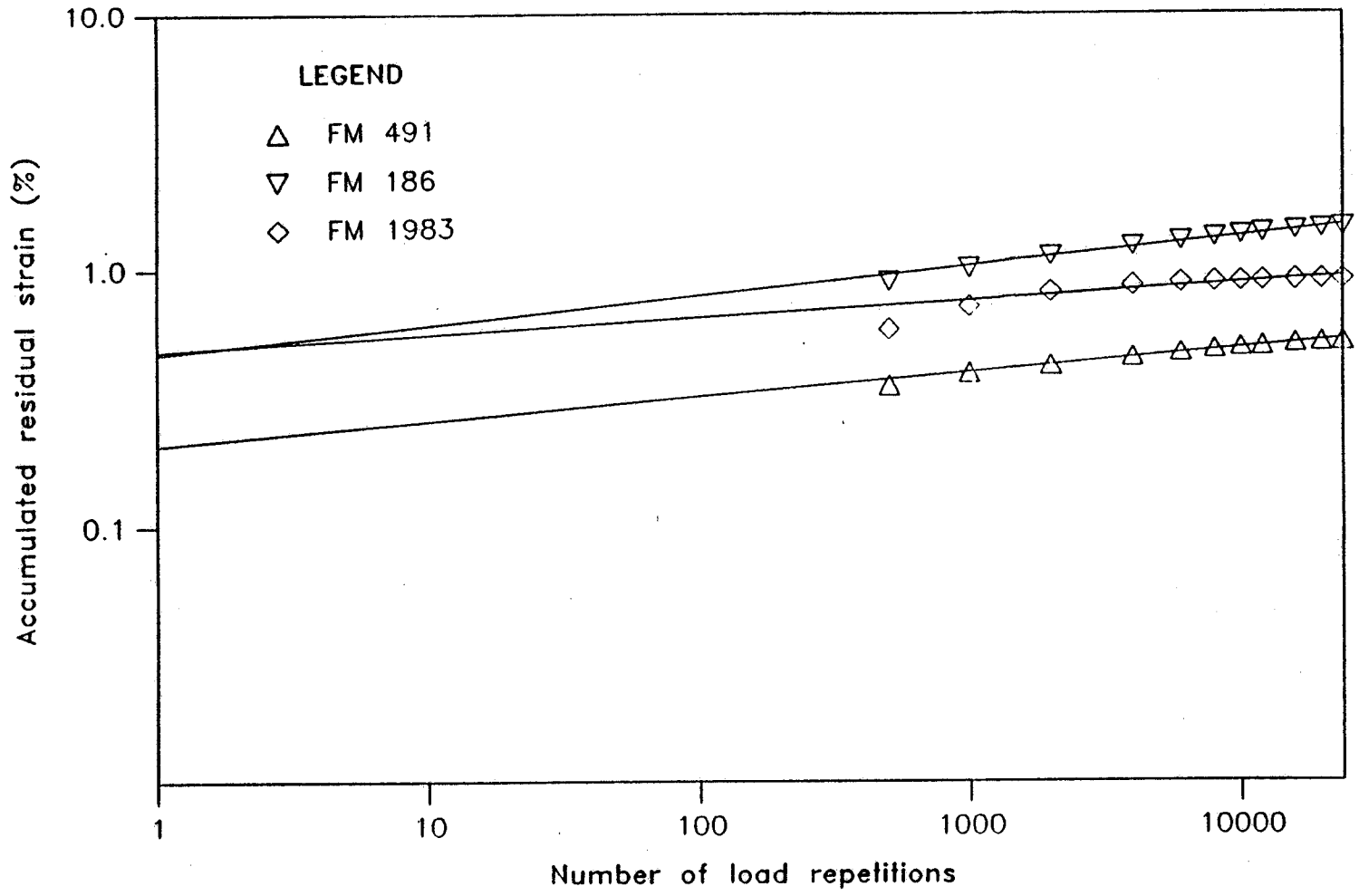

FIGURE 27 Repeated load test—base course materials

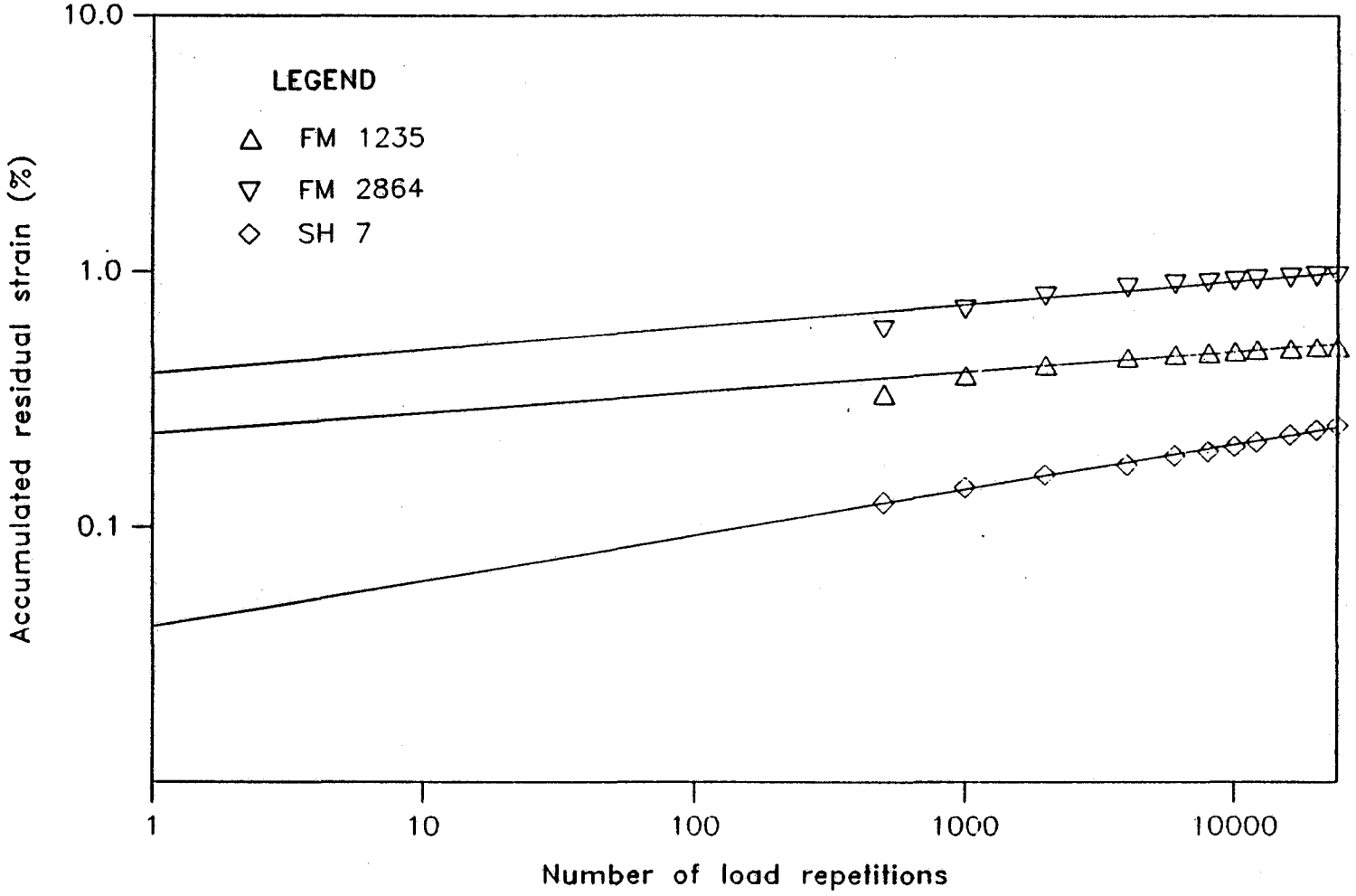

FIGURE 27 Continued

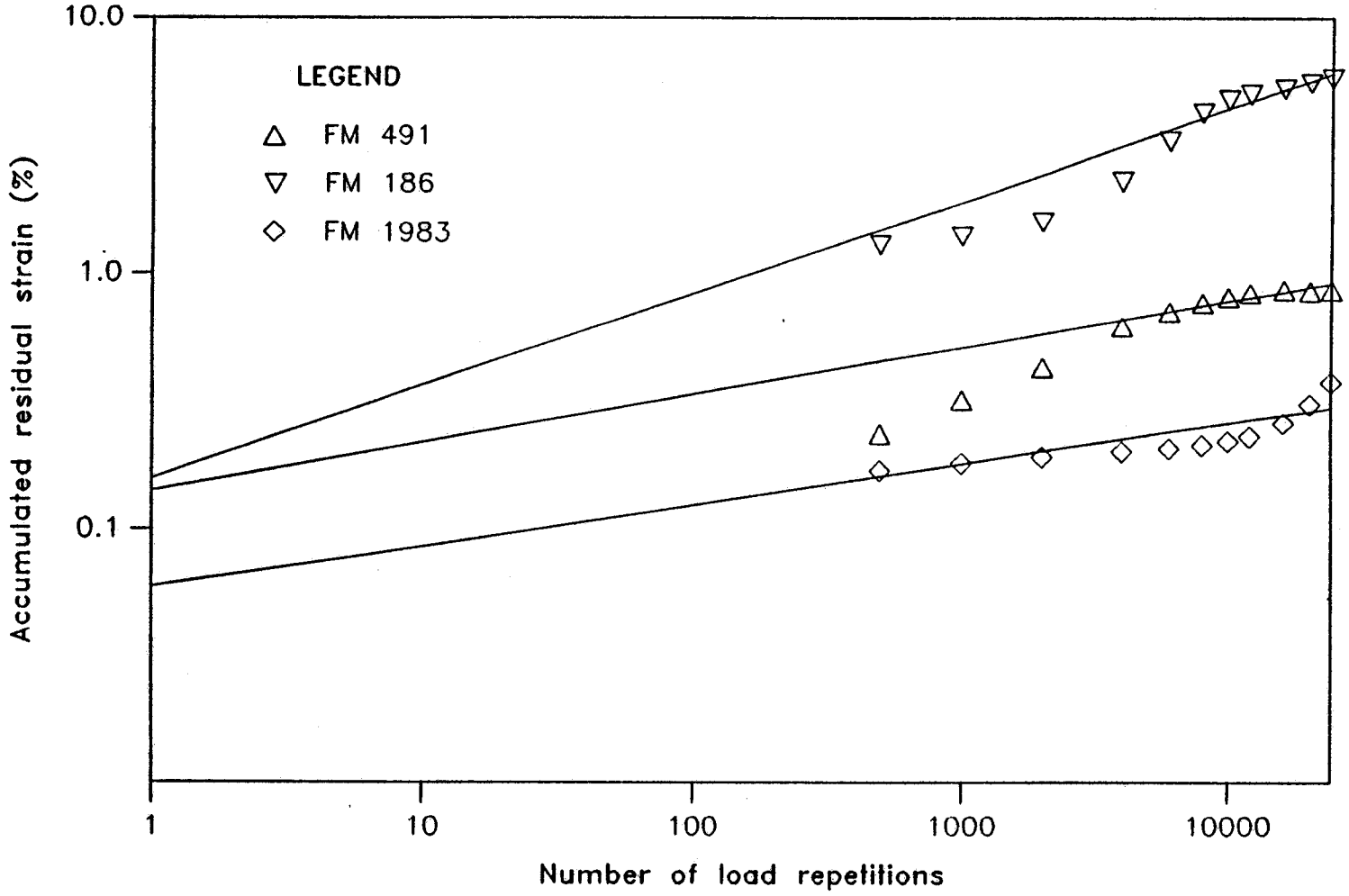

FIGURE 28 Repeated load test—subgrade materials

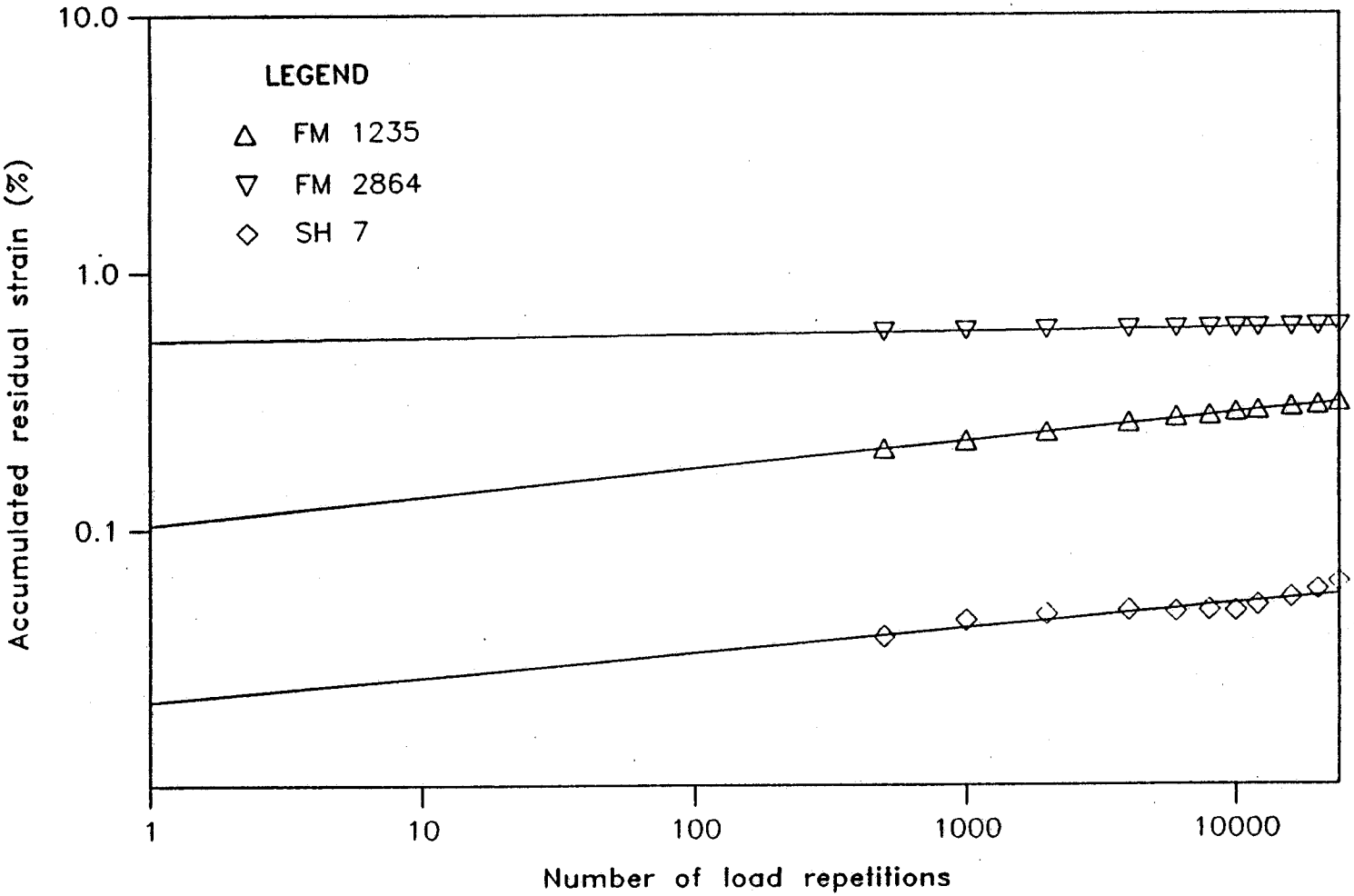

FIGURE 28 Continued

TABLE 7 LABORATORY RUTTING PARAMETERS—BASE COURSE AND SUBGRADE

Sample	Location	Rutting Parameter		Resilient Modulus (ksi)
		Intercept a (x 10^{-4})	Slope b	
Base Course				
FM491	#5	20.862	0.094	32.39
FM186	#6	46.970	0.115	20.52
FM1983	#5	48.176	0.067	52.35
FM1235	#5	23.057	0.081	41.27
FM2864	#3	39.428	0.094	34.04
SH7	#4	4.091	0.178	40.25
Subgrade				
FM491	#8(bot)	14.043	0.187	8.25
FM186	#12(bot)	15.711	0.363	9.28
FM1983	#11	5.943	0.159	11.61
FM1235	#13(top)	10.421	0.107	13.45
FM2864	#10	53.388	0.013	14.11
SH7	#5	2.126	0.094	35.60

C. Identification of Rutting Parameters

Residual Deformation Rate 'b'

The 'b' value in Equation (2) may be referred to as the rate with which the residual deformation will take place. The greater the magnitude of 'b', the more pronounced the residual deformation will be. Monismith and others (20) suggested that 'b' may depend on the material type. Rauhut and Jordhal (30) observed that α $(= 1 - b)$ varies within a narrow range with the deviator stress and the moisture content, but is greatly affected by the clay content of the material. They further observed that α is essentially independent of the stress state for the granular base course material. Majidzadeh and co-workers (31, 32, 33) observed that 'm' $(= 1 - b)$ is almost a constant for silty clay material (Figure 6). Khedr's work (34) showed that 'm' is nearly a constant for granular base course materials, too (Figure 8). To investigate the behavior of 'b' in detail, with respect to different pavement materials, a thorough literature survey was conducted.

As observed by above mentioned researchers, it was found that the 'b' value stayed within a narrow range for a given material type. Also, 'b' showed a significant decreasing trend with a decrease in the clay content of a subgrade material. Accordingly, the subgrade materials were broadly classified into three groups, namely, heavy clay (CH–clay), light or silty clay and clayey silt (CL–ML) and, clayey, silty or uniform sand (SC–SM). The 'b' values from the laboratory test data, from this study and from past research work by others, are presented in Table 8 for the three groups of subgrades. The table indicates the spread of 'b' values in a set of data, with average 'b' values for the individual data set and for each material group marked with 'X' . The average 'b' value decreases from 0.236 for the CH-clay group to 0.142 for the SC-SM group. The CL-ML group has a value in between of 0.162. For the base course materials, there were comparatively few sets of repeated load test results available. Table 8 shows the 'b' values for two base course materials, namely, gravelly sand and crushed limestone. Since there was no significant difference in the 'b' values between these two types of materials, it was decided to calculate one average value of 'b' $(= 0.125)$ for the base course materials.

The considerable spread in the 'b' values within individual sets of data and also within each material group could be due to several reasons. One probable reason for this, the effect of the differences in the volumetric moisture content among the

TABLE 8 VARIATION OF 'b' VALUE FOR DIFFERENT MATERIALS

Material Type	Rate of Accumulation of Residual Strain 'b'- Value	Reference
	0.0 0.1 0.2 0.3 0.4	
CH - Clay (High plasticity)		Edris (22) Townsend (27) Average
CL - ML (Low plasticity clay and clayey silt)		Monismith (20) Rauhut (30) (33) Hamilton (49) Cuyahoga (49) Franklin (49) Natural Edris (22) (33) Licking Average
SC - SM (Clayey sand and silty sand)		(33) Auglaize (33) Carrol (33) Licking FM1983 SH7 FM491 Lentz (23) Average
Base Course Materials		(26) Limestone (19) Penn. (19) Virginia FM1235 FM491 FM186 (26) Gravel FM2864 SH7 FM1983 Average
	0.0 0.1 0.2 0.3 0.4	

test specimens, is discussed in Chapter VI. Other slightly influential factors could be the differences in loading conditions and the specimen placement conditions such as density.

First Cycle Strain 'a'

The 'a' value in Equation (2) is the amount of residual strain caused by the first cycle of loading. Monismith and others (20) suggested that 'a' could be a function of the stress level, the previous stress history, and the placement conditions. Majidzadeh and co-workers (31, 32, 33) showed that 'A' ($=a$) varies inversely with the dynamic modulus ($\approx$ resilient modulus) for silty clay subgrade materials (Figure 7). In the same plot, 'A' shows very little variation with the applied stress. Khedr (34) correlated 'A' with the resilient modulus and a function of the applied stress (Chapter II). Again, the influence of the applied stress, when taken together with the resilient modulus, was found to be negligible. An apparent reason for this behavior may be that the direct effect of applied stress could be overshadowed by the inclusion of the resilient modulus. It is widely accepted that the resilient modulus of a material is highly influenced by the applied stress and also by the placement conditions.

Hence, in this study, the behavior of 'a' was investigated with respect to the resilient modulus of a specimen, measured under the same loading conditions as used in the corresponding repeated load test. Furthermore, the investigation was conducted separately for each of the four groups of pavement materials, for which a corresponding average value 'b' could be assigned. This would facilitate a simple means of identifying an 'a' and a 'b', given the soil classification of a pavement material. Figures 29, 30, 31 and 32 show the behavior of 'a' with respect to the resilient modulus for the four groups of materials, CH–clay, CL–ML, SC–SM, and base course materials, respectively. In the figures, the data for different materials and from different test programs are identified by different symbols. Out of the sets of data used to calculate the 'b' value for each material group, only those with tabulated resilient modulus values were used to establish the behavior of 'a'. Since the data do not come from a single controlled experiment, no attempt was made to generate statistical trends. Instead, the data from different materials in a group were given equal weights by selecting only an equal number of data points representing the behavior of each different material. It can be seen from the figures that some sets of data are clustered into narrow regions, because of the limitations in the ranges of loading conditions used

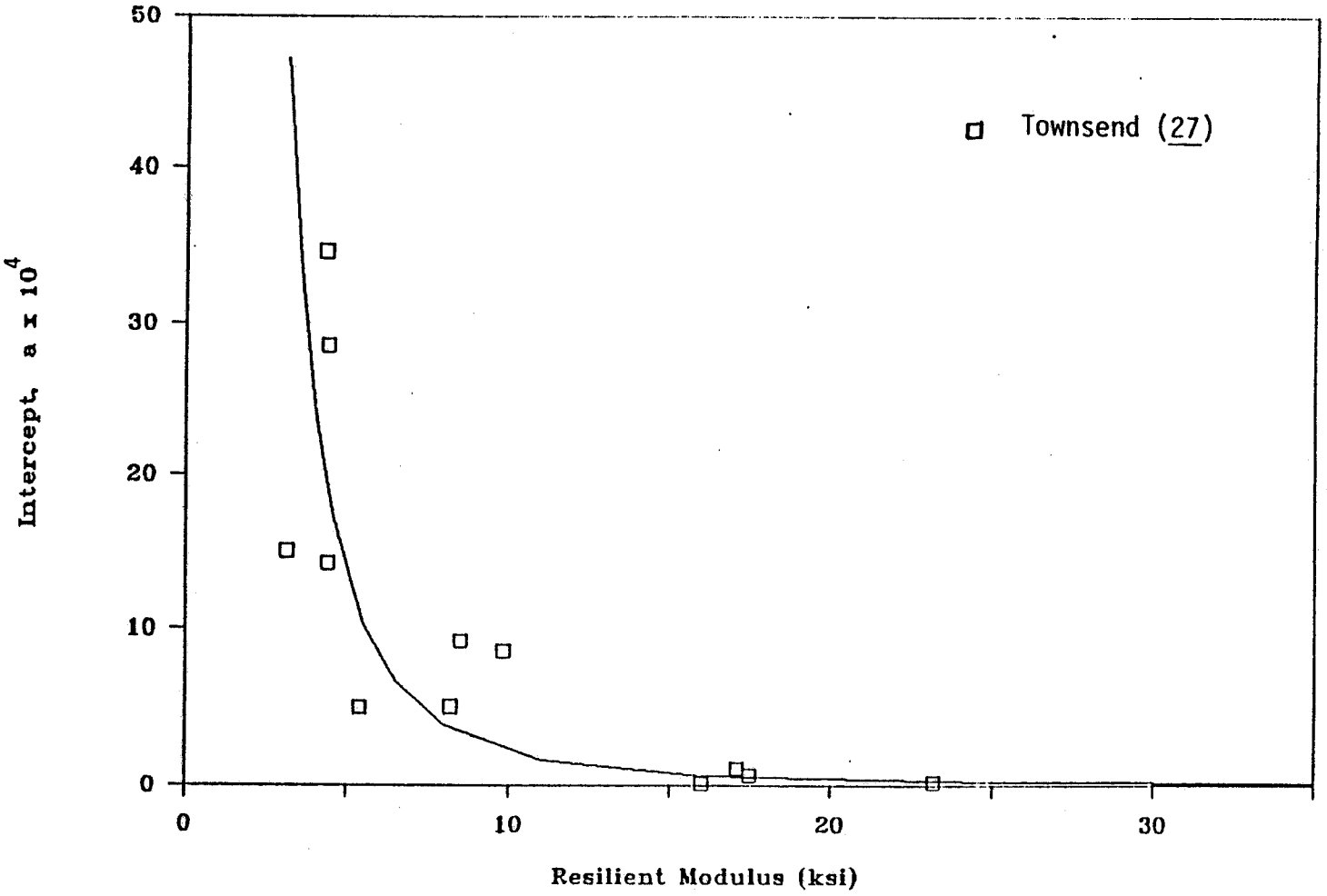

FIGURE 29 Variation of 'a' values—CH-clay(subgrade)

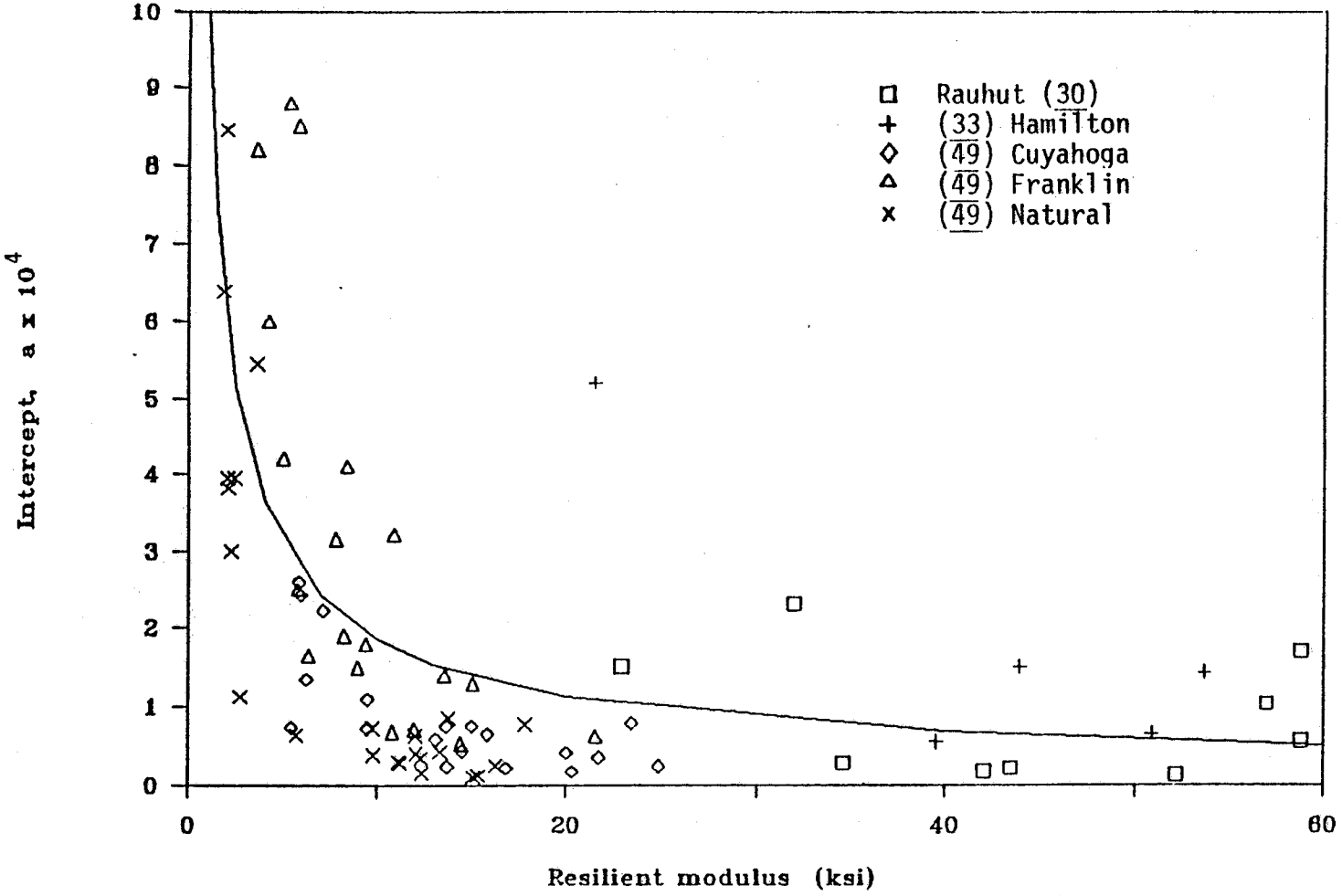

FIGURE 30 Variation of 'a' values—CL-ML(subgrade)

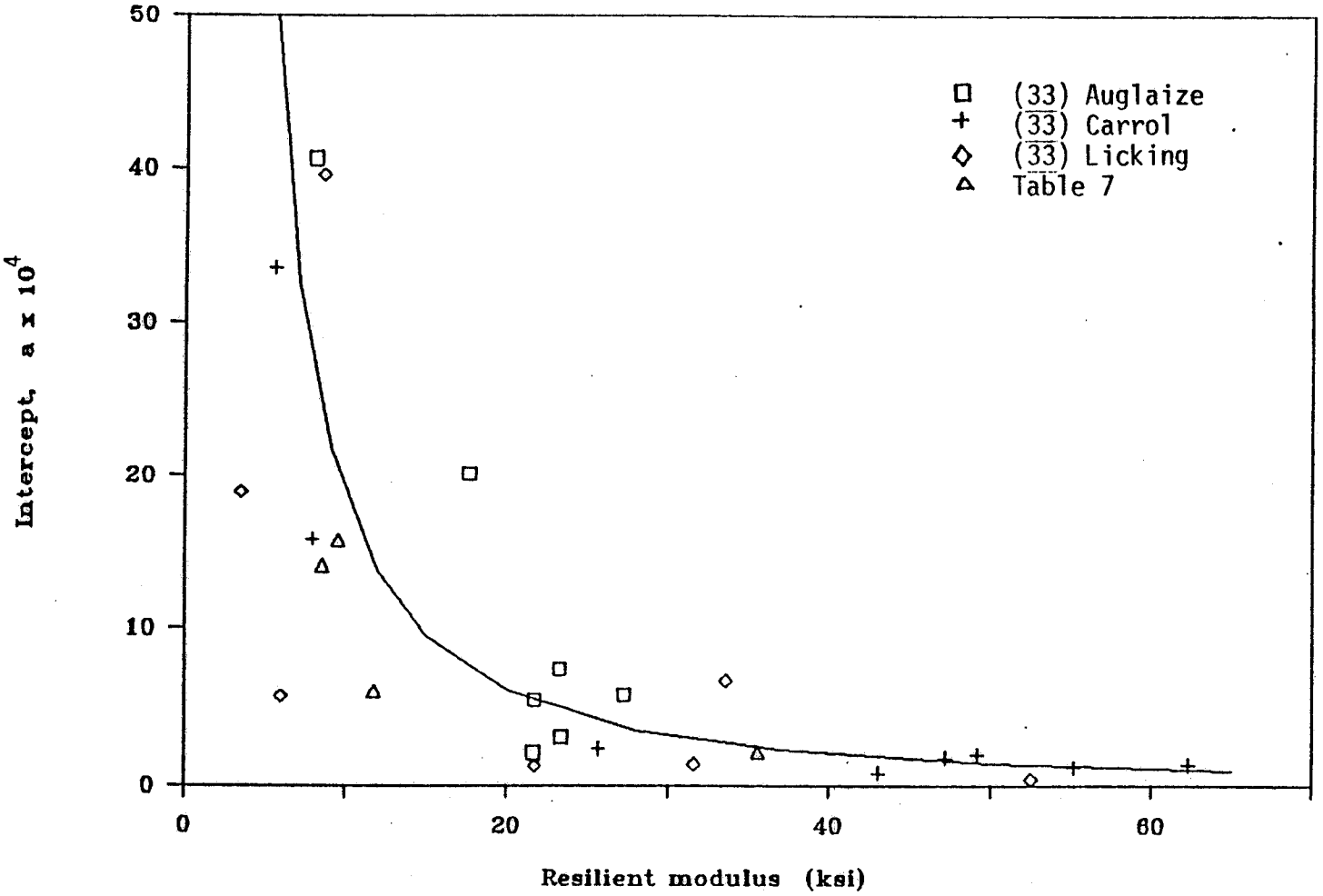

FIGURE 31 Variation of '*a*' values—SC-SM(subgrade)

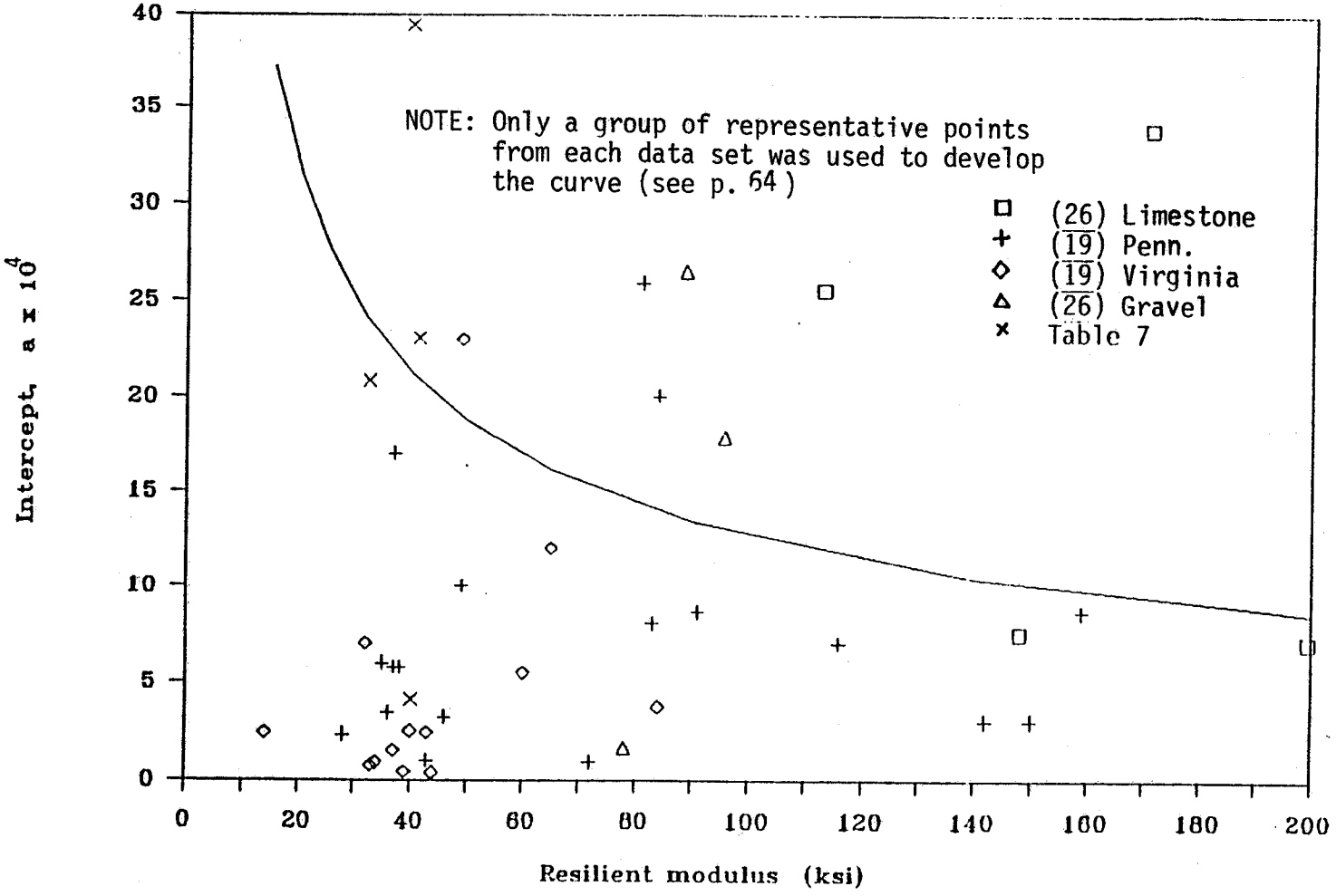

FIGURE 32 Variation of 'a' values—base course materials

in individual investigations. The above procedure eliminated the effect of any bias due to these limited ranges. Since a stiffer specimen may have a smaller permanent deformation at the first cycle of loading and vice versa, it is logical to assume 'a' to vary inversely with the resilient modulus. Hence, a hyperbolic curve with asymptotes at both X and Y axes was fitted to those selected data points using the Least Squares method. However, all of the data points available are shown in the figures with the fitted curves.

Table 9 shows the average 'b' values for the four different groups of pavement materials and the behavior of the corresponding 'a' value with respect to the resilient modulus. Thus, with a knowledge of the soil type of a pavement material, sufficient to identify the group it belongs to, its permanent deformation behavior can be approximately determined by the 'b' and the 'a' values given in Table 9. A field NDT test could be used to determine the resilient moduli of the pavement layers, with which the value of 'a' can be determined. This simple and approximate method of identifying permanent deformation behavior of a pavement material will be used in the next chapter to develop a rut depth prediction procedure.

TABLE 9 RUTTING PARAMETERS FOR PAVEMENT MATERIALS

Material	Rutting Parameter	
	Intercept a x 10^4	Slope b
Base Course	174 $M_R^{-0.57}$	0.125
Subgrade		
Heavy Clay (CH-clay)	933 $M_R^{-2.64}$	0.236
Clayey Silt/ Silty Clay (CL-ML)	10 $M_R^{-0.73}$	0.162
Clayey/Silty Sand (SC-SM)	750 $M_R^{-1.61}$	0.142

* M_R - Resilient Modulus (in ksi)

CHAPTER V

RUT DEPTH PREDICTION PROCEDURE

In Chapter II, two different methodologies for predicting the rut depth of a pavement were discussed. The second method, the Mechano-lattice program is used in this study. This chapter describes how the Mechano-lattice program was used to calculate the rut depths of different types of low-volume pavements. The study was designed in such a way that the resulting database could be used to predict the rut depth of any type of a low-volume road in the state of Texas. A multi-dimensional interpolation technique uses this database to predict the rut depth value of a pavement. The required inputs are the resilient modulus of both the base layer and the subgrade of the pavement and the soil classification of the subgrade. This procedure incorporates the technique of approximate determination of permanent deformation behavior of a pavement material, developed in Chapter IV.

A. Creating a Data Base of Rut Depths

Out of the two methodologies described for rut depth prediction, the first, the method of superposition calculates permanent deformation in each layer of the pavement, using a relationship between the permanent deformation and the stress state in that layer (36). Then the rut depth at the surface is determined by summing permanent deformation in each of the layers. The Mechano-lattice program, on the other hand, approaches the problem by considering the pavement as one integrated unit. It is claimed that it incorporates any interaction effects between the layers that may affect not only the distribution of stresses, but also the permanent deformation in the system. Therefore, it was decided to employ the Mechano-lattice program to create a data base of rut depths using a number of different configurations of low-volume road pavement sections.

Since in a low-volume road, the effect of the surface treatment is negligible on the structural performance of the pavement as a whole, the surface-treated layer was completely left out of the simulation. A few preliminary runs of the Mechano-lattice program showed the effect of the absence of this layer to be negligible.

Input data for the Mechano-lattice program require three basic material parameters and the thickness of the pavement layers. Elastic modulus, accumulated residual strain after a specified number of load repetitions and the Poisson's ratio are the

three material parameters. The Poisson's ratio did not have a significant effect on the output over the possible range of variation, and therefore, it was kept constant for each of the two layers throughout the study. This reduced the total number of input parameters to five, namely, the elastic modulus of both the base course and the subgrade, the accumulated residual strain of both the base course and the subgrade and the thickness of the base layer. It was decided to use the resilient modulus in place of the elastic modulus for both the layers because the difference is negligible for the type of materials under consideration. In order to include all possible types of low-volume pavements in the state of Texas, the input parameters were varied within a wide range of values, as shown in Table 10. The accumulated residual strain (rutting potential) in each layer was estimated for 300,000 load repetitions. This simulation study produced rut depths for 162 different pavement sections. The calculated rut depths represent the depression caused by 300,000 load repetitions, measured under a 4 ft. straight edge placed across the wheel path. The database of rut depths is tabulated in Appendix B.

B. A Simplified Procedure for Rut Depth Prediction

The response from a FWD test on a low-volume road can be interpreted through the LOADRATE program (10) to estimate the resilient modulus of both the base course and the subgrade. Additional information regarding the soil classification of the material used for the subgrade will help determine approximate values for the intercept (a) and the slope (b) of their permanent deformation behavior (Chapter IV). A value for the number of load repetitions is chosen so that the accumulated residual deformation per each layer, as calculated by $\epsilon_p = a\ N^b$, remains within the range of values used for the Mechano-lattice simulation (Table 10). The resilient moduli and the residual deformation behavior of each of the layers and the thickness of the base layer complete the information required for a prediction of rut depth. By using a multidimensional polynomial interpolation routine (50), the Mechano-lattice rut depth output values are interpolated (or extrapolated within limits) to produce a value of rut depth for the road. If desired, the allowable number of vehicle passes until the road reaches a specified terminal rut depth can be predicted. The procedure is written as a computer code and is listed in Appendix C. It can be incorporated to the LOADRATE program. If the resilient moduli of the pavement materials are known otherwise, the program can be used to predict the rut depth without using the

TABLE 10 INPUT PARAMETERS FOR MECHANO-LATTICE RUNS

Parameter	Unit	Level		
		1	2	3
Resilient Modulus	psi			
-Base Course		100,000	70,000	40,000
-Subgrade		25,000	15,000	5,000
Accumulated Residual Strain	in/in			
-Base Course		0.0075	0.0025	
-Subgrade		0.0100	0.0060	0.0020
Base Thickness	in.	18.0	12.0	6.0

LOADRATE program. If more accurate predictions of the rut depth are required, it is recommended that the permanent deformation behavior of each material layer be determined in the laboratory. Then those values can be used directly as input for the rutting potential.

CHAPTER VI

DISCUSSION

A. Interaction Effects of Rutting Potential on Rut Depth

As mentioned earlier, the Mechano-lattice program considers the interaction effects of rutting potential between the different layers, while the method of superposition ignores those effects. This study provides an opportunity to examine these interaction effects and their importance in the rut depth calculations.

In the Mechano-lattice program, the response of the subgrade is approximated by a unit-deep artificial layer, which simulates a semi-infinite space. It is thus impossible to determine an effective depth of the subgrade layer that contributes to the total amount of rutting. However, the thickness of the base course is known and its contribution to rutting can be quantified. Suppose, in a hypothetical case, the rutting potential of the base course is varied while keeping all of the other parameters constant. Then, according to the superposition method, the difference in the rut depths in the two pavement configurations should be equal to the change in the residual deformation in the base layer. This observation is based on the assumption that the rutting potential of a material layer will not affect the calculation of stress distribution in the method of superposition.

Consider two pavement sections, each with a 6-inch thick base layer, but one having a higher rutting potential than the other and say, accumulated residual strains of 0.0075 and 0.0025 respectively, for 300,000 load repetitions. Then, the difference in the rut depths between the two sections, estimated by the superposition method is as follows:

Rut depth (case 1) = 0.0075 x 6 + contribution of subgrade

Rut depth (case 2) = 0.0025 x 6 + contribution of subgrade (same)

Difference in rut depth = 0.0050 x 6

= 0.0300 in.

This difference in the rut depths will vary linearly with the thickness of the base course as shown in Figure 33. However, for the two sections considered, the differences in the rut depths calculated by the Mechano-lattice program for different base

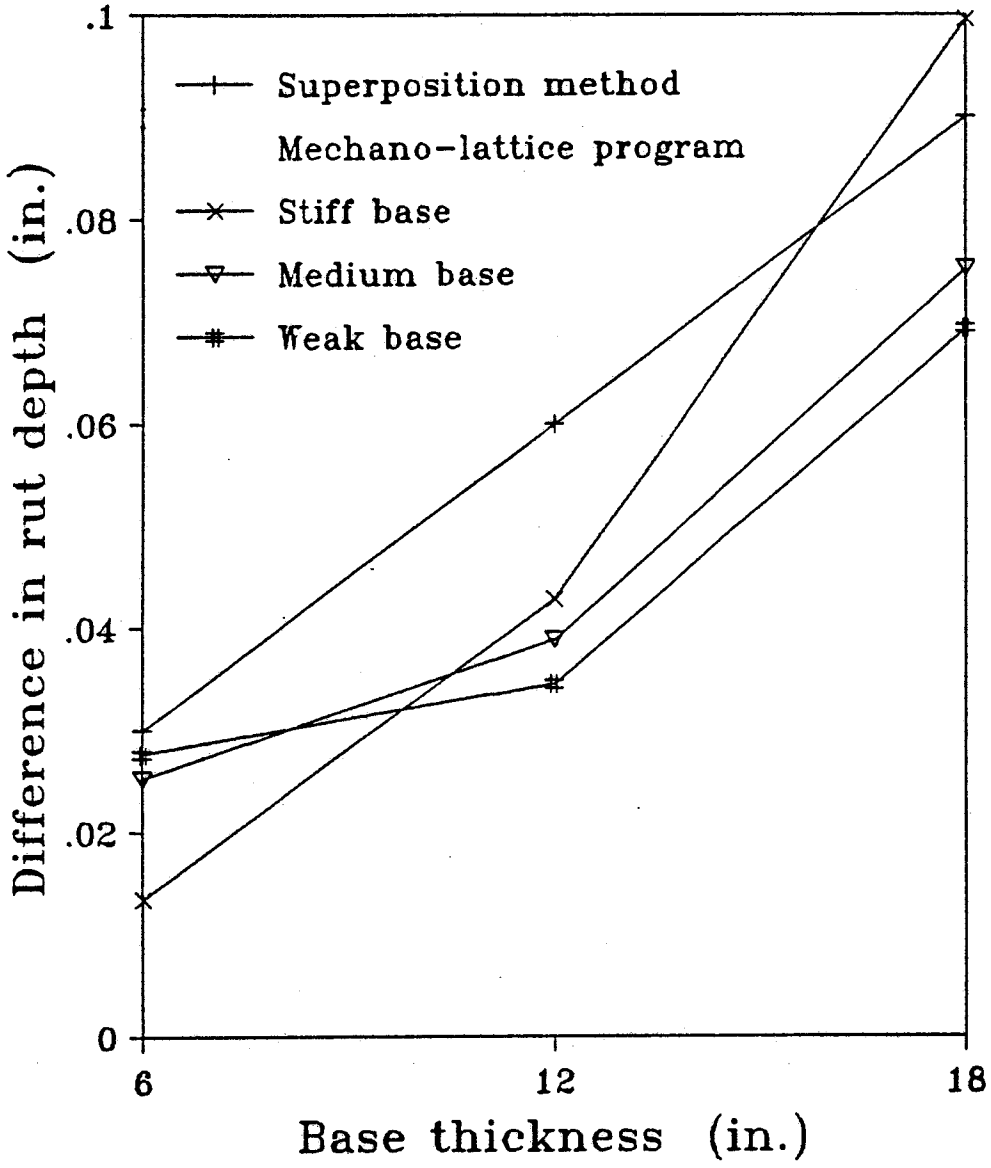

FIGURE 33 Comparison of rut depth predictions of the superposition method and the Mechano-lattice program

course stiffnesses (high, medium or low resilient modulus values), can be seen to be non-linear (Figure 33). In fact, when the base course is strong and thin (say, 6 inches), the difference (= 0.0135 in.) is smaller than that estimated by the method of superposition (= 0.0300 in.). The reason may be that, in this case, the contribution to the rut depth comes mainly from the subgrade, and thus, a change in rutting potential in the base layer does not have much influence on the whole. On the other hand, if the base layer is sufficiently thick, its permanent deformation will significantly contribute to the rut depth in the pavement and the differences calculated by the two methods will agree closely. For example, for a stiff 18 inch thick base course layer, the difference computed by the Mechano-lattice program is 0.0996 in., as compared to 0.0900 in. by the method of superposition. In contrast, when the base layer is weak, even though it may be 18 in. thick, the subgrade layer will experience a higher stress level and thus will contribute more to the overall rut depth. The computed difference in rut depths in this case is 0.0692 in. This illustration clearly shows that any method which ignores the interaction effects may not provide a correct estimate of the rut depth.

B. The Effect of Soil Moisture on '*b*' Value

In Table 8, the mean '*b*' value for each of the soil material groups has a considerably large spread. This may be due to the variations in the volumetric concentrations of the aggregate and the pore water in the materials used. The following expression appears to fit the data displayed in Table 8:

$$b = b_a \theta_a + b_w \theta_w \tag{7}$$

where,

b_a = the '*b*' value for dry aggregate, and is approximately equal to 0.02 (51)

(Note: It can be shown that the rate of permanent deformation is related to the creep rate and this value is calculated from the latter.)

b_w = the '*b*' value for pore water, found to be 0.60 (from regression analysis using data from Table 8)

θ_a = the volumetric concentration of the aggregate particles, and

θ_w = the volumetric water content.

Table 11 shows the mean 'b' value for most of the studies reviewed in this paper, their standard deviations, the mean of the predicted values of 'b' by Equation (7) and their standard deviations. The table indicates an acceptable degree of correspondence between the observed and the predicted values. The relation in Equation (7) was suggested by the rule of mixtures. The volumetric water and aggregate contents can be calculated simply with standard engineering measurements using the following equations:

$$\theta_w = \frac{\gamma_t}{\gamma_w} \frac{w}{1+w} \tag{8}$$

$$\theta_a = \frac{\gamma_t}{\gamma_w} \frac{1}{G_s(1+w)} \tag{9}$$

where,

w = gravimetric water content

γ_t = total unit weight

γ_w = unit weight of water, and

G_s = specific gravity of solids.

C. Sensitivity of the Rut Depth Prediction

The rut depth database (Appendix B) developed using the Mechano-lattice program shows the variation of rut depth due to a change in the resilient modulus of either the base course or the subgrade within a wide range. A careful inspection of the data reveals that a change in the resilient modulus of the base course alone would change the rut depth only slightly. To illustrate the effect of the subgrade type and its stiffness on rutting using the proposed procedure, let us consider a low-volume road with a 6 inch thick base course of resilient modulus of 50,000 psi and with different subgrade material types ranging from heavy clay (CH group) to silty sand (SC-SM group). The resilient modulus of the subgrade layer is varied from that of the low through the high range. Rut depths are calculated for 200,000 passes of a 9000 lb. single wheel load.

Figure 34 shows the rut depths obtained for various road sections. It can be seen that the potential of rutting depends on the material type as well as the resilient modulus of the subgrade. Rutting is seen to be the most severe in heavy clay (CH)

TABLE 11 PREDICTING 'b' USING EQUATION (7)

Material	Mean of 'b'	Coefficient of Variation of 'b'	Mean of Predicted 'b'	Coefficient of Variation of Predicted 'b'	Reference
Subgrade					
CH - Clay	0.26	0.10	0.25	0.04	Edris (22)
CH - Clay	0.20	0.12	0.26	0.02	Townsend (27)
CL - Clay	0.18	0.02	0.20	0.01	Monismith (20)
CL - Clay	0.18	0.12	0.18	0.04	Rauhut (30)
CL - Clay	0.21	0.06	0.17	0.03	(33) Hamilton
ML - Silt	0.21	0.11	0.15	0.04	Edris (22)
ML - Silt	0.11	0.04	0.17	0.03	(33) Licking
SM - Sand	0.11	0.02	0.12	0.00	(33) Auglaize
SM - Sand	0.16	0.02	0.13	0.02	(33) Carrol
SM - Sand	0.18	0.09	0.14	0.03	(33) Licking
SC - Sand	0.16		0.15		FM1983
SP - SM	0.09		0.08		SH7
SC - Sand	0.19		0.21		FM491
SC - Sand	0.36		0.22		FM186
Base Course					
GRAVEL	0.11	0.02	0.08	0.01	(26) Gravel
GRAVEL	0.09		0.13		FM2864
GRAVEL	0.18		0.12		SH7
GRAVEL	0.07		0.08		FM1983
CR. LIMESTONE	0.08		0.08		FM1235
CR. LIMESTONE	0.09		0.13		FM491
CR. LIMESTONE	0.12		0.14		FM186

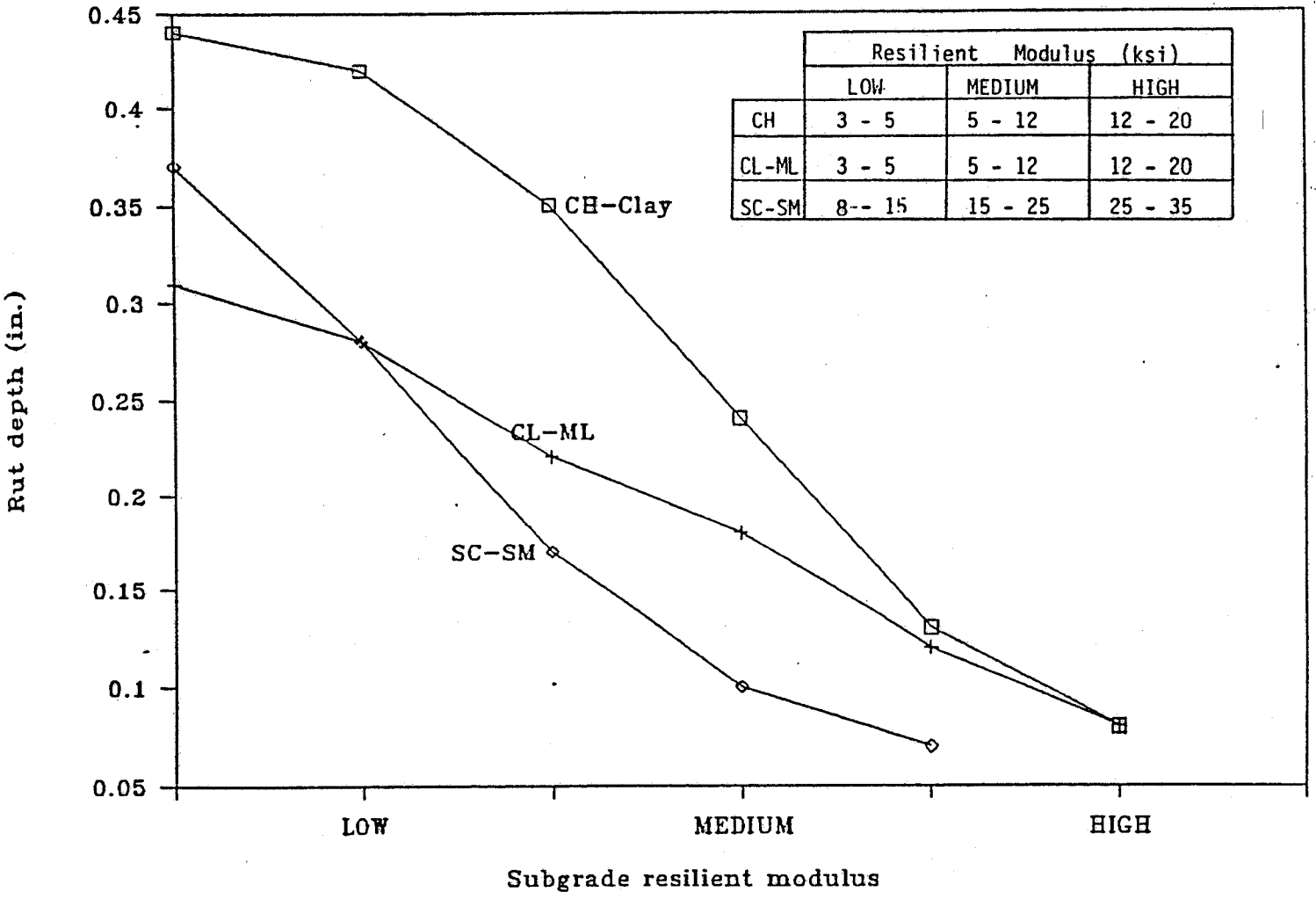

FIGURE 34 Effect of subgrade type and modulus on rut depth

subgrade. A sandy (SC-SM) subgrade with a resilient modulus of 3000 psi can result in as much rutting as a clayey (CL-ML) subgrade of that stiffness. However, this is an unrealistic comparison, since a loose sand can easily have a modulus much higher than that. On the other hand, a "stiff" sandy subgrade will have a rut depth much smaller than a "stiff" clay.

CHAPTER VII

SUMMARY AND CONCLUSIONS

A mechanistic, but yet simple procedure for rut depth prediction in low-volume roads is presented in this study. The method requires the resilient modulus of both the base course and the subgrade, the thickness of the base layer and the soil classification of the subgrade material. A comprehensive database of rut depths computed using the Mechano-lattice program is interpolated to predict the rut depth of a particular road. The permanent deformation behavior of each of the material layers, which is needed for interpolation, is estimated using the material type of the layer and its resilient modulus. These relationships were established by using laboratory test data from this study and from the past research work as reported in the literature. In the process of laboratory repeated load testing, existing procedures were critically examined in order to simulate the field conditions properly in the laboratory. The resilient modulus of a pavement material layer is estimated from the response of a commonly used NDT device. To verify the field NDT predictions of resilient moduli, a laboratory resilient test program too was envisaged. This study also provided an opportunity to investigate the importance of the interaction effects of permanent deformation behavior in different material layers on the prediction of rut depth.

The following conclusions can be drawn from this study.

1. At the present time, it appears that the logarithmic plot between the accumulated residual strain and the number of load repetitions is adequate for comparing the rutting behavior of various soil materials.

2. The rate of residual deformation (b value) can be generally classified into four groups of pavement soil materials, namely, heavy clay (CH), light or silty clay and clayey silt (CL-ML), clayey or silty sand (SC-SM), and the base course materials.

3. The first cycle strain (a value) varies inversely with the resilient modulus of the material layer.

4. The 'a' and 'b' values can be calculated based upon the soil classification and the resilient modulus.

5. The 'b' value appears to be related by a rule of mixtures to the 'b' values of the solids and the water.

6. The BISDEF computer program using FWD responses and the PDCP predict the resilient moduli of the pavement layers quite successfully.

7. The interaction effects of the permanent deformation behavior of different pavement layers can have a significant impact upon the rut depth calculation of a pavement.

REFERENCES

1. *AASHTO Guide for Design of Pavement Structures.* American Association of State Highway and Transportation Officials, Washington, DC, 1986.

2. M.Y. Shahin and S.D. Kohn. *Pavement Maintenance Management for Roads and Parking Lots.* CERL–TR–M–294, U.S. Army Construction Engineering Research Laboratory, Champaign, IL, Oct. 1981.

3. *Pavement Management Guide.* Roads and Transportation Association of Canada, Ottawa, Canada, 1977.

4. M.S. Hoffman and M.R. Thompson. Comparative Study of Selected Nondestructive Testing Devices. In *Transportation Research Record 852*, TRB, National Research Council, Washington, DC, 1982, pp. 32–41.

5. E.G. Kleyn, J.H. Maree and P.F. Savage. The Application of a Portable Pavement Dynamic Cone Penetrometer to Determine In Situ Bearing Properties of Road Pavement Layers and Subgrades in South Africa. *Proc., 2nd European Symposium on Penetration Testing*, Amsterdam, May 1982, pp. 277–283.

6. E.J. Yoder and M.W. Witczak. *Principles of Pavement Design.* 2nd Ed., John Wiley Sons, Inc., New York, NY, 1975.

7. K.M. Chua. *Evaluation of Moduli Backcalculation Programs for Low Volume Roads.* Presented at 1st International Symposium on Nondestructive Testing of Pavements and Backcalculation of Moduli, Baltimore, MD, June 1988.

8. M. S. Hoffman and M.R. Thompson. Backcalculating Nonlinear Resilient Moduli from Deflection Data. In *Transportation Research Record 852*, TRB, National Research Council, Washington, DC, 1982, pp. 42–51.

9. J. Uzan. MODULUS User's Guide. In *Determination of Asphaltic Concrete Pavement Structural Properties by Nondestructive Testing.* by R.L. Lytton et al., Final Report, Research Foundation Project RF2076, Texas Transportation Institute, College Station, TX 77843, Apr. 1986.

10. K.M. Chua and R.L. Lytton. Load Rating of Light Pavement Structures. In *Transportation Research Record 1043*, TRB, National Research Council, Washington, DC, 1985, pp. 89–101.

11. M.S. Mamlouk. Use of Dynamic Analysis in Predicting Field Multilayer Pavement Moduli. In *Transportation Research Record 1043*, TRB, National Research Council, Washington, DC, 1985, pp. 113–121.

12. K.M. Chua. *Determination of CBR and Elastic Modulus of Soils Using a Portable Dynamic Cone Penetrometer.* Presented at 1st International Symposium on Penetration Testing, Orlando, FL, Mar. 1988.

13. C.L. Monismith, H.B. Seed, F.G. Mitry and C.K. Chan. Prediction of Pavement Deflections from Laboratory Tests. *Proc., 2nd International Conference on Structural Design of Asphalt Pavements*, MI, 1967, pp. 109–140.

14. T. Rwebangira, R.G. Hicks and M. Truebe. Determination of Pavement Layer Structural Properties for Aggregate-Surfaced Roads. In *Transportation Research Record 1106*, TRB, National Research Council, Washington, DC, 1987, pp. 215–221.

15. S.F. Brown. Laboratory Testing for Use in the Prediction of Rutting in Asphalt Pavements. In *Transportation Research Record 616*, TRB, National Research Council, Washington, DC, 1976, pp. 22–27.

16. AASHTO T 274–82 (1986). *Standard Method of Test for Resilient Modulus of Subgrade Soils.* American Association of State Highway and Transportation Officials, Washington, DC, 1986.

17. New Standard Test Method for Resilient Modulus of Untreated Soils (ASTM Preliminary). In *Determination of Asphaltic Concrete Pavement Structural Properties by Nondestructive Testing.* by R.L. Lytton et al., Final Report, Research Foundation Project RF7026, Texas Transportation Institute, College Station, TX 77843, Apr. 1986.

18. R.D. Barksdale. Laboratory Evaluation of Rutting in Base Course Materials. *Proc., 3rd International Conference on the Structural Design of Asphalt Pavements*, London, 1972, pp. 161–174.

19. I.V. Kalcheff and R.G. Hicks. A Test Procedure for Determining the Resilient Properties of Granular Materials. *Journal of Testing and Evaluation*, ASTM, Vol. 1, No. 6, Nov. 1973, pp. 472–479.

20. C.L. Monismith, N. Ogawa and C.R. Freeme. Pavement Deformation Characteristics of Subgrade Soils due to Repeated Loading. In *Transportation Research Record 537*, TRB, National Research Council, Washington, DC, 1974, pp. 1–17.

21. J.R. Morgan. The Response of Granular Materials to Repeated Loading. *Proc., Australian Road Research Board*, Vol. 3, Part 2, 1966, pp. 1178–1192.

22. E.V. Edris, Jr. and R.L. Lytton. *Dynamic Properties of Subgrade Soils, Including Environmental Effects.* TTI-2-18-74-164-3, Texas Transportation Institute, College Station, TX 77843, May 1976.

23. R.W. Lentz. Permanent Deformation of Cohesionless Subgrade Material Under Cyclic Loading. Ph.D. thesis, Michigan State University, 1979.

24. V.K. Khosla and R.D. Singh. Influence of Number of Cycles on Strain. *Canadian Geotechnical Journal*, Vol. 15, 1978, pp. 584–592.

25. P.N. Gaskin, G.P. Raymond, F.Y. Addo-abedi and J.S. Lau. Repeated Compressive Loading of a Sand. *Canadian Geotechnical Journal*, Vol. 16, 1979, pp. 798–802.

26. E.E. Chisolm and F.C. Townsend. *Behavioral Characteristics of Gravelly sand and Crushed Limestone for Pavement Design.* FAA-RD-75-177, U.S. Army Engineer Waterways Experiment Station, Vicksburg, MS, Sept. 1976.

27. F.C. Townsend and E.E. Chisolm. *Plastic and Resilient Properties of Heavy Clay Under Repetitive Loadings.* FAA-RD-76-107, U.S. Army Engineer Waterways Experiment Station, Vicksburg, MS, Nov. 1976.

28. H.A. Loffti, C.W. Schwartz and M.W. Witzack. *Compaction Specification for the Control of Subgrade Rutting.* Presented at Transportation Research Board 67th Annual Meeting, Washington, DC, Jan. 1988.

29. W.J. Kenis. Predictive Design Procedures: A Design Method for Flexible Pavements using the VESYS Structural Subsystem. *Proc., 4th International Conference on Structural Design of Asphalt Pavements*, MI, 1977, pp. 101–130.

30. J.B. Rauhut and P.R. Jordhal. *Effects on Flexible Highways of Increased Legal Vehicle Weights using VESYS IIM.* FHWA-RD-77-116, Austin Research Engineers Inc., Austin, TX 78746, Jan. 1978.

31. K. Majidzadeh, S. Khedr and H. Guirguis. Laboratory Verification of a Mechanistic Subgrade Rutting Model. In *Transportation Research Record 616*, TRB, National Research Council, Washington, DC, 1976, pp. 34–37.

32. K. Majidzadeh, F. Bayomy and S. Khedr. Rutting Evaluation of Subgrade Soils in Ohio. In *Transportation Research Record 671*, TRB, National Research Council, Washington, DC, 1978, pp. 75–84.

33. F. Bayomy. The Effect of Soil Type and Saturation on Subgrade Rutting Parameters. M.S. Thesis, Ohio State University, 1977.

34. S. Khedr. Deformation Characteristics of Granular Base Course in Flexible Pavements. In *Transportation Research Record 1043*, TRB, National Research Council, Washington, DC, 1985, pp. 131–138.

35. K. H. Tseng and R.L. Lytton. *Prediction of Permanent Deformation in Flexible Pavement Materials.* Presented at ASTM Symposium on the Implication of Aggregates in the Design Construction and Performance of Flexible Pavements, New Orleans, LA, Dec. 1986.

36. C.L. Monismith, Rutting prediction in Asphalt Concrete Pavements. In *Transportation Research Record 616*, TRB, National Research Council, Washington, DC, 1976, pp. 2–8.

37. G.M. Dorman and C.T. Metcalf. Design Curves for Flexible Pavements Based on Layered System Theory. In *Highway Research Record 71*, HRB, Washington, DC, 1965, pp. 69–84.

38. C.L. Monismith and D.B. McLean. *Design Considerations for Asphalt Pavements.* TE–71–8, Institute of Transportation and Traffic Engineering, University of California, Berkeley, 1971.

39. W.O. Yandell. New Method of Simulating Layered Systems of Unbound Granular Material. In *Transportation Research Record 1022*, TRB, National Research Council, Washington, DC, 1985, pp. 91–98.

40. W.O. Yandell. Mechano-Lattice Prediction of Pavement Performance. *Proc., 4th Conference on Asphaltic Pavements for Southern Africa*, Capetown, 1984, pp. 201–215.

41. W.O. Yandell. Measurement and Prediction of Forward Movement and Rutting in Pavements Under Repetitive Wheel Loads. In *Transportation Research Record 888*, TRB, National Research Council, Washington, DC, 1982, pp. 77–84.

42. M. McVay and Y. Taesiri. Cyclic Behavior of Pavement Base Materials. *Journal of Geotechnical Engineering*, ASCE, Vol. 111, No. 1, Jan. 1985, pp. 1–17.

43. J.B. Sousa and C.L. Monismith. *Dynamic Response of Paving Materials.* Presented at Transportation Research Board 66th Annual Meeting, Washington, DC, Jan. 1987.

44. J.J. Allen and M.R. Thompson. Significance of Variably Confined Triaxial Testing. *Journal of Transportation Engineering*, ASCE, Vol. 100, No. 4, Nov. 1984, pp. 827–843.

45. *Test Procedures for Characterizing Dynamic Stress-Strain Properties of Pavement Materials.* Transportation Research Board Special Report 162, National Research Council, Washington, DC, 1975.

46. R.G. Hicks. Factors Influencing the Resilient Properties of Granular Materials. Ph.D. Thesis, University of California, Berkeley, 1970.

47. S.F. Brown, A.K.F. Lashine and A.F.L. Hyde. Repeated Load Testing of a Silty Clay. *Geotechnique*, Vol. 25, No. 1, pp. 95–114.

48. A.J. Bush III. *Computer Program BISDEF.* U.S. Army Engineer Waterways Experiment Station, Vicksburg, MS, Nov. 1985.

49. S.A.H. Khedr, Variations of Parameters of Permanent Deformation Mechanistic Model. M.S. Thesis, Ohio State University, Mar. 1975.

50. W.H. Press, B.P. Flannery, S.A. Tenkolsky and W.T. Vetterling. *Numerical Recipes: The Art of Scientific Computing.* Cambridge University Press, Cambridge, 1987, pp. 77–101.

51. K.M. Chua and R.L. Lytton. Time-Dependent Properties of Embedment Soils Back Calculated from Deflections of Buried Pipes. *Speciality Geomechanics Symposium, Interpretation of Field Testing for Design Parameters*, Institute of Engineers, Adelade, Australia, Aug. 1986.

APPENDIX A

RESILIENT TEST RESULTS OF BASE COURSE AND SUBGRADE SAMPLES

TABLE 12 RESILIENT MODULUS VALUES OF BASE COURSE SAMPLES

Location	Sample	Confining Pressure (psi)	Deviator Stress (psi)	Resilient Modulus (ksi)
Dist 21	BE0	30	10.8	40.44
FM 491		30	21.5	36.74
#5		30	37.1	38.98
		30	47.9	42.69
		30	63.9	42.04
		20	10.7	32.60
		20	21.4	29.51
		20	36.8	27.85
		20	47.3	32.65
		10	10.3	22.04
		10	21.0	20.83
		10	35.6	17.90
		5	10.1	20.32
		5	20.2	14.63
		1	10.2	13.83

TABLE 12 Continued

Location	Sample	Confining Pressure (psi)	Deviator Stress (psi)	Resilient Modulus (ksi)
Dist 21	BE1	30	10.8	39.94
FM 491		30	21.6	33.75
# 5		30	37.1	36.30
		30	47.5	38.98
		30	63.5	39.67
		30	10.7	54.07
		20	10.7	32.17
		20	21.1	28.18
		20	36.8	30.61
		20	47.1	29.18
		10	10.2	20.96
		10	20.8	18.61
		10	36.1	19.49
		5	10.4	18.02
		5	20.1	14.36
		1	9.9	13.51

TABLE 12 Continued

Location	Sample	Confining Pressure (psi)	Deviator Stress (psi)	Resilient Modulus (ksi)
Dist 21	BER	30	10.3	-
FM 491		30	20.6	57.83
# 5		30	36.2	49.44
		30	46.8	46.48
		30	62.6	42.09
		20	10.2	59.70
		20	20.6	44.72
		20	36.1	36.44
		20	46.3	32.38
		10	9.9	41.97
		10	20.2	32.39
		10	35.0	22.09
		5	9.3	22.63
		5	19.7	22.74
		1	9.8	21.24

TABLE 12 Continued

Location	Sample	Confining Pressure (psi)	Deviator Stress (psi)	Resilient Modulus (ksi)
Dist 21	BC0	30	10.8	47.39
FM 186		30	21.0	44.05
#6		30	36.6	39.50
		30	47.0	43.55
		30	63.3	44.62
		20	10.7	41.37
		20	21.0	36.67
		20	36.5	32.48
		20	46.7	36.49
		20	62.6	34.90
		10	10.3	28.77
		10	20.7	23.57
		10	36.3	19.46
		5	10.2	18.38
		5	16.6	7.63
		1	9.8	14.78

TABLE 12 Continued

Location	Sample	Confining Pressure (psi)	Deviator Stress (psi)	Resilient Modulus (ksi)
Dist 21 FM 186 #6	BC1	30	10.6	42.24
		30	21.4	38.38
		30	37.0	38.96
		30	47.3	40.68
		30	63.0	40.47
		30	10.8	70.78
		20	10.4	34.02
		20	21.0	28.65
		20	36.4	28.58
		20	46.9	30.17
		20	10.4	48.43
		10	10.0	22.11
		10	20.7	17.65
		10	35.0	17.81
		10	10.0	29.34
		5	10.3	14.00
		5	20.4	10.31
		5	9.5	21.86
		1	10.0	12.39
		1	8.9	14.66

TABLE 12 Continued

Location	Sample	Confining Pressure (psi)	Deviator Stress (psi)	Resilient Modulus * (ksi)
Dist 8	BA1	30	10.9	-
FM 1983		30	21.7	66.90
#5		30	35.6	72.42
		30	47.5	92.97
		30	63.0	88.03
		20	10.8	-
		20	21.2	45.67
		20	35.5	51.73
		20	47.1	66.22
		10	10.3	48.69
		10	21.1	31.69
		10	34.5	36.98
		5	9.8	27.43
		5	18.5	17.38
		1	9.8	24.67

* Obtained from corrected Ram readings

TABLE 12 Continued

Location	Sample	Confining Pressure (psi)	Deviator Stress (psi)	Resilient Modulus * (ksi)
Dist 8	BD0	30	11.3	67.96
FM 1235		30	22.4	63.33
#5		30	38.1	58.73
		30	48.1	62.55
		30	62.7	65.89
		20	10.8	60.12
		20	22.5	42.72
		20	38.3	53.65
		20	48.3	56.63
		10	10.6	47.27
		10	21.7	37.20
		10	37.9	35.90
		5	10.7	34.07
		5	21.2	27.29
		1	10.5	30.20

* Obtained from corrected Ram readings

TABLE 12 Continued

Location	Sample	Confining Pressure (psi)	Deviator Stress (psi)	Resilient Modulus (ksi)
Dist 8	BD1	30	11.0	68.90
FM 1235		30	22.7	-
#5		30	37.8	60.52
		30	48.5	67.01
		30	64.4	74.57
		30	10.7	-
		20	11.0	58.42
		20	22.9	44.74
		20	38.0	53.44
		20	47.5	56.60
		20	10.5	-
		10	10.7	41.91
		10	22.6	38.81
		10	37.6	39.44
		5	10.5	35.40
		5	22.2	29.01
		1	10.3	28.63

TABLE 12 Continued

Location	Sample	Confining Pressure (psi)	Deviator Stress (psi)	Resilient Modulus (ksi)
Dist 8	BDR	30	10.5	-
FM 1235		30	21.0	78.34
#5		30	35.9	77.17
		30	46.9	66.25
		30	62.8	80.66
		20	10.7	-
		20	20.9	61.39
		20	35.9	56.13
		20	46.5	55.78
		10	10.5	63.96
		10	20.5	41.27
		10	35.5	38.00
		5	10.2	44.95
		5	20.1	32.29
		1	10.2	41.50

TABLE 12 Continued

Location	Sample	Confining Pressure (psi)	Deviator Stress (psi)	Resilient Modulus * (ksi)
Dist 11	BB0	30	10.8	98.61
FM 2864		30	21.6	54.65
#3		30	37.1	54.47
		30	46.5	65.34
		30	63.6	58.08
		20	10.7	96.70
		20	21.3	41.68
		20	37.0	46.07
		20	47.2	47.20
		10	10.3	48.59
		10	20.8	29.22
		10	36.4	38.86
		5	10.0	46.83
		5	20.0	21.20
		1	9.8	29.66

* Obtained from corrected Ram readings

TABLE 12 Continued

Location	Sample	Confining Pressure (psi)	Deviator Stress (psi)	Resilient Modulus (ksi)
Dist 11	BB1	30	10.8	61.25
FM 2864		30	21.5	50.75
#3		30	38.4	-
		30	48.2	87.39
		30	63.9	83.28
		20	10.6	43.83
		20	21.4	38.76
		20	37.1	69.01
		20	47.7	70.29
		20	63.5	83.23
		10	10.1	29.33
		10	20.6	27.00
		10	37.8	42.39
		5	10.6	18.13
		5	21.1	24.80
		1	10.4	17.29

TABLE 12 Continued

Location	Sample	Confining Pressure (psi)	Deviator Stress (psi)	Resilient Modulus (ksi)
Dist 11 FM 2864 #3	BB2	30	10.8	80.13
		30	21.5	50.80
		30	36.7	48.90
		30	47.4	58.58
		30	62.5	62.92
		20	10.6	59.40
		20	21.0	38.08
		20	36.7	39.24
		20	47.1	46.92
		10	10.2	38.59
		10	20.3	25.10
		10	36.3	27.95
		5	9.6	23.33
		5	19.9	28.05
		1	8.9	16.23

TABLE 12 Continued

Location	Sample	Confining Pressure (psi)	Deviator Stress (psi)	Resilient Modulus (ksi)
Dist 11 SH 7 #4	BF0	30	10.3	61.41
		30	21.0	53.84
		30	36.6	55.91
		30	46.5	64.21
		30	61.9	70.33
		30	10.2	89.77
		20	10.2	46.57
		20	20.9	40.11
		20	36.2	48.16
		20	46.3	49.98
		20	9.9	57.55
		10	9.8	29.40
		10	20.3	25.52
		10	35.5	34.73
		5	9.7	24.79
		5	19.4	19.50
		1	9.4	20.88

TABLE 12 Continued

Location	Sample	Confining Pressure (psi)	Deviator Stress (psi)	Resilient Modulus (ksi)
Dist 11	BFR	30	10.3	113.85
SH 7		30	20.0	92.03
#4		30	35.2	76.74
		30	45.3	77.92
		30	60.4	77.09
		20	10.0	73.88
		20	20.0	69.10
		20	35.0	55.60
		20	44.9	56.59
		10	9.8	43.77
		10	20.1	40.25
		10	34.5	40.07
		5	9.4	25.18
		5	18.8	24.84
		1	9.3	25.49

TABLE 13 RESILIENT MODULUS VALUES OF SUBGRADE SAMPLES

Location	Sample	Confining Pressure (psi)	Deviator Stress (psi)	Resilient Modulus (ksi)
Dist 21	PO	1	2.0	-
FM 491		1	5.2	8.91
#7 (top)		1	7.8	7.17
		1	11.4	5.52
		4	5.1	10.01
		4	7.7	7.42
		4	11.6	7.05
		8	5.2	13.58
		8	7.9	10.56
		8	11.8	9.91
		8	15.9	7.50
		8	23.2	4.61

TABLE 13 Continued

Location	Sample	Confining Pressure (psi)	Deviator Stress (psi)	Resilient Modulus (ksi)
Dist 21 FM 491 #8 (top)	MO	1	5.1	10.33
		1	7.8	8.86
		1	11.4	7.32
		4	5	9.96
		4	7.7	8.36
		4	11.6	8.97
		8	2.2	27.06
		8	5.2	11.53
		8	7.9	9.36
		8	11.8	10.11

TABLE 13 Continued

Location	Sample	Confining Pressure (psi)	Deviator Stress (psi)	Resilient Modulus * (ksi)
Dist 21	F0	1	2.1	-
FM 491		1	5.1	8.44
#10 (top)		1	7.8	7.40
		1	11.3	6.52
		4	5.0	8.36
		4	7.7	7.44
		4	11.4	7.01
		8	5.1	12.65
		8	7.7	7.95
		8	11.7	8.28

* Obtained from corrected Ram readings

TABLE 13 Continued

Location	Sample	Contining Pressure (psi)	Deviator Stress (psi)	Resilient Modulus * (ksi)
Dist 21	H0	1	2.1	-
FM 186		1	5.3	9.08
#8 (bot)		1	8.1	8.92
		1	11.8	7.77
		4	2.2	-
		4	5.4	10.62
		4	8.3	10.49
		4	12.1	10.13
		8	2.0	-
		8	5.3	12.43
		8	8.3	12.25
		8	12.2	13.20

* Obtained from corrected Ram readings

TABLE 13 Continued

Location	Sample	Confining Pressure (psi)	Deviator Stress (psi)	Resilient Modulus (ksi)
Dist 21	KO	1	2.0	33.06
FM 186		1	5.2	11.15
#9 (bot)		1	7.7	8.18
		1	11.7	13.84
		4	2.1	26.35
		4	5.2	11.40
		4	7.8	7.88
		8	2.1	23.03
		8	5.2	10.87
		8	7.7	7.62

TABLE 13 Continued

Location	Sample	Confining Pressure (psi)	Deviator Stress (psi)	Resilient Modulus (ksi)
Dist 8	S1	1	2.2	32.75
FM 1983		1	5.2	22.21
#7,9,10		1	8.1	17.43
		1	11.7	18.40
		4	2.2	49.80
		4	5.3	24.98
		4	8.1	21.08
		4	11.9	18.98
		8	2.2	52.57
		8	5.2	28.66
		8	8.1	24.14
		8	11.8	22.60

TABLE 13 Continued

Location	Sample	Confining Pressure (psi)	Deviator Stress (psi)	Resilient Modulus (ksi)
Dist 8	S3	1	2.1	35.93
FM 1983		1	5.3	22.90
#7,9,10		1	8.1	19.34
		1	11.6	16.30
		4	2.1	48.13
		4	5.2	29.74
		4	8.2	25.39
		4	11.8	21.92
		8	2.0	52.68
		8	5.2	46.31
		8	8.2	31.00
		8	11.8	26.87

TABLE 13 Continued

Location	Sample	Confining Pressure (psi)	Deviator Stress (psi)	Resilient Modulus * (ksi)
Dist 8	I0	1	5.3	9.37
FM 1235		1	8.2	8.19
#8 (top)		1	12.1	7.55
		4	5.1	9.35
		4	8.1	8.98
		4	11.8	7.23
		8	5.2	14.80
		8	8.1	9.76
		8	11.6	7.91

* Obtained from corrected Ram readings

TABLE 13 Continued

Location	Sample	Confining Pressure (psi)	Deviator Stress (psi)	Resilient Modulus (ksi)
Dist 8	L0	1	5.3	18.88
FM 1235		1	8.1	14.98
#8 (bot)		1	11.7	10.41
		4	5.3	17.19
		4	8.1	14.19
		4	11.7	10.00
		8	5.2	15.36
		8	8.1	12.66
		8	11.7	10.57

TABLE 13 Continued

Location	Sample	Confining Pressure (psi)	Deviator Stress (psi)	Resilient Modulus * (ksi)
Dist 8	G0	1	2.3	-
FM 1235		1	5.4	9.17
#9 (top)		1	8.1	8.51
		1	11.8	7.51
		4	2.3	-
		4	5.3	8.83
		4	8.1	8.08
		4	11.9	7.88
		8	5.2	9.56
		8	7.6	8.76
		8	11.9	10.44

* Obtained from corrected Ram readings

TABLE 13 Continued

Location	Sample	Confining Pressure (psi)	Deviator Stress (psi)	Resilient Modulus (ksi)
Dist 11 FM 2864 #5	00	1	5.4	16.13
		1	8.0	11.78
		1	11.2	6.87
		4	5.3	15.18
		4	7.9	11.18
		4	11.2	6.99
		8	5.2	15.18
		8	7.8	11.29
		8	11.1	5.93

TABLE 13 Continued

Location	Sample	Confining Pressure (psi)	Deviator Stress (psi)	Resilient Modulus (ksi)
Dist 11	U0	1	4.7	39.15
FM 2864		1	7.9	19.77
#8 (top)		1	11.4	14.55
		1	19.0	9.87
		4	4.8	46.73
		4	8.0	23.51
		4	11.4	15.82
		8	4.8	56.60
		8	7.9	27.44
		8	11.5	19.66

TABLE 13 Continued

Location	Sample	Confining Pressure (psi)	Deviator Stress (psi)	Resilient Modulus (ksi)
Dist 11 FM 2864 #8 (bot)	E0	1	5.3	12.76
		1	8.0	11.18
		1	12.0	9.77
		4	5.3	12.81
		4	7.9	10.89
		4	11.8	9.25
		8	5.2	21.03
		8	8.1	13.10
		8	12.0	9.91

* Obtained from corrected Ram readings

TABLE 13 Continued

Location	Sample	Contining Pressure (psi)	Deviator Stress (psi)	Resilient Modulus (ksi)
Dist 11	NO	1	5.4	14.95
FM 2864		1	8.1	12.52
#9 (top)		1	11.6	10.32
		4	5.4	14.32
		4	8.1	12.25
		4	11.5	10.00
		8	5.4	14.41
		8	8.1	11.63
		8	11.5	9.82

TABLE 13 Continued

Location	Sample	Confining Pressure (psi)	Deviator Stress (psi)	Resilient Modulus (ksi)
Dist 11	T2	1	5.2	-
SH 7		1	8.2	70.90
#5		1	11.9	42.23
		4	5.1	-
		4	8.2	65.25
		4	11.9	48.71
		8	4.8	-
		8	8.1	94.40
		8	11.9	59.44

TABLE 13 Continued

Location	Sample	Confining Pressure (psi)	Deviator Stress (psi)	Resilient Modulus (ksi)
Dist 11	T1	1	5.3	46.10
SH 7		1	8.5	37.90
#6		1	11.7	31.50
		4	2.0	-
		4	5.1	59.50
		4	8.5	44.70
		4	11.7	40.90
		8	1.9	
		8	4.8	44.90
		8	8.5	52.50
		8	11.8	52.70

APPENDIX B

RUT DEPTH DATABASE

TABLE 14 RUT DEPTHS CALCULATED BY MECHANO-LATTICE PROGRAM

Rut Depth (in.)	Resilient Modulus Base (psi)	Subgrade (psi)	Accumulated Base (in/in)	Perm. Def. Subgrade (in/in)	Thickness of Base (in.)
0.3191	100000	25000	0.0075	0.0100	6.0
0.2223	100000	25000	0.0075	0.0060	6.0
0.1253	100000	25000	0.0075	0.0020	6.0
0.2804	100000	25000	0.0075	0.0100	12.0
0.2152	100000	25000	0.0075	0.0060	12.0
0.1502	100000	25000	0.0075	0.0020	12.0
0.2609	100000	25000	0.0075	0.0100	18.0
0.2216	100000	25000	0.0075	0.0060	18.0
0.1831	100000	25000	0.0075	0.0020	18.0
0.3431	100000	15000	0.0075	0.0100	6.0
0.2556	100000	15000	0.0075	0.0060	6.0
0.1680	100000	15000	0.0075	0.0020	6.0
0.3030	100000	15000	0.0075	0.0100	12.0
0.2491	100000	15000	0.0075	0.0060	12.0
0.1951	100000	15000	0.0075	0.0020	12.0
0.2705	100000	15000	0.0075	0.0100	18.0
0.2451	100000	15000	0.0075	0.0060	18.0
0.2168	100000	15000	0.0075	0.0020	18.0
0.5286	100000	5000	0.0075	0.0100	6.0
0.4580	100000	5000	0.0075	0.0060	6.0
0.3882	100000	5000	0.0075	0.0020	6.0
0.4519	100000	5000	0.0075	0.0100	12.0
0.4172	100000	5000	0.0075	0.0060	12.0
0.3831	100000	5000	0.0075	0.0020	12.0
0.3674	100000	5000	0.0075	0.0100	18.0
0.3503	100000	5000	0.0075	0.0060	18.0
0.3331	100000	5000	0.0075	0.0020	18.0
0.3019	70000	25000	0.0075	0.0100	6.0
0.2002	70000	25000	0.0075	0.0060	6.0
0.0991	70000	25000	0.0075	0.0020	6.0
0.2912	70000	25000	0.0075	0.0100	12.0
0.2185	70000	25000	0.0075	0.0060	12.0
0.1458	70000	25000	0.0075	0.0020	12.0
0.2702	70000	25000	0.0075	0.0100	18.0
0.2249	70000	25000	0.0075	0.0060	18.0
0.1797	70000	25000	0.0075	0.0020	18.0
0.3549	70000	15000	0.0075	0.0100	6.0
0.2600	70000	15000	0.0075	0.0060	6.0
0.1652	70000	15000	0.0075	0.0020	6.0
0.3099	70000	15000	0.0075	0.0100	12.0
0.2490	70000	15000	0.0075	0.0060	12.0
0.1882	70000	15000	0.0075	0.0020	12.0
0.2804	70000	15000	0.0075	0.0100	18.0
0.2473	70000	15000	0.0075	0.0060	18.0
0.2137	70000	15000	0.0075	0.0020	18.0

TABLE 14 Continued

Rut Depth (in.)	Resilient Modulus Base (psi)	Subgrade (psi)	Accumulated Perm. Def. Base (in/in)	Subgrade (in/in)	Thickness of Base (in.)
0.5322	70000	5000	0.0075	0.0100	6.0
0.4561	70000	5000	0.0075	0.0060	6.0
0.3798	70000	5000	0.0075	0.0020	6.0
0.4610	70000	5000	0.0075	0.0100	12.0
0.4231	70000	5000	0.0075	0.0060	12.0
0.3842	70000	5000	0.0075	0.0020	12.0
0.3900	70000	5000	0.0075	0.0100	18.0
0.3688	70000	5000	0.0075	0.0060	18.0
0.3475	70000	5000	0.0075	0.0020	18.0
0.3110	40000	25000	0.0075	0.0100	6.0
0.2031	40000	25000	0.0075	0.0060	6.0
0.0837	40000	25000	0.0075	0.0020	6.0
0.3130	40000	25000	0.0075	0.0100	12.0
0.2263	40000	25000	0.0075	0.0060	12.0
0.1403	40000	25000	0.0075	0.0020	12.0
0.2946	40000	25000	0.0075	0.0100	18.0
0.2344	40000	25000	0.0075	0.0060	18.0
0.1750	40000	25000	0.0075	0.0020	18.0
0.3755	40000	15000	0.0075	0.0100	6.0
0.2687	40000	15000	0.0075	0.0060	6.0
0.1618	40000	15000	0.0075	0.0020	6.0
0.3356	40000	15000	0.0075	0.0100	12.0
0.2600	40000	15000	0.0075	0.0060	12.0
0.1842	40000	15000	0.0075	0.0020	12.0
0.3013	40000	15000	0.0075	0.0100	18.0
0.2548	40000	15000	0.0075	0.0060	18.0
0.2087	40000	15000	0.0075	0.0020	18.0
0.5424	40000	5000	0.0075	0.0100	6.0
0.4541	40000	5000	0.0075	0.0060	6.0
0.3670	40000	5000	0.0075	0.0020	6.0
0.4840	40000	5000	0.0075	0.0100	12.0
0.4343	40000	5000	0.0075	0.0060	12.0
0.3834	40000	5000	0.0075	0.0020	12.0
0.3977	40000	5000	0.0075	0.0100	18.0
0.3750	40000	5000	0.0075	0.0060	18.0
0.3498	40000	5000	0.0075	0.0020	18.0
0.3056	100000	25000	0.0025	0.0100	6.0
0.2086	100000	25000	0.0025	0.0060	6.0
0.1119	100000	25000	0.0025	0.0020	6.0
0.2376	100000	25000	0.0025	0.0100	12.0
0.1727	100000	25000	0.0025	0.0060	12.0
0.1082	100000	25000	0.0025	0.0020	12.0
0.1613	100000	25000	0.0025	0.0100	18.0
0.1258	100000	25000	0.0025	0.0060	18.0
0.0934	100000	25000	0.0025	0.0020	18.0
0.3247	100000	15000	0.0025	0.0100	6.0
0.2374	100000	15000	0.0025	0.0060	6.0
0.1500	100000	15000	0.0025	0.0020	6.0
0.2528	100000	15000	0.0025	0.0100	12.0
0.1993	100000	15000	0.0025	0.0060	12.0

TABLE 14 Continued

Rut Depth (in.)	Resilient Modulus Base (psi)	Subgrade (psi)	Accumulated Perm. Def. Base (in/in)	Subgrade (in/in)	Thickness of Base (in.)
0.1457	100000	15000	0.0025	0.0020	12.0
0.1901	100000	15000	0.0025	0.0100	18.0
0.1588	100000	15000	0.0025	0.0060	18.0
0.1280	100000	15000	0.0025	0.0020	18.0
0.4915	100000	5000	0.0025	0.0100	6.0
0.4217	100000	5000	0.0025	0.0060	6.0
0.3523	100000	5000	0.0025	0.0020	6.0
0.3681	100000	5000	0.0025	0.0100	12.0
0.3355	100000	5000	0.0025	0.0060	12.0
0.3038	100000	5000	0.0025	0.0020	12.0
0.2607	100000	5000	0.0025	0.0100	18.0
0.2453	100000	5000	0.0025	0.0060	18.0
0.2300	100000	5000	0.0025	0.0020	18.0
0.2767	70000	25000	0.0025	0.0100	6.0
0.1747	70000	25000	0.0025	0.0060	6.0
0.0732	70000	25000	0.0025	0.0020	6.0
0.2524	70000	25000	0.0025	0.0100	12.0
0.1794	70000	25000	0.0025	0.0060	12.0
0.1072	70000	25000	0.0025	0.0020	12.0
0.1951	70000	25000	0.0025	0.0100	18.0
0.1491	70000	25000	0.0025	0.0060	18.0
0.1039	70000	25000	0.0025	0.0020	18.0
0.3400	70000	15000	0.0025	0.0100	6.0
0.2453	70000	15000	0.0025	0.0060	6.0
0.1505	70000	15000	0.0025	0.0020	6.0
0.2643	70000	15000	0.0025	0.0100	12.0
0.2037	70000	15000	0.0025	0.0060	12.0
0.1433	70000	15000	0.0025	0.0020	12.0
0.1957	70000	15000	0.0025	0.0100	18.0
0.1628	70000	15000	0.0025	0.0060	18.0
0.1296	70000	15000	0.0025	0.0020	18.0
0.5025	70000	5000	0.0025	0.0100	6.0
0.4262	70000	5000	0.0025	0.0060	6.0
0.3502	70000	5000	0.0025	0.0020	6.0
0.4006	70000	5000	0.0025	0.0100	12.0
0.3648	70000	5000	0.0025	0.0060	12.0
0.3230	70000	5000	0.0025	0.0020	12.0
0.2920	70000	5000	0.0025	0.0100	18.0
0.2713	70000	5000	0.0025	0.0060	18.0
0.2508	70000	5000	0.0025	0.0020	18.0
0.2834	40000	25000	0.0025	0.0100	6.0
0.1736	40000	25000	0.0025	0.0060	6.0
0.0643	40000	25000	0.0025	0.0020	6.0
0.2785	40000	25000	0.0025	0.0100	12.0
0.1918	40000	25000	0.0025	0.0060	12.0
0.1059	40000	25000	0.0025	0.0020	12.0
0.2254	40000	25000	0.0025	0.0100	18.0
0.1652	40000	25000	0.0025	0.0060	18.0
0.1056	40000	25000	0.0025	0.0020	18.0
0.3642	40000	15000	0.0025	0.0100	6.0

TABLE 14 Continued

Rut Depth (in.)	Resilient Modulus Base (psi)	Subgrade (psi)	Accumulated Perm. Def. Base (in/in)	Subgrade (in/in)	Thickness of Base (in.)
0.2574	40000	15000	0.0025	0.0060	6.0
0.1506	40000	15000	0.0025	0.0020	6.0
0.2974	40000	15000	0.0025	0.0100	12.0
0.2216	40000	15000	0.0025	0.0060	12.0
0.1461	40000	15000	0.0025	0.0020	12.0
0.2256	40000	15000	0.0025	0.0100	18.0
0.1790	40000	15000	0.0025	0.0060	18.0
0.1328	40000	15000	0.0025	0.0020	18.0
0.5197	40000	5000	0.0025	0.0100	6.0
0.4327	40000	5000	0.0025	0.0060	6.0
0.3456	40000	5000	0.0025	0.0020	6.0
0.4287	40000	5000	0.0025	0.0100	12.0
0.3786	40000	5000	0.0025	0.0060	12.0
0.3287	40000	5000	0.0025	0.0020	12.0
0.3322	40000	5000	0.0025	0.0100	18.0
0.3034	40000	5000	0.0025	0.0060	18.0
0.2749	40000	5000	0.0025	0.0020	18.0

APPENDIX C

COMPUTER CODE FOR RUT DEPTH PREDICTION PROCEDURE

```
10 '*****************************************************
20 ' RUT DEPTH PREDICTION PROGRAM FOR LOW-VOLUME ROADS
30 '                        BY
40 '                  K. A. S. YAPA
50 '*****************************************************
60 ' Pavement Systems, Texas Transportation Institute,
70 ' TTI Building, Texas A & M University,
80 ' College Station, Texas 77843.
90 ' (409)-845-9910.
100 ' 18th JULY 1988.
105 ' MODIFIED TO SUIT LOADRATE - 7/1/89
110 '
120 'This program predicts the rut depth of a low-volume road by using a data
130 'base of rut depths calculated by the Mechano-lattice program. A
140 'multi-dimensional polynomial interpolation routine is used to
150 'interpolate among the input parameters. Required inputs are the
160 'resilient modulus and the material classification of both the base
170 'course and the subgrade layers and the thickness of the base layer.
180 'Optionally, laboratory data from a permanent deformation test for
190 'each material layer can be input, in place of the material
200 'classification.
210 '
220 '*****************************************************
222 INIOPT = 2: REM This alllows the program to run alone
224 '*****************************************************
230 DIM RUT(2, 3, 3, 3, 3)
240 '
250 ' LOAD THE DATA BASE INTO AN ARRAY
260 '
270 FOR I = 1 TO 2
280 FOR J = 1 TO 3
290 FOR K = 1 TO 3
300 FOR L = 1 TO 3
310 READ RUT(I, J, K, L, 1), RUT(I, J, K, L, 2), RUT(I, J, K, L, 3)
320 NEXT L: NEXT K: NEXT J: NEXT I
330 '
340 ' READ THE ORIGINAL INPUT PARAMETERS
350 '
360 FOR I = 1 TO 3
370 READ XM(I), XL(I), XK(I), XJ(I), XI(I)
380 NEXT I
390 '
400 ' GOTO SUBROUTINE INPUT1 ---------------------------------
420 GOSUB 3000
421 ' LOOP TO CALCULATE RUT DEPTHS FOR EACH FWD SECTION
422 '
423 IF INIOPT = 2 THEN NC = 1
424 '
425 FOR INC = 1 TO NC
426 '
427 REM GOTO SUBROUTINE INPUT2
428 GOSUB 4111
430 '
432 'GOTO INPUT1 IF ANY CORRECTIONS ARE NEEDED
436 IF CORR = 1 THEN GOSUB 3000
438 '
440 ' SELECT PARAMETERS FOR INTERPOLATION
450 '
460 FOR I = 1 TO 2
470 FOR J = 1 TO 3
480 FOR K = 1 TO 3
490 FOR L = 1 TO 3
500 FOR M = 1 TO 3
510 '
```

```
520 ' M - BASE THICKNESS
530 '
540 Y1(M) = RUT(I, J, K, L, M)
550 X1(M) = XM(M): NEXT M
560 '
570 ' CALL THE INTERPOLATION ROUTINE
580 '
590 NUM = 3: X = XMM: GOSUB 2010
600 YLTEMP(L) = Y: XMFLAG = XFLAG
610 NEXT L
620 '
630 ' L - SUBGRADE RUTTING POTENTIAL
640 '
650 FOR LL = 1 TO 3: X1(LL) = XL(LL): Y1(LL) = YLTEMP(LL): NEXT LL
660 NUM = 3: X = XLL: GOSUB 2010
670 YKTEMP(K) = Y: XLFLAG = XFLAG
680 NEXT K
690 '
700 ' K - SUBGRADE RESILIENT MODULUS
710 '
720 FOR KK = 1 TO 3: X1(KK) = XK(KK): Y1(KK) = YKTEMP(KK): NEXT KK
730 NUM = 3: X = XKK: GOSUB 2010
740 YJTEMP(J) = Y: XKFLAG = XFLAG
750 NEXT J
760 '
770 ' J - BASE RESILIENT MODULUS
780 '
790 FOR JJ = 1 TO 3: X1(JJ) = XJ(JJ): Y1(JJ) = YJTEMP(JJ): NEXT JJ
800 NUM = 3: X = XJJ: GOSUB 2010
810 YITEMP(I) = Y: XJFLAG = XFLAG
820 NEXT I
830 '
840 ' I - BASE RUTTING POTENTIAL
850 '
860 FOR II = 1 TO 2: X1(II) = XI(II): Y1(II) = YITEMP(II): NEXT II
870 NUM = 2: X = XII: GOSUB 2010
880 RUTCAL = Y * CYL / 300000!: XIFLAG = XFLAG
890 '
900 ' GOTO SUBROUTINE OUTPUT ------------------------------------
910 '
920 GOSUB 5020
925 NEXT INC
930 INPUT "DO YOU WANT TO RERUN THE PROGRAM: 0=NO,1=YES"; ENDOP
940 IF ENDOP = 1 THEN : GOTO 420
950 '
960 ' DATA BASE OF RUT DEPTHS
970 '
980 DATA       0.2609 ,         0.2804 ,         0.3191
990 DATA       0.2216 ,         0.2152 ,         0.2223
1000 DATA       0.1831 ,         0.1502 ,         0.1253
1010 DATA       0.2705 ,         0.3030 ,         0.3431
1020 DATA       0.2451 ,         0.2491 ,         0.2556
1030 DATA       0.2168 ,         0.1951 ,         0.1680
1040 DATA       0.3674 ,         0.4519 ,         0.5286
1050 DATA       0.3503 ,         0.4172 ,         0.4580
1060 DATA       0.3331 ,         0.3831 ,         0.3882
1070 DATA       0.2702 ,         0.2912 ,         0.3019
1080 DATA       0.2249 ,         0.2185 ,         0.2002
1090 DATA       0.1797 ,         0.1458 ,         0.0991
1100 DATA       0.2804 ,         0.3099 ,         0.3549
1110 DATA       0.2473 ,         0.2490 ,         0.2600
1120 DATA       0.2137 ,         0.1882 ,         0.1652
1130 DATA       0.3900 ,         0.4610 ,         0.5322
1140 DATA       0.3688 ,         0.4231 ,         0.4561
```

```
1150 DATA       0.3475 ,          0.3842 ,          0.3798
1160 DATA       0.2946 ,          0.3130 ,          0.3110
1170 DATA       0.2344 ,          0.2263 ,          0.2031
1180 DATA       0.1750 ,          0.1403 ,          0.0837
1190 DATA       0.3013 ,          0.3356 ,          0.3755
1200 DATA       0.2548 ,          0.2600 ,          0.2687
1210 DATA       0.2087 ,          0.1842 ,          0.1618
1220 DATA       0.3977 ,          0.4840 ,          0.5424
1230 DATA       0.3750 ,          0.4343 ,          0.4541
1240 DATA       0.3498 ,          0.3834 ,          0.3670
1250 DATA       0.1613 ,          0.2376 ,          0.3056
1260 DATA       0.1258 ,          0.1727 ,          0.2086
1270 DATA       0.0934 ,          0.1082 ,          0.1119
1280 DATA       0.1901 ,          0.2528 ,          0.3247
1290 DATA       0.1588 ,          0.1993 ,          0.2374
1300 DATA       0.1280 ,          0.1457 ,          0.1500
1310 DATA       0.2607 ,          0.3681 ,          0.4915
1320 DATA       0.2453 ,          0.3355 ,          0.4217
1330 DATA       0.2300 ,          0.3038 ,          0.3523
1340 DATA       0.1951 ,          0.2524 ,          0.2767
1350 DATA       0.1491 ,          0.1794 ,          0.1747
1360 DATA       0.1039 ,          0.1072 ,          0.0732
1370 DATA       0.1957 ,          0.2643 ,          0.3400
1380 DATA       0.1628 ,          0.2037 ,          0.2453
1390 DATA       0.1296 ,          0.1433 ,          0.1505
1400 DATA       0.2920 ,          0.4006 ,          0.5025
1410 DATA       0.2713 ,          0.3648 ,          0.4262
1420 DATA       0.2508 ,          0.3230 ,          0.3502
1430 DATA       0.2254 ,          0.2785 ,          0.2834
1440 DATA       0.1652 ,          0.1918 ,          0.1736
1450 DATA       0.1056 ,          0.1059 ,          0.0643
1460 DATA       0.2256 ,          0.2974 ,          0.3642
1470 DATA       0.1790 ,          0.2216 ,          0.2574
1480 DATA       0.1328 ,          0.1461 ,          0.1506
1490 DATA       0.3322 ,          0.4287 ,          0.5197
1500 DATA       0.3034 ,          0.3786 ,          0.4327
1510 DATA       0.2749 ,          0.3287 ,          0.3456
1520 '
1530 'INPUT PARAMETERS USED IN CREATING THE DATA BASE
1540 '
1550 DATA 18, 0.0100, 25000, 100000, 0.0075
1560 DATA 12, 0.0060, 15000,  70000, 0.0025
1570 DATA  6, 0.0020,  5000,  40000, 0.0000
1580 END
2000 '*****************************************************************
2010 'SUBROUTINE FOR POLYNOMIAL INTERPOLATION
2020 '*****************************************************************
2022 ' X - VALUE OF THE PARAMETER
2024 ' X1(I) - PARAMETER VALUES USED IN THE DATA BASE
2030 ' Y1(I) - RUT DEPTHS FROM DATA BASE CORRESPONDING TO PARAMETER
2040 ' Y - INTERPOLATED VALUE
2050 ' NUM - NUMBER OF LEVELS OF THE PARAMETER
2060 '
2070 NS = 1
2080 DIF = ABS(X - X1(1))
2090 FOR A = 1 TO NUM
2100 DIFT = ABS(X - X1(A))
2110 '
2120 ' SELECT THE BEST STARTING POINT
2130 '
2140 IF DIFT < DIF THEN : NS = A: DIF = DIFT
2150 C(A) = Y1(A): D(A) = Y1(A)
2160 NEXT A
2170 XFLAG = 0
```

```
2180 '
2190 'ENFORCE LIMITS ON EXTRAPOLATION (MAXIMUM = 1.5 * DIFFERENCE BETWEEN TWO
2200 'CONSECUTIVE PARAMETER LEVELS)
2202 '
2210 IF DIF > 1.5 * (ABS(X1(1) - X1(2))) THEN GOTO 2220 ELSE GOTO 2260
2220 DIF = 1.5 * (ABS(X1(1) - X1(2)))
2230 IF NS = 1 THEN : X = X1(1) + DIF
2240 IF NS = NUM THEN : X = X1(NUM) - DIF
2250 XFLAG = X
2260 Y = Y1(NS)
2270 NS = NS - 1
2280 BEND = 1
2290 FOR B = 1 TO BEND
2300 AEND = NUM - B
2310 FOR A = 1 TO AEND
2320 HO = X1(A) - X
2330 HP = X1(A + B) - X
2340 W = C(A + 1) - D(A)
2350 DEN = HO - HP
2360 DEN = W / DEN
2370 '
2380 ' D - CORRECTION FROM THE LOWER LEVEL
2390 ' C - CORRECTION FROM THE UPPER LEVEL
2400 '
2410 D(A) = HP * DEN
2420 C(A) = HO * DEN
2430 NEXT A
2440 '
2450 ' PICK THE SHORTEST PATH TO MOVE
2460 '
2470 IF (2 * NS) < AEND THEN : DY = C(NS + 1): GOTO 2490:    ELSE GOTO 2480
2480 DY = D(NS): NS = NS - 1
2490 Y = Y + DY
2500 NEXT B
2510 RETURN
3000 '*************************************************************************
3010 ' SUBROUTINE INPUT1
3020 '*************************************************************************
3022 '
3023 'USE IF ONLY RUT LEVELS ARE NEEDED
3024 '
3025 IF INIOPT <> 2 GOTO 3080
3026 CLS : INPUT "JOB DESCRIPTION :"; AA$
3030 INPUT "Resilient Modulus - Base Course (psi)"; EBA
3040 INPUT "Resilient Modulus - Subgrade (psi)"; ESG
3050 INPUT "Thickness of Base Layer (in)"; TBA
3053 INPUT "# of Equivalent Standard Wheel (9000 lbs) Passes"; EQPASS
3054 INPUT "Allowable Rut Depth (in.)"; RALLOW
3056 INPUT "Existing Rut Depth (in.)"; REXIST
3060 CLS
3070 '
3080 LOCATE 4, 10: PRINT "INPUT DATA OPTIONS: "
3090 LOCATE 6, 10: PRINT " 1) Require subgrade material"
3100 LOCATE 7, 10: PRINT "    classification to determine approximate "
3110 LOCATE 8, 10: PRINT "    rutting potentials."
3120 LOCATE 10, 10: PRINT " 2) Require laboratory data on residual deforma- "
3130 LOCATE 11, 10: PRINT "    tion behavior of base and subgrade."
3140 LOCATE 15, 10: INPUT "OPTION: 1=SOIL CLASS, 2=LAB DATA "; OPP
3150 '
3160 IF OPP = 2 THEN GOTO 3450
3170 IF OPP <> 1 THEN GOTO 3060
3182 '
3190 REM BASE COURSE MATERIALS ARE CLASSIFIED INTO ONLY ONE GROUP.
3192 '
```

```
3200 CLS : LOCATE 4, 10: PRINT "Subgrade Material Type :"
3210 LOCATE 7, 10: PRINT "1) Heavy Clay - (CH)"
3220 LOCATE 9, 10: PRINT "2) Light/Silty Clay, Clayey Silt - (CL-ML)"
3230 LOCATE 11, 10: PRINT "3) Clayey/Silty/Uniform Sand - (SC-SM)"
3240 LOCATE 15, 10: INPUT "ENTER SELECTION & <RET> "; MSG
3250 GOTO 4000
3450 CLS : LOCATE 4, 10: PRINT "Laboratory Data Input:"
3460 LOCATE 6, 10: PRINT "Log a - Intercept of the Straight Line Fit on a "
3470 LOCATE 7, 10: PRINT "        Log-Log Plot of Accumulated Residual Strain"
3480 LOCATE 8, 10: PRINT "        vs. Number of Load Repetitions"
3490 LOCATE 10, 10: PRINT "b     - Slope of the Straight Line Fit"
3492 PRINT : PRINT
3500 INPUT "Log a - Base Course Material"; LGABA
3510 INPUT "b     - Base Course Material"; BBA
3520 INPUT "Log a - Subgrade Material"; LGASG
3530 INPUT "b     - Subgrade Material"; BSG
3540 '
3550 ABA = 10 ^ LGABA: ASG = 10 ^ LGASG
3560 IF ((ABA * 50000! ^ BBA) < .03470 LOCATE 7, 10: PRINT "        Log-Log Plot of Accumulated Residual Strain"
3480 LOCATE 8, 10: PRINT "        vs. Number of Load Repetitions"
3490 LOCATE 10, 10: PRINT "b     - Slope of the Straight Line Fit"
3492 PRINT : PRINT
3500 INPUT "Log a - Base Course Material"; LGABA
3510 INPUT "b     - Base Course Material"; BBA
3520 INPUT "Log a - Subgrade Material"; LGASG
3530 INPUT "b     - Subgrade Material"; BSG
3540 '
3550 ABA = 10 ^ LGABA: ASG = 10 ^ LGASG
3560 IF ((ABA * 50000! ^ BBA) < .015) AND ((ASG * 50000! ^ BSG) < .016) GOTO 4000
3570 CLS : BEEP: PRINT "Input Data are Incompatible. Check & Re-enter!":
3580 GOTO 3080
3590 '
4000 ' SKIP IF ONLY RUT LEVELS ARE CALCULATED
4010 IF INIOPT = 2 GOTO 4050
4012 '
4014 ' OBTAIN THE TRUCK PASSES AND ALLOWABLE AND MEASURED RUT LEVELS FROM
4016 ' THE MAIN PROGRAM
4018 '
4020 EQPASS = PA
4030 RALLOW = RX
4040 REXIST = RM
4050 RETURN
4111 '*********************************************************
4112 'SUBROUTINE INPUT2 ---------------------------------
4113 '*********************************************************
4114 'SKIP IF ONLY RUT LEVELS ARE CALCULATED
4115 IF INIOPT = 2 GOTO 4200
4116 '
4120  EBA = E1(INC)
4130  ESG = E2(INC)
4140  TBA = BA(INC)
4200 IF OPP <> 1 GOTO 4599
4260 '
4261 REM APPROXIMATE METHOD TO DETERMINE RUTTING BEHAVIOR
4265 '
4270 ' e(p) = a* N^b
4272 ' a - FIRST CYCLE STRAIN      (ABA,ACH,ACL,ASM)
4274 ' b - RESIDUAL DEFORMATION RATE  (BBA,BCH,BCL,BSM)
4275 ' N - # OF WHEEL PASSES  (CYL)
4276 ' a = aa * Mr^ab
4278 ' aa - COEFFICIENT   (AABA,AACH,AACL,AASM)
4280 ' ab - EXPONENT   (ABBA,ABCH,ABCL,ABSM)
4282 ' Mr - RESILIENT MODULUS (ksi)    (EBA,ESG)
4284 '
```

```
4300 AABA = .0174: AACH = .0933: AACL = .001: AASM = .075
4310 ABBA = -.57: ABCH = -2.64: ABCL = -.73: ABSM = -1.61
4320 BBA = .125: BCH = .236: BCL = .162: BSM = .142
4322 '
4324 'CALCULATE "a" AND "b" ("a" IS KEPT WITHIN PRACTICAL LIMITS)
4326 '
4330 ABA = AABA * (EBA / 1000) ^ ABBA
4335 IF ABA > .0035 THEN ABA = .0035
4340 IF MSG <> 1 GOTO 4370
4350 BSG = BCH
4352 ASG = AACH * (ESG / 1000) ^ ABCH
4360 IF ASG > .004 THEN ASG = .004
4370 IF MSG <> 2 GOTO 4390
4375 BSG = BCL
4380 ASG = AACL * (ESG / 1000) ^ ABCL
4385 IF ASG > .001 THEN ASG = .001
4390 IF MSG <> 3 GOTO 4430
4400 BSG = BSM
4410 ASG = AASM * (ESG / 1000) ^ ABSM
4420 IF ASG > .005 THEN ASG = .005
4430 '
4599 REM USE IF ONLY RUT LEVELS ARE NEEDED
4600 '
4605 IF INIOPT <> 2 GOTO 4660
4610 CLS : REM DISPLAY INPUT DATA
4620 LOCATE 2, 10: PRINT "JOB : "; AA$
4630 LOCATE 4, 10: PRINT "Resilient Modulus (psi) - Base     = "; EBA
4640 LOCATE 6, 10: PRINT "                        - Subgrade = "; ESG
4650 LOCATE 8, 10: PRINT "Thickness of Base Layer           = "; TBA; " in."
4652 LOCATE 10, 10: PRINT "# of Equivalent Standard Wheel Passes ="; EQPASS
4654 LOCATE 12, 10: PRINT "Allowable Rut Depth ="; RALLOW; " in."
4656 LOCATE 14, 10: PRINT "Measured Rut Depth ="; REXIST; " in."
4660 IF OPP <> 1 GOTO 4770
4690 LOCATE 16, 10: IF MSG = 1 THEN PRINT "Subgrade      - CH - Clay"
4700 LOCATE 16, 10: IF MSG = 2 THEN PRINT "Subgrade      - CL-ML "
4710 LOCATE 16, 10: IF MSG = 3 THEN PRINT "Subgrade      - SC-SM"
4740 GOTO 4820
4750 '
4760 '
4770 LOCATE 16, 10: PRINT "Base Course Material - "
4780 LOCATE 17, 10: PRINT "            Log a = "; LGABA; ",     b = "; BBA
4790 LOCATE 19, 10: PRINT "Subgrade Material    - "
4800 LOCATE 20, 10: PRINT "            Log a = "; LGASG; ",     b = "; BSG
4810 '
4820 LOCATE 22, 10: INPUT "DO YOU WANT ANY CORRECTIONS - 0=NO, 1=YES"; CORR
4830 IF CORR = 1 THEN RETURN
4840 IF CORR <> 0 GOTO 4820
4850 '
4860 'ASSIGN VALUES TO INTERPOLATION PARAMETERS
4870 '
4880 CYL = 300000!
4890 XII = ABA * CYL ^ BBA
4900 XLL = ASG * CYL ^ BSG
4902 IF XII > .015 THEN XII = .015
4904 IF XLL > .016 THEN XLL = .016
4906 IF XLL < .001 AND TBA < 10 THEN XLL = .001
4910 XMM = TBA: XJJ = EBA: XKK = ESG
4915 ' Controls extrapolations
4920 IF TBA < 10 AND ESG > 20000 AND EBA > 100000 THEN XJJ = 100000
4930 IF TBA < 10 AND EBA < 60000 AND ESG > 30000 THEN XKK = 30000
4940 IF TBA < 6 AND EBA < 60000 AND ESG > 30000 THEN XMM = 6
4950 IF TBA < 6 AND EBA < 30000 AND ESG > 30000 THEN XJJ = 30000
4960 RETURN
5000 '*************************************************************************
```

```
5020 'SUBROUTINE OUTPUT
5030 '*****************************************************************
5035 '
5038 IF RUTCAL < 0 THEN RUTCAL = 0!
5041 RFINAL(INC) = RUTCAL * EQPASS / CYL
5043 REXTRA = RALLOW - REXIST
5044 IF RUTCAL = 0 THEN PASSES(INC) = 0: GOTO 5100
5045 PASSES(INC) = CYL * REXTRA / RUTCAL
5100 IF INIOPT <> 2 GOTO 5400
5110 CLS
5120 IF EQPASS = 0 GOTO 5210
5140 LOCATE 6, 10: PRINT "EQUIVALENT STANDARD WHEEL PASSES ="; EQPASS
5150 LOCATE 8, 10: PRINT "RUT DEPTH CAUSED        = "; RFINAL(1); " in."
5210 LOCATE 10, 10: PRINT "ALLOWABLE RUT DEPTH     = "; RALLOW; " in."
5215 LOCATE 12, 10: PRINT "EXISTING RUT DEPTH      = "; REXIST; " in."
5220 LOCATE 14, 10: PRINT "ALLOWABLE WHEEL PASSES  = "; PASSES(1)
5225 IF PASSES(1) = 0 THEN : LOCATE 16, 5: PRINT "INPUT DATA MAY BE INCOMPATIBLE. CHECK & RERUN!"
5230 PRINT : PRINT
5400 RETURN
```